Addis Ababa University

Addis Ababa Institute of Technology

School of Electrical and Computer Engineering

Study on Conversion of Existing HVAC Lines to Hybrid HVAC/HVDC Transmission Line to Increase Transmission Capacity and Efficiency

[Case of GIBE III – Addis Ababa 400KV line]

A thesis Submitted to Addis Ababa Institute of Technology, School of Graduate Studies, Addis Ababa University

In Partial Fulfillment of the Requirement for the Degree of

Master of Science in Electrical Engineering (Electrical Power Engineering)

By Amare Assefa Ashagire

Advisor: Dr.-Ing. GETACHEW BIRU WORKU

December 2015, Addis Ababa

Addis Ababa University

Addis Ababa Institute of Technology

School of Electrical and Computer Engineering

Study on Conversion of Existing HVAC Lines to Hybrid HVAC/HVDC Transmission Line to Increase Transmission Capacity and Efficiency

[Case of GIBE III – Addis Ababa 400KV line]

APPROVED BY BOARD OF EXAMINERS

Dr. Yalemzewid Negash	
Chairman, Department of Graduate Committee	**Signature**
Dr.Ing- Getachew Biru	
Advisor	**Signature**
Dr. Mengesha Mamo	
Internal Examiner	**Signature**
Prof. N.P Singh	
External Examiner	**Signature**

Declaration

I, the undersigned, declare that this thesis is my original work, has not been presented for fulfillment of a degree in this or any other university, and all sources and materials used for the thesis have been acknowledged.

All examiners' comments are duly incorporated.

Name: Amare Assefa

Signature: _____

Place: Addis Ababa

This thesis has been submitted for examination with my approval as a university advisor.

Dr.-Ing Getachew Biru _____

Advisor's Name Signature

Acknowledgment

First and foremost, I would like to express my sincere gratitude to my advisor Dr.-Ing. Getachew Biru for his invaluable advice, incessant guidance and continuous encouragement throughout the course of my study both in undergraduate and postgraduate study. His deep knowledge on his field, hardworking attitude and way of teaching are always inspiring me as a model to follow in my future study and work. I would, also, like to express my gratitude to ATPdraw-EMTP educational software developer, Prof Hans kr. Holden from NTNU, Norway and QuickField software owner, Tera analysis Ltd for providing software's for our simulation.

As well, I would like to thank all my colleagues in the School of Electrical and Computer Engineering for providing such an excellent education and research environment. Finally, I would like to express my deepest appreciation to my family for their encouragement, support, and understanding through my work have meant more I can ever express.

Abstract

Ethiopia's economy has been one of the fastest growing economy in the world with two digit figures in the last decade. Consequently, the rate of electric consumption has also been increasing very fast. A large number of new consumers has been recently connected to the grid or waiting to be connected. Infrastructure development boosted on different areas like, new country-wise railway developments, Addis Ababa light rail system, large new irrigation, new Industrial zone development and electricity export consumers.

Gilgel gibe III hydropower project is one of mega project undertaken by the government of Ethiopia. The objective of the project is to enhance the hydropower generation capacity of the country through developing a plant with a capacity of 1870 MW. The project is expected to raise the present installed capacity from 2268 MW to 4138 MW. A total of 402km new 400 KV HVAC double circuit transmission line is constructed from Gibe III – Wolayita – Akaki II substation with a capacity of 1500MVA.

In the near future the government is trying to finance for Gibee VI and Gibee V hydro power plant with combined capacity of 2100MW as part of a series of cascade dams on the Gibe River. The existing transmission line capacity cannot able to evacuate such power, therefore new transmission line construction is a must to evacuate power to load center, Addis Ababa.

This thesis studies the technical and economic feasibility of converting existing 400KV HVAC line from Gibe III – Wolyita- Addis Ababa to Hybrid HVAC/HVDC line to upgrade the power transmission capacity. The new line will have a bipolar 500 KV HVDC as part of the whole transmission line

In our study we have observed that we can increase the transmission efficiency from 1500MVA to 2.5GW. The investment cost for constructing new single circuit 400KV HVAC line about 855,978,477.20 USD. (17,958,428,451.66 Birr). The Hybrid HVAC/HVDC line costs 439,173,420.00 USD (9,200,683,149.00 Birr). This price reduction is about 416,805,057.20 USD (8,732,065,948.34 Birr). From Investment point of view, the total reduction of cost is about 49%. Considering the active power loss and corona loss of the two systems, the hybrid HVAC/HVDC line 97% efficient while HVAC system is 91%. The environmental effects like audible noise and radio interference as well as electric level is essentially under standard. It is found that the hybrid HVAC/HVDC line is found to be technically and economically feasible.

Key words: Hybrid HVAC/HVDC, HVDC, HVAC, Radio interference, Audible noise, loss cost

Table of Content

List of Figures

List of Tables

Acronyms

A	Ampere
Ac/ac	Alternate Current
AIS	Air insulated swicthgear
CAD	Canadian Dollar
CC	Capacitor Commutation
CIGRÉ CSC Current Source Converter	Conseil International des Grands Réseaux Électriques (International Council for Large Electric Systems)
DC/dc	Direct Current
DFIG	Double fed Induction Generator
EEPCo	Ethiopian Electric Power Corporation
EPC	Engineering, procurement and construction cost
ESIA	Environment and Social Impact Assessment
F	Farad
GIS	Gas insulated substation
H	Henry
HVAC	High Voltage Alternate Current
HVDC	High Voltage Direct Current
IRR	Interest return rate
k	kilo
km	kilo meter
LC	Line Commutation
LCC	Line Commutated Converters
MVAR	Mega Volt Amper Reactive
MW	Mega Watt
NPV	Net present value
pu	per unit
RAP	Resettlement Action Plan
RoW	Right of Way
SCR	Silcon controled rectfier
V	Volt
VSC	Voltage Source Converter
WTG	Wind Turbine Generator

CHAPTER ONE

Introduction

1.1 Background

An electric power system can be considered as the integration of a generation system, transmission system a sub-transmission system and a distribution system. Generation system and transmission system together referred as bulk power transfer systems. Transporting bulk power from generation station to consumer areas is conveyed by using high voltage network. High voltage alternating current (HVAC) lines dominates power transmission systems. However, for long distance transmission, High voltage direct current (HVDC) power lines possess many advantages over HVAC lines in economics, power transmission capability, system stability, reliability, control, low short circuit current levels, structural simplicity, and low line power losses.

With the growth of industry and population in Ethiopia, the demand of electric power is increasing exponentially everywhere, which has led to overloading and stability problems of the existing high voltage transmission lines. To tackle this problem, various options have been under study and implementation. One of the methods, which has gained serious attention in the last decade is the use of High Voltage Direct Current (HVDC) for transmission of bulk of power. Converting existing double circuit high voltage alternating current (HVAC) transmission line to hybrid HVAC/HVDC system is an alternative method to high voltage alternating current (HVAC) transmission system to transport bulk power over hundreds of kilometers. Hybrid HVAC/HVDC transmission system is superior compared to HVAC transmission system in terms of efficiency, voltage drop, operating cost, system stability, reliability, control, low short circuit current levels [1]. In order to enhance the efficiency and power transmission capacity of the existing HVAC, converting them to hybrid HVAC/HVDC transmission system can be a promising option.

Gigel gibe III hydropower project is one of mega project undertaken by the government of Ethiopia. The project is located in the Southern Nations Nationalities & Peoples Regional State in Wolayta and Dawro Zones at about 470 km south west of Addis Ababa on the road via Shashemene. It is situated along the lower course of the Omo River, some 155 km downstream of the Gilgel Gibe II Powerhouse. The objective of the project is to enhance the hydropower generation capacity of the country through developing a plant with a capacity of 1870 MW and with an annual energy production of 6,500 GWh, this in turn is expected to raise the present installed capacity 2268 MW [as 2014] of the country by 82 percent. The project has the aim of ensuring exportation of power to the neighboring countries through regional Interconnection Transmission System so that Ethiopia will be in a place of gaining hard currency through sells of electricity.

The power transmission about 55 km from Gibe III main station to Wolaita II substation and about 342 km from Wolaita II substation to Akaki II substation. The tower is a double circuit 400 kV, 3-phase, twin AAAC "ASTER 851" conductor, two optical fiber cable (OPGW). This research focuses on studying the technical and economic feasibility of converting double circuit to hybrid HVAC/HVDC transmission for improving the transmission capacity and efficiency.

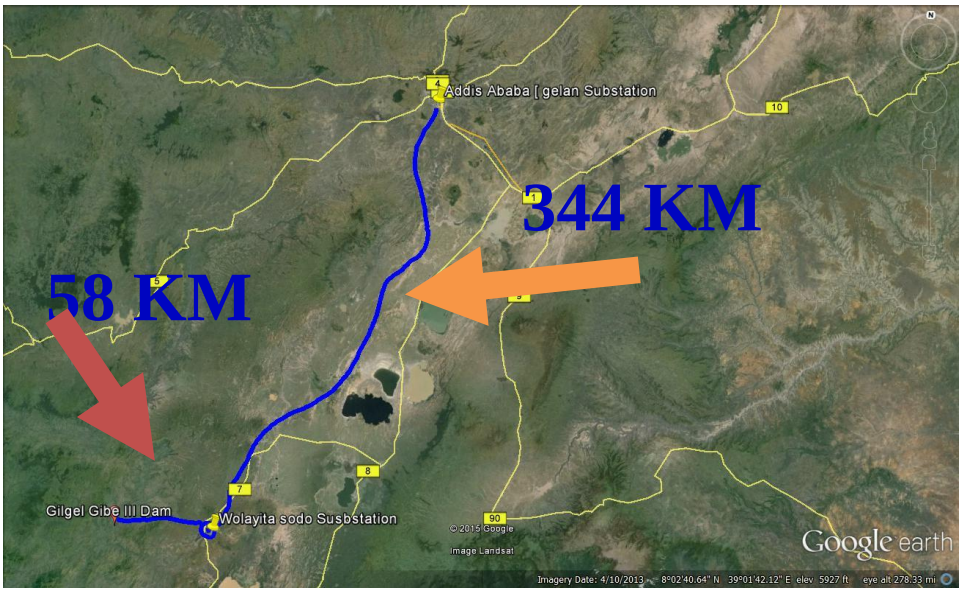

Figure 0:1 Gibee III – Addis Ababa 400KV double circuit route

1.2 Problem Statement and Motivation

Ethiopia, as a fast growing country on sub- Saharan region, has a huge plan to expand its power generation and transmission capacity to meet the ever growing energy need for industrialization and population growth. In addition to that, Ethiopian Electric Power (EEP) is currently striving to be a power hub of east Africa by selling powers to neighborhood countries like Kenya, Djibouti, Sudan, and South Sudan, as Ethiopia possesses many huge rivers which can generate green energy at affordable cost. It is obvious that the combined internal and external energy need have put a huge pressure on the existing power infrastructure, leading to overloading of transmission lines beyond their capacity. The inadequacy of the transmission lines has also contributed to the power interruptions and instability of the power system. Therefore, ways and means have to be found to raise the efficiency and power transmission capacity of the lines. As constructing new HVAC transmission line is expensive, this thesis studies the technical and economic feasibility of converting existing transmission lines to hybrid HVAC/HVDC transmission system.

1.3 Objective of the Thesis

General Objective

The general objective of this thesis is to study the technical and economic feasibility of converting double HVAC transmission lines into hybrid HVAC/HVDC system for increasing transmission capacity and efficiency as compared to existing HVAC system.

Specific Objectives

Taking one existing HVAC transmission lines as a sample, the study has the following specific objectives:

1. To study and evaluate the technical details of converting HVAC into hybrid HVAC/HVDC system.
2. To evaluate, corona effect of audible noise (AN) and radio interference contribution of the system.
3. To evaluate changes in conductor size, insulation, various spacings between conductors and the earth.

4. To compute the electric and magnetic fields around the conductors as an important input for further design of the HVDC.
5. To investigate the changes in the mechanical structure of the tower.
6. To Evaluate and compare the cost of the implementation of the hybrid HVAC/HVDC system. This will be compared with the benefits of the HVDC and expressed in monetary terms.

1.4 Methodology

Data collection: The study has been started from literature review to get information on current developments on the area. Data from EEP planning and GIBE III project office has been collected for analyzed.

Modeling: Based on the information obtained from this study, Modeling and analyzing the technical details of converting the HVAC system to hybrid AC/DC system has been done.

Design: After modeling and Identifying sample transmission lines (from Gibee III to Akaki), design of components of a transmission line has been done.

Simulation: Hybrid HVAC/HVDC model has been simulated by using electromagnetic transient simulation program ATP-EMTP and evaluated its performance and behavior.

Result: Finally, economic feasibility study of the model has been conducted to evaluate its practicability and cost effectiveness.

1.5 Thesis outline

The thesis consists of the following chapters.

- *Chapter 1* presents a brief introduction, background, motivation, and problem statement, a brief description of methodology and thesis outline.
- *Chapter 2* explains the theoretical background and literature reviews of the study area by different authors.
- *Chapter 3* describes modeling and designing of hybrid HVAC/HVDC components.
- *Chapter 4* presents the technical and economical comparison of hybrid HVAC/HVDC model.
- *Chapter 5* presents the simulation result of hybrid HVAC/HVDC model.
- *Chapter 6 gives* the conclusion and recommendation of the thesis.

CHAPTER TWO

Literature Review and Theoretical Back Ground

2.1. Switchyard

In a power system there are four common types of electric substations. The first type is the switchyard, which is located at a generating station. This type of substation connects the generating units to the utility grid and also provide electric power on generation station. Switchyards tend to be large installations that are needed to be designed and constructed carefully by considering future plan of the plant. The second type of substation, known as the customer substation, it functions as a primary substation to specified industrial customers. The third type of substation is referred to as a system station. The main purpose is to transfer bulk power between two networks. System stations typically serve as the end points for transmission lines originating from generating switchyards and provide the electrical power for circuits that feed transformer stations. The fourth type of substation is the distribution station. These are the most common type of substation electric power system which located near to load centers. Their target to distribute power with distribution voltage levels to customers.

High voltage switchyard comprising high voltage switchgears and devices with different insulating system, air or gas (SF_6). Air Insulated switch gear (AIS) are cost effective high voltage substations up to 800KV, which are more popular where space restriction and environmental effect is not severe. All electrical and electromechanical part of a switch gear is assembled on the site. Since the installation is taken place on open area during AIS case, safety requirement should be taken as major part of the site. Gas insulated substations (GIS) basically compact and small in size. It is possible to install in middle of urban areas to the basement of power generating building. Each electrical, electromechanical parts, and controlling components of GIS must be factory assembled with high accuracy. In switchyard arrangement

the most common types are Single bus, Double bus–double breaker, Main and transfer (inspection) bus, Double bus–single breaker, Ring bus and Breaker-and-a-half.

2.2. HVAC transmission

The main target behind the electric transmission system is the interconnection of the electric energy producing power plants or generating stations with the loads which is most of the time located hundreds of kilometer away. A three-phase AC system is used for most transmission lines. The operating frequency varies from is 60 Hz in the North America. and 50 Hz in other continents. The three-phase system has three phase conductors. The system voltage is defined as the rms voltage between the conductors, also called line-to-line voltage. The voltage between the phase conductor and ground, called line-to-ground voltage, is equal to the line-to-line voltage divided by the square root of three [3].

High voltage level with hundreds of kilovolt be selected for transmission. The main significance of using high-voltage transmission lines is that, high-voltage transmission lines transport power over long distances much more efficiently than lower-voltage distribution lines for two main reasons. First, high-voltage transmission lines take advantage of the power equation, that is, power is equal to the voltage times current. Therefore, increasing the voltage allows one to decrease the current for the same amount of power. Second, since transport losses are a function of the square of the current flowing in the conductors, increasing the voltage to lower the current drastically reduces transportation losses. Plus, reducing the current allows one to use smaller conductor sizes. [2]

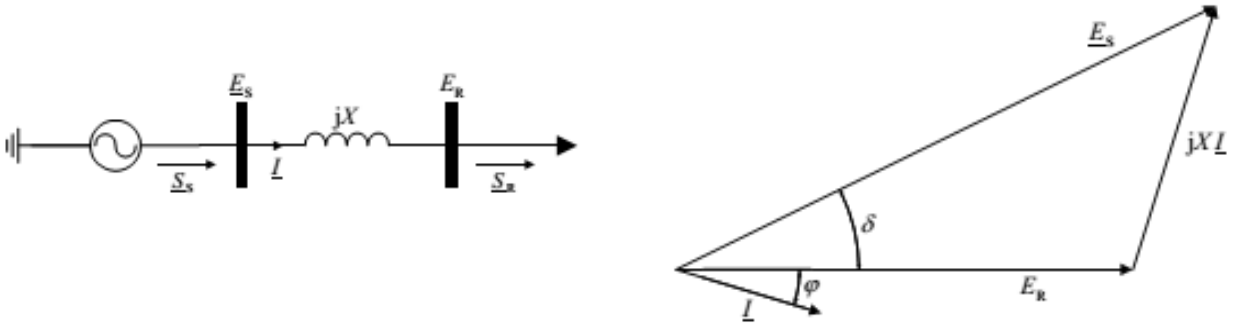

a Line diagram

b) Phasor diagram

Figure 2:1 Model of Electrical power transmission through Alternating current (AC) system

Electric power transfer through a transmission line in which the complex power S is transmitted from the sending end to the receiving end. The line reactance X corresponds to the series impedance of an electrical over-head transmission line, for simplicity the shunt capacities (and also the line resistance) have been neglected. E_S and E_R represent the complex busbar voltages at the sending and the receiving end, respectively, where E_R is a reference voltage assumed to be real-valued I is the complex line current.

The apparent power can be represented as,

$$\bar{S}_R = E_R I^* = P_R + jQ_R \tag{2.1}$$

and

$$I = \frac{\bar{E}_S - E_R}{jX} \tag{2.2}$$

From the above Phasor diagram and apparent power equation, we can easily calculate that

$$S_R = E_R \frac{E_S \sin\delta + j[E_s \cos\delta - E_R]}{jX}$$

The active power component P_R can be calculated as,

$$P_R = \frac{E_R E_s}{X} \sin\delta \tag{2.3}$$

The reactive component

$$Q_R = \frac{E_R E_s \cos\delta - {E_R}^2}{X} \tag{2.4}$$

Similarly, at sending end side

$$P_S = \frac{E_s E_R}{X} \sin\delta \tag{2.5}$$

$$Q_s = \frac{{E_s}^2 - E_s E_R \cos\delta}{X} \tag{2.6}$$

For the above equations, when $\delta = 0$ no active power can be transferred through the line. When $E_s > E_R$, Q_s and Q_R are positive therefore reactive power is transmitted from the sending to the receiving end of the line. If $E_s < E_R$, then Q_s and Q_R become negative, i.e. reactive power is flowing from the receiving end to the sending end of the line.

Figure 2.2 shows the Phasor diagram representation when δ=0, the reactive power loss on the transmission line can be calculated as the difference of sending end reactive component to receiving reactive component.

$$Q_{loss} = Q_s - Q_R = \frac{(E_s{}^2 - E_R{}^2)}{X} = XI^2 \qquad (2.7)$$

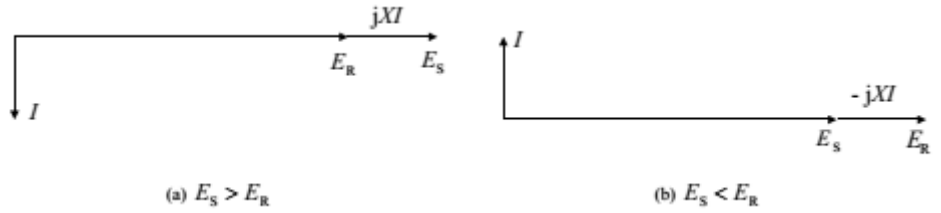

Figure 2:2Phasor diagram for δ=0

Transmission of lagging current, i.e., the transmission of positive reactive power from the sending to the receiving end, causes a voltage drop in receiving end voltage. Similarly, transmission of leading current, i.e. the transmission of negative reactive power from the sending to the receiving end, causes a voltage raise in receiving end voltage. When δ=0 the transmission of reactive power mainly depends on the difference between the voltage magnitudes at the ends of the line.

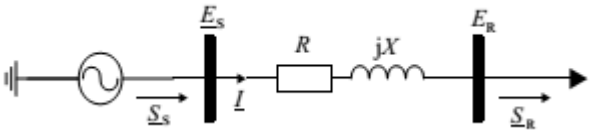

Figure 2:3 Sing line representation of HVAC line

Taking a more detailed representation of the transmission line that now also considers the ohmic series resistance R (see Figure 2.3) and allowing any possible values of $0 \neq \delta$, and, it can be found that the active and reactive losses on the transmission line and Q, respectively, can be expressed as a function of the power transfer.

$$P_{loss} = RI^2 = R\frac{(P_R{}^2 + Q_R{}^2)}{E^2{}_R} \qquad (2.8)$$

$$Q_{loss} = XI^2 = X\frac{(P_R{}^2 + Q_R{}^2)}{E^2{}_R} \quad (2.9)$$

Form the above formula it can be deduced that increasing active power transfer P_R results into increasing both reactive and active losses on the line, and with increasing reactive power transfer Q_R, both active and reactive losses on the line increase. Furthermore, the equations show that for a given transmission power, the losses on the line can be reduced by increasing the operating voltage and hence decreasing the line current I.

The above stated deductions provide the basic framework for the engineering practice of long distance power transmission. Since the line reactance X and the ohmic series resistance Rare proportional to the transmission line length, for long lines X and R will take high values which in turn lead to the constraints in long-distance power transmission

HVAC transmission line

The HVAC power transmission line is one of the major components of an electric power system. Its major function is to transport electric energy, with minimal losses, from the power sources to the load centers, usually separated by long distances.

The main purpose of any configuration of transmission tower is to carry the overhead transmission line conductors and earth wires above the ground during design every tower type has to:

- Withstand all the variety of forces that it is exposed to with regards to the. These forces include normal air loads, extreme wind loads, ice loads, loads during erection and maintenance and the changing of conductor sag when the conductor expands and contracts with normal daily current loads. In some cases, tower designs must with stand loads imposed by extreme conditions such as in earth quake, cyclone and tornado areas [10].
- Maintain electrical clearances between live conductors and any earthed body in the vicinity of the tower such that the energized lines do not include any hazardous voltage that could render the operation of the transmission lines dangerous to the environment and the public.
- Provide a proper a path for earth fault during lightning. Hence, the tower must also exhibit low resistance to ground during transient lighting overvoltage.

Depending on network requirement of power system, the tower may be designed to cater for single 3 –phase circuit, double 3-phase circuit, multiple voltages circuits and with direct current transmission either monopolar, bipolar construction. In certain countries, due to land constraints new transmission lines always built on double circuit towers and old single circuits are upgraded to double circuit to optimize the use of land settlement [10].

The major components of high voltage transmission lines are

a. Towers and structures
b. Foundations
c. Conductors and earth wire (including joints)
d. Insulators

Each of these components has its own function that enables power to be transmitted safely and reliably through transmission lines.

a. Towers and structures

The purpose of tower is to support conductors. The tower is composed of tower body, earth wire peaks, cross arm, and both flange and diagonal (Fig 2.4). The materials of towers are usually wood or steel. Wood is mostly used for low voltage to Medium [11].

The transmission tower is an important accessory and the performance of the transmission line depends very much on the design of the transmission tower. The electric transmission towers or pylons can be classified several ways. The most obvious and visible tower types are

- Lattice structure
- Tubular pole structure
- Guyed V tower

Lattice structure

Traditionally self-supporting lattice structures are used for electric transmission line towers (Fig - 2.4). The use of self-supporting type lattice structures for transmission lines in highest voltage transmission is common everywhere. The advantage of lattice structures is can be erected easily in very inaccessible locations and different terrain topologies as the tower members can be easily transported. Lattice structures are light and cost effective. The main disadvantage of lattice

structure is that it requires more ROW (Right Of Way). Right Of Way is the stretch of land acquired along the route length of line keeping the towers in the middle of ROW width.

The ROW width is most of the time standardize according to the standard set by responsible authorities or government agency. As the voltage label of high voltage transmission increases, the ROW also increases.

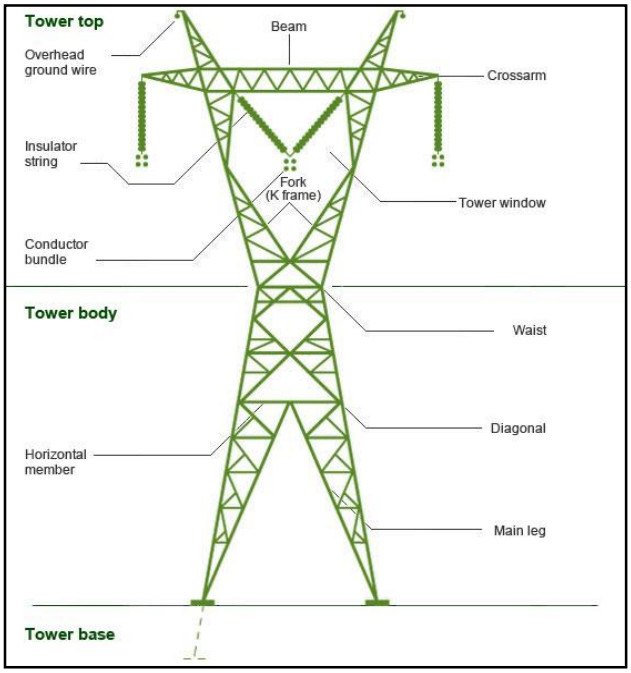

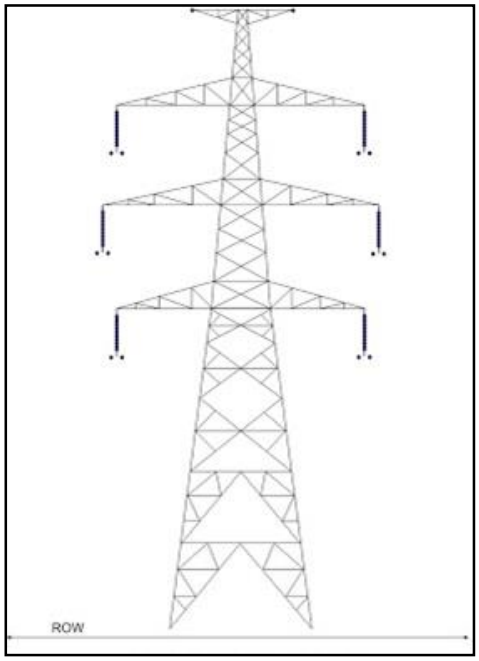

Figure 2:4 Lattice tower (single circuit) [12] Figure 2:5 Double circuit lattice tower [12]

Guyed-V transmission towers

The lattice guyed-V transmission towers has also been used by the transmission companies in cases where more space is available. These are simple, easy and cheaper to install. The guyed towers also require less time for installation. The main disadvantage is that these towers require more space due to presence of guy wires. See the sketch of the tower (fig: 2.6). This tower uses two string insulators per phase arranged in V form.

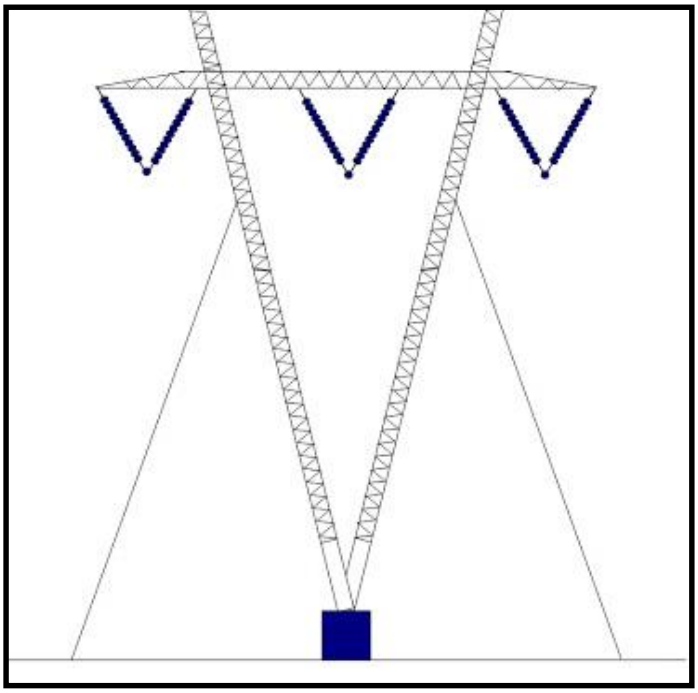

Figure 2:6 Guyed V-tower with double insulator strings per phase conductor [12]

Tubular pole structure

In urban and populated areas and due to public resentment the use of lattice structures has been restricted. So alternative transmission structures are adopted. Steel tubular pole structures have been used quite successfully by some power companies for high and extra high tension transmission lines. The installation of these structures are costly but requires less time. See the sketch of a tubular steel pole structure (Fig-2.7). The tubular structure can be a single tubular form or H-form. Like Lattice tower it can also be designed for carrying two or more circuits.

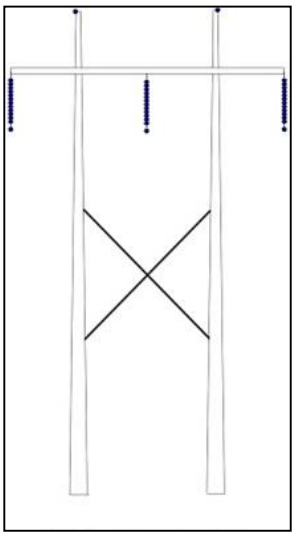

Figure 2:7 Tubular steel H frame tower single circuit [12]

b. Foundation

The purpose of tower foundation is to transmit to ground the mechanical loads that are due to the tower and conductor so that the loads do not cause any settlement or movement which would affect the stability of the tower [10]. The loads are the resultant of the dead weight of the tower and the wind forces that act up on the tower and the conductor. These forces result in uplift and compression forces which is transmitted to the lower legs to the foundation. Therefore, it is important that the foundation is designed correctly to resist these forces in order to ensure the stability of the tower [13]

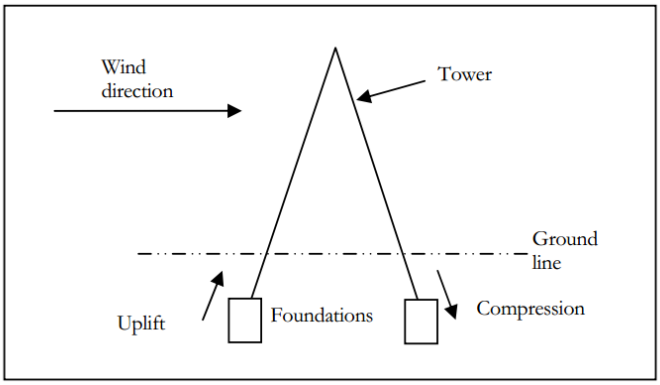

Figure 2:8 uplift and compression forces on tower foundations [13]

Tower foundation design needs to consider the properties of the soil on which the tower is standing. These are determined by conducting soil investigation which are performed in site and

the soil properties are analyzed in the laboratory. The soil property classification is based on measurement of grain size, density, shear-length, compressibility, chemical composition and moisture content [14]

There are basically four types of tower foundation:

Steel grillage: This type of foundation basically usually used on the upper layers of the soil have relatively low bearing capacities. It serves to evenly distribute the load in order to avoid bearing capacity failure and to ensure any ground settlement is evenly catered for. Steel reinforcement bars are built into the concrete cast to increase its strength. It is also commonly referred to as the 'pad and chimney' foundation due to the shape of its design. Fig 2.9 shows a typical steel grillage foundation.

Format other similarly.

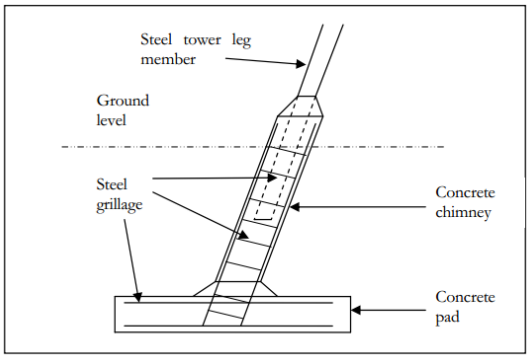

Figure 2:9 Typical construction of transmission tower steel grillage foundation. [13]

- **Pile foundation**

This type of foundation is necessary for very poor soils. It transmits the load to the lower ground layers which are more stable. Several piles may be required for each tower foundation depending on the load capacity of the piles. A few types piles are normally used which include steel sections, precast concrete section and steel screw anchor [14].

- **Strip footing**

These are used in good denser soils with high bearings capacity so that the weight of the structure is transferred adequately to the ground. Its construction is similar to the steel grillage foundation but with a much smaller pad [14]

- **Anchor foundation**

In areas where there is very hard and rocky ground, it may not be economically feasible to excavate and construct concrete foundation. Instead, the stability the rock ground is used as a base for the tower leg. This is done by grouting the steel reinforcement bars into predrilled holes is the rock, figure 2-15 shows typical tower anchor foundation

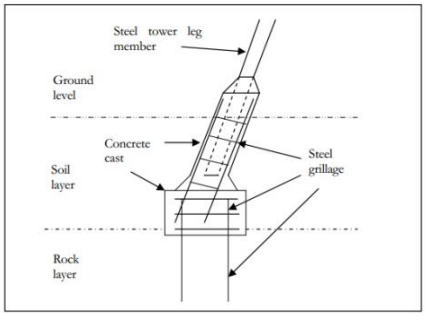

Figure 2:10 typical construction of transmission tower rock anchor foundation [13]

Conductors and grounding wires

The materials which are used as conductors for overhead transmission lines should have the following electrical and physical properties.

- It should have a high conductivity
- It should have sufficient tensile strength.
- It should have a high melting point and thermal stability.
- It should be flexible to permit us to handle easily and to transport to the site easily.
- It should be corrosion resistance

In a power system, high voltage transmission line conductor is one of essential component. It is intended to carry rated current up to their design temperature up to the thermal limit. To successfully maintain the purpose, conductors must able to maintain the sag throughout the lines so that the clearance from the ground can be within the limits of standard.

Currently two main conductors' types that are currently used by high voltage transmission utilities. ACSR conductor (Aluminum conductor Steel reinforced) and AAAC (All Aluminum Alloy conductor).

Figure 2:11: ACSR conductor (Aluminum conductor Steel reinforced)

ACSR conductor (Aluminum conductor Steel reinforced): this conductor type gets its name from its construction which is galvanized steel strands surrounded by aluminum steel strands. A layer of grease is normally applied on the steel strands to provide extra corrosion protection. Fig 2.12 shows typical ACSR stranding arrangement.

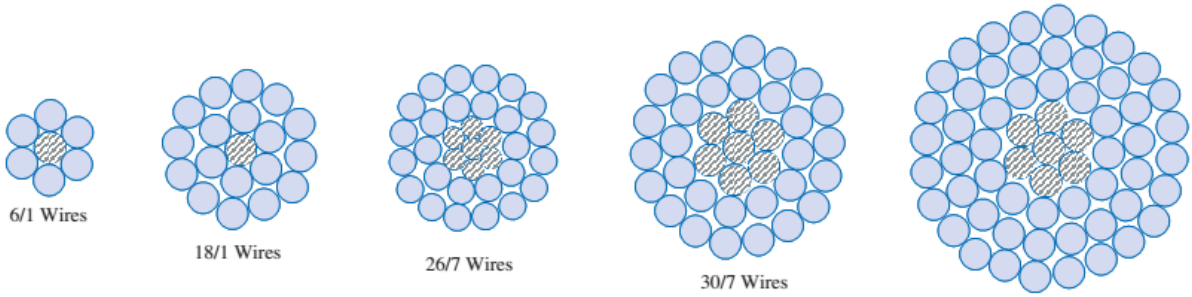

Figure 2:12 ACSR conductor stranding arrangement [15]

AAAC (All Aluminum Alloy conductor): this type of conductor is made up of strands of alloys. These alloys often containing silicon and/or magnesium, which intended to provide high breaking strength and good electrical conductivity.

Figure 2:13 All Aluminum Alloy conductor

Insulators: In a power system network High-voltage insulators have a major contribution for the operational safety and operating efficiency of transmission systems of electrical power, and it is therefore Insulators must meet particularly high demands in terms of reliability and insulators are used to separate line conductors from each other and from supporting structure electrically.

There are different types of insulators exist among them long rod insulators made of porcelain and cap and pin insulators made of glass or porcelain. Currently composite insulators have gained great importance in recent years in the field of insulation technology for medium and high-voltage overhead transmission lines and substations. [16]

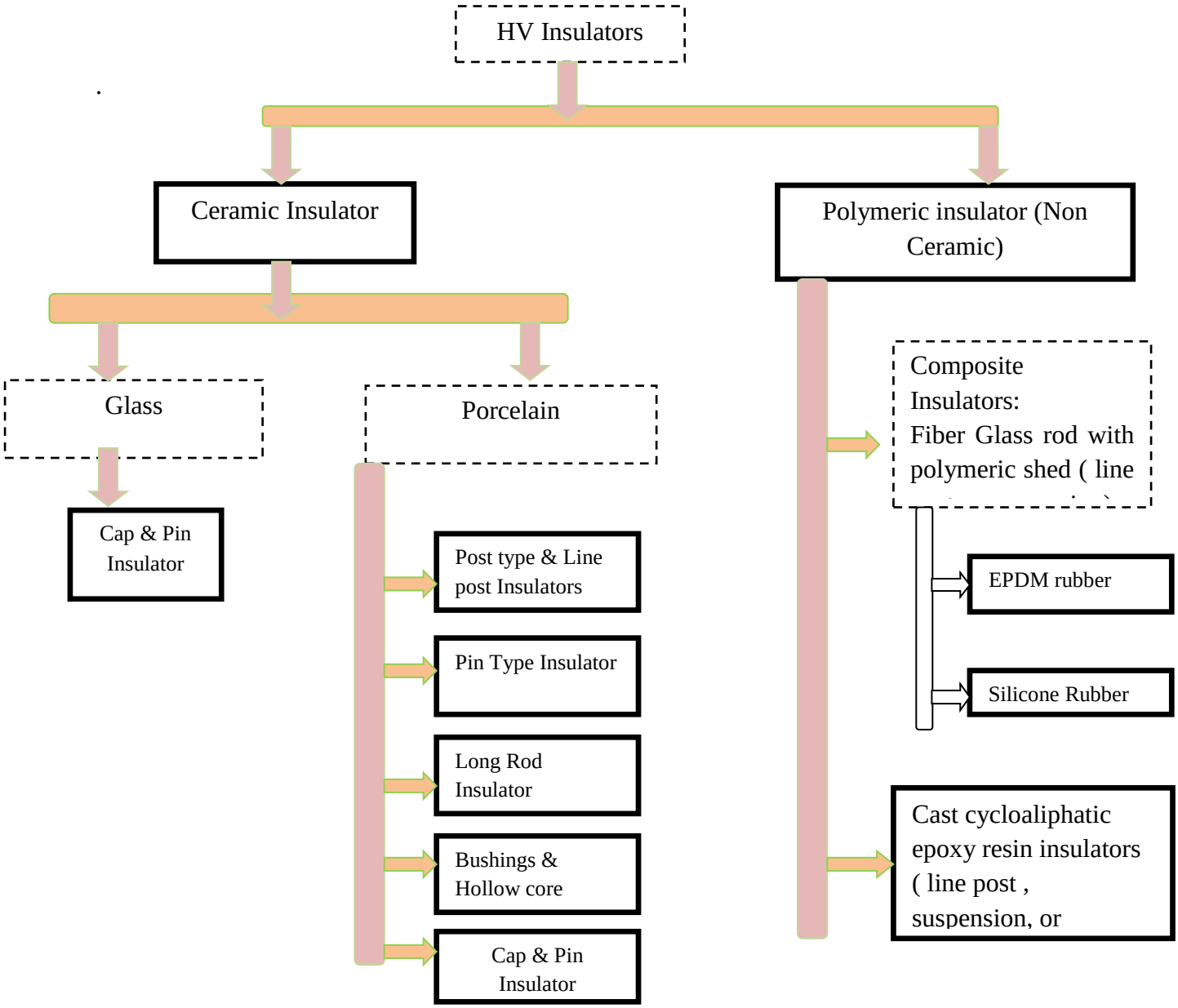

Figure 2:14 Types of insulators

Both HVAC or HVDC insulators are of key importance for the operational safety and operating efficiency of transmission systems of electrical power. In addition to both long rod insulators of conventional design made of porcelain and cap and pin insulators made of glass or porcelain, as were previously used as standard, composite insulators have gained great importance in recent years in the field of insulation technology for medium and high-voltage overhead transmission lines and substations. [16]

Currently composite insulators have convincing qualities and efficiency when designed appropriately, both in terms of construction and in terms of material selection. From previous design perspective it is not possible to optimize mechanical and electrical performance separately in conventional insulators (porcelain or glass), these properties can be considered individually when selecting materials for composite insulators. The physical structure of composite insulator can be divided into three parts

1. Rod section
2. shed-like housing
3. Metal fittings

During design thee Rod of high mechanical strength choosen for taking up the external loads.The shed-like housing surrounding the rod, designed to provide creepagedistance and electrical insulation and the Metal fittings are there at either end of the rod for transmission of the mechanical loads.

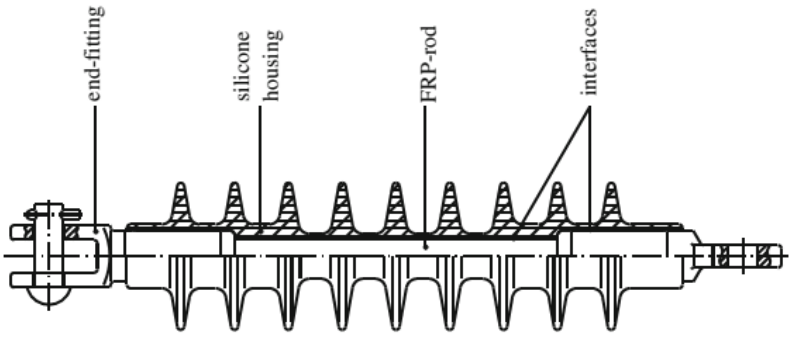

Figure 2:15 component of Composite insulators. [15]

Nowadays composite insulator is taking dominance on high voltage transmission utilities for is its low weight, which has a positive feedback for designing lighter towers. During high-voltage

lines, the weight of conventional insulators may account for almost 20 % of the entire vertical load on a tower. By contrast, composite insulators allow a weight saving of up to more than 90 % compared to conventional insulators [15]. The sensitivity of the composite structure to impact loads caused by power arc, dynamic mechanical forces is much lower than that of a conventional insulator.

2.3. HVDC transmission

The development of HVDC transmission system dates back to the 1930s when mercury arc rectifiers were invented. In 1941, the first HVDC transmission system contract for a commercial HVDC system was placed: 60 MW were to be supplied to the city of Berlin through an underground cable of 115 km in length. In 1945, this system was ready for operation. However, due to the end of World War II, the system was dismantled and never became operational. It was only in 1954 that the first HVDC (10 MW) transmission system was commissioned in Gotland. Since the 1960s, HVDC transmission system is now a mature technology and has played a vital part in both long distance transmission and in the interconnection of systems [10].

In a power system technology, the original motivation for the emergence of DC technology was transmission system efficiency, many scholars confirm that the power loss of a DC line is lower than that of a corresponding AC line of the same power rating. However, this required the use of HVDC transmission line and development of converter station both at receiving and sending end side.

The invention of the high-voltage mercury valves half a century ago paved the way for the development of HVDC transmission. By 1954, the first commercial DC link came successfully into operation and was soon followed by several other schemes orders of magnitude larger. The success of the new technology immediately triggered research and development into an alternative solid-state valve, which by the mid-1960s had already displaced the use of mercury arc valves in new schemes. The early history and technical development of the HVDC technology are described in [8].

Substantial progress made in the ratings and reliability of thyristor valves has increased the competitiveness of HVDC schemes. DC transmission has lower transmission losses and cost than equivalent AC lines, but requires terminal equipment which adds to the cost and power

losses. Thus traditionally, the DC option has been found economically viable only when the distance involved is long and the amount of energy to be transferred is large.

As it was explained in Section 2.3 on HVAC system, the active power transmission is essentially dependent on the angle δ. However, to maintain static stability the angle δ in a transmission line should typically below or equal to 30^o

Referring equation 2.7, the reactive power is only slightly influenced by the angle δ, but it is greatly dependent on the voltages. However, since these voltages are related to the reactive power balance on both sides, the major part of the reactive power requirement of the transmission link is taken from that network side, which has better reserves of reactive power. Thus, the a.c. system has an automatic compensation mechanism in this respect as well.

HVDC transmission systems, when installed, often form the backbone of an electric power system. They combine high reliability with a long useful life. Their core component is the power converter, which serves as the interface to the AC transmission system. The conversion from AC to DC, and vice versa, is achieved by controllable electronic switches (valves) in a3-phase bridge configuration. The following figure shows application examples of HVDC transmission systems. [47]

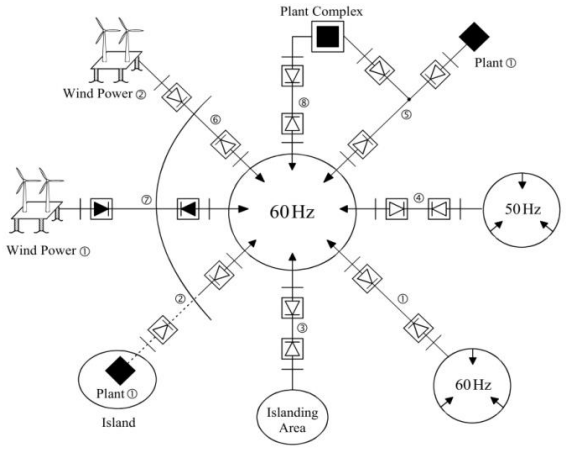

Figure 2:16 Application of HVDC transmission system [19]

As we can see from Fig 2.16, HVDC transmission link application can be explained below

1. Bulk power transmission through overhead lines for long distances
2. Bulk power transmission through submarine cable

3. Fast and precise control of the flow of energy over an HVDC link
4. To link systems with different frequencies using an Asynchronous Back-to-Back.
5. Multi terminal DC link.
6. To link renewable energy sources, such as wind power, when it is located far away from the consumer.

The basic circuit diagram of an equivalent DC transmission link is shown in Fig 2.17 [17]. The indices 1 and 2 indicate the sending and receiving ends respectively. The voltages sV_{il} and sV_{i2} represents the number of series are ideal in that they do not contain the resistive voltage drops of the two terminal stations,

$$V_{i1} = V_{i01}\cos\alpha - d_{x1}\frac{I}{I_m}V_{iom1}$$
$$V_{i2} = V_{i02}\cos\gamma - d_{x2}\frac{I}{I_m}V_{iom2} \qquad (2.10)$$

where γ *extinction angle*

α *commutaion angle*

$d_x \frac{V_{iom}}{I_m}$ *Internal resistance*

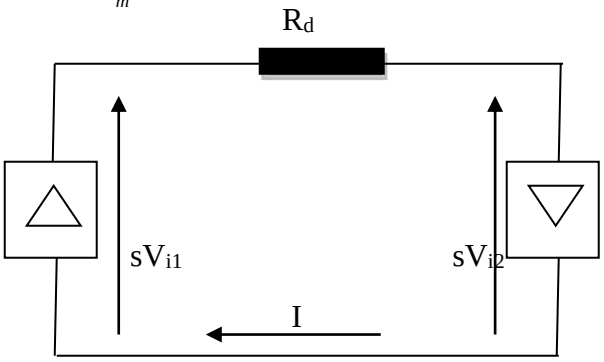

Figure 2:17 Basic circuit of d.c. transmission.

Extinction angle (y): the extinction angle is the angle between the end of commutation and the next intersection of the two alternating voltages. The angle is used to control the voltage level as well as blocking ability of the valve.

Commutation angle: The commutation angle is also called firing angle, defined from the crossover point of phase voltages, which is the earliest point when a thyristor can assume

conduction. If the commutation operates $90^o < \delta < 180^o$, the converter operates in the inverting mode whereas if δ operates below 90^o the converter is on rectifier mode.

:

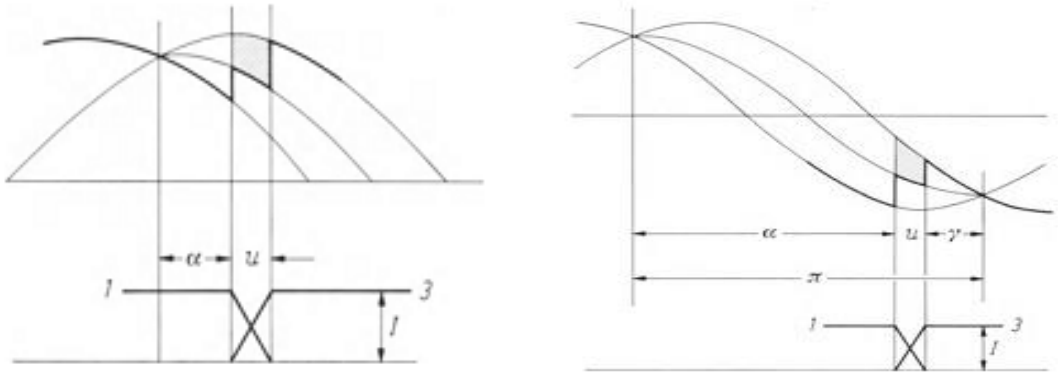

(a) (b)

Figure 2:18 Convertor operation (a) Rectifier mode (b) Inverter mode.

The ohmic resistances in the converters can be placed on the DC side making use of the approximation. For this reason, R_d is the total ohmic resistance encountered by the direct current on its path from the source voltage of the converter on one side to the source voltage of the converter on the other side in a commutation-free condition.

$$\frac{I}{I_m} = \frac{sV_{i1} - sV_{i2}}{I_m R_d} = \frac{sV_{io1}\cos\alpha - sV_{io1}\cos\gamma}{I_m R_d} \qquad (2.11\ a)$$

If we use $\underline{s_m}$ to represent the number of series-connected six-pulse groups, which are in service on both sides in normal operation, and take V_{im} to represent the nominal voltage of an inverter group and p_m, the nominal power on the inverter side, we obtain

$$\frac{p_2}{p_m} = \frac{S_2}{S_m} \cdot \frac{V_{i2}}{V_{im}} \cdot \frac{sV_{i1} - sV_{i2}}{I_m R_d} \qquad (2.11\ b)$$

Compared with HVAC equation the load angle δ has disappeared, and would indeed be a quite pointless concept, since the two AC networks interconnected by the DC link need not even have the same frequency [17]. However, the loss of the load angle δ also leads to the loss of the advantage of automatic power adaptation.

Moreover, Eqn 2.5 and Eqn 2.11 differ basically in structure. Instead of the voltage product we now have their difference so that the power equation of the DC system resembles the reactive power equation of the AC system. Furthermore, since R_d is far smaller than X in eqn 2.11, the voltage dependence of the DC power (p) is many times greater than that of the reactive power in an AC system.

HVDC Transmission Line Systems

In a power system, HVDC transmission basically refers to the generated AC power from a power plant is converted to DC power before its transmission. At the receiving end there is an inverter which facilitate the inversion to its original AC power and then distributed to domestic commercial or industrial customers. Such power transmission method makes it possible to transmit electric power in an economic way through up-conversion of voltage, which is an advantage in existing AC transmission technology and to overcome many disadvantages associated with AC power transmission as well.

Considering application, geographical location and technology HVDC transmission system categorized in to two main topologies. Two-terminal and multi terminal HVDC transmission systems are common.

In two terminal configurations, there are only two HVDC converter stations, HVDC rectifier at sending end and HVDC inverter at receiving end. Most of Electrical and electromechanical component of the rectifier station is almost the same as those of the inverter station, but AC-side filter configuration and reactive-power compensation method are different. The main difference is, extra Shunt reactors may be used on inverter side to provide inductive compensation for AC harmonic filters, especially under light-load conditions [19] on rectifier side extra shunt capacitor is installed for reactive power compensation. Multi terminal configuration is used when generation location is remote need to be connected across different geographically isolated regions or different areas within one country. [19]

HVDC system requires an electronic converter for its ability of converting electrical energy from ac-dc or vice versa. Currently there are two basic configuration types of three-phase converters are used on HVDC system, Current source converters (CSC) and voltage source converters (VSC).

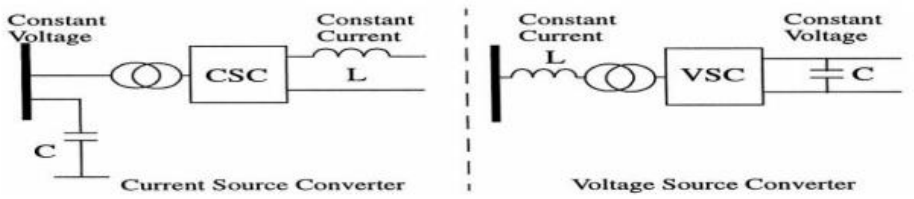

Figure 2:19 Converter configuration

HVDC with current Source Converter

The thyristor, or silicon-controlled rectifier (SCR), has been the only solid-state switch used in the process of HVDC conversion, prior to the availability of high-power turn-off switching devices. The thyristor converter is still the most cost-effective solution for large-power and long-distance power transmission.

SCR-based conversion provides active power controllability (i.e. rectification and inversion) at the expense of large and varying demand of reactive power. Both the rectification and inversion processes consume reactive power, because the commutation is performed by the voltage source and the leakage reactance of the converter transformer generally dominates the commutation circuit. Therefore, the fundamental component of the current always lags that of the voltage.

Moreover, for inverter operation, as the commutation overlap is not known at the instant of firing, an extinction angle of the order of 15 must be allowed to prevent commutation failure and this increases further the consumption of reactive power, which will be of the order of between 50 and 60 % of the active power in normal operation [21]. As the reactive power consumption varies with load, the filters and extra capacitors must be switched by means of circuit breakers to match the converter reactive power requirement. If the commutation circuit inductance is compensated by means of series capacitance, unity power factor is possible; this is the purpose of the so-called CCC (Capacitor-Commutated Converter or Conversion.

Despite their limited controllability, static line commutated conversion (LCC) of high reliability are now used extensively in the power transmission field, either as long-distance interconnections or back-to-back asynchronous links. The conventional thyristor-based LCC technology is at present superior to self-commutating VSC transmission in terms of capital cost, power losses and reliability for large-scale HVDC transmission [21]

HVDC with Voltage Source Converter

The voltage source converter HVDC system is a fast developing technology, which uses insulated gate bipolar transistor (IGBT) switches and pulse width modulation (PWM). The basic module of the voltage source converter is the three phase bridge built with Integrated Gate Bipolar Transistors, shunted by diodes in the reverse direction. Fig 2.20 shows basic circuit diagram of a transmission system with voltage source converters.

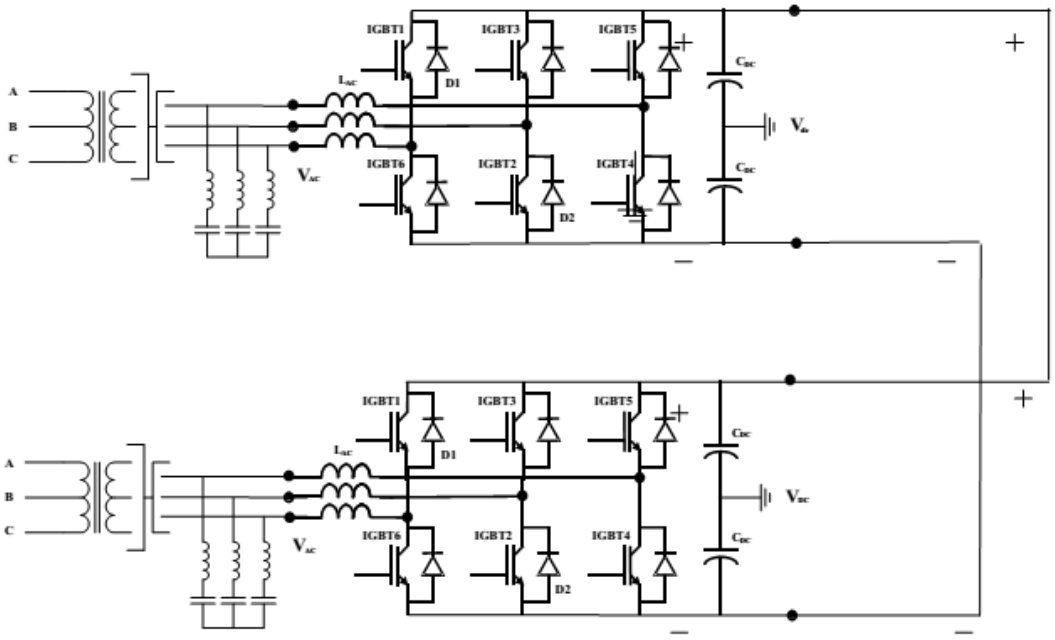

Figure 2:20Voltage source converter [23]

The HVAC systems supplying the converters do not need to have high short circuit capacity or at the receiving end do not need to have its own generation. VSC has a black start capacity and can supply an island without generation [23]. A black start is the process of restoring a power station to operation without relying on the external electric power transmission network. Typically, a standard transformer and a series converter reactor (inductance) connect the converter to the network. Because of the PWM system only small AC filter is needed. At the DC side, two capacitors connected in series serves as a filter. The midpoint of the capacitors is grounded. If the system operates as a floating system, the converter is not actually grounded to another circuit or ground.

The converters can operate automatically without communication between the stations. The system can regulate both the amplitude and phase angle of the AC voltage. This means the independent regulation of the active and reactive power. The direction of power transfer depends on the voltage. The current flows from the converter operating at a higher voltage than the other. The reversal of the power flow requires the reversal of current direction and not the reversal on the voltage. The system is suitable for multi-terminal operation.

HVDC converter configuration

Most of the HVDC power converters with thyristor valves are assembled in a converter bridge using a 12-pulse configuration. The 12-pulse converter consists of two 6-pulse valve bridges connected in series on the DC side, and are supplied by converter transformers with the AC-side windings in parallel. Both bridges are operated at the same control angle. As shown in Figure 2.21, one 6-pulse bridge is fed by Y-connected valve side windings and the other by Delta connected valve side windings.

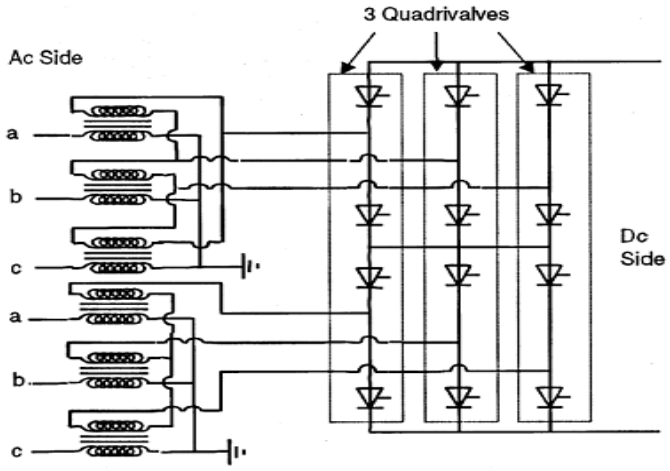

Figure 2:21 12 pulse configuration [23]

There are in principle four possible configurations for overhead HVDC transmission line systems. Monopolar, bipolar, homopolar and back to back systems are the basic main system configuration of HVDC

Monopole system:

Monopole with Electrode Return

One type of a monopole system with earth electrodes is shown in Figure 2.26 In this system, earth or sea is used as one conductor line and thereby two converter stations must be grounded necessarily. Since considerable direct current flows through earth or sea continuously, it will give rise to transformer magnetism saturation and underground metal-objects electrochemistry corrosion. The advantage of the system is it decreases the HVDC line cost but lack of reliability and flexibility of the of the system can be considered as drawback.

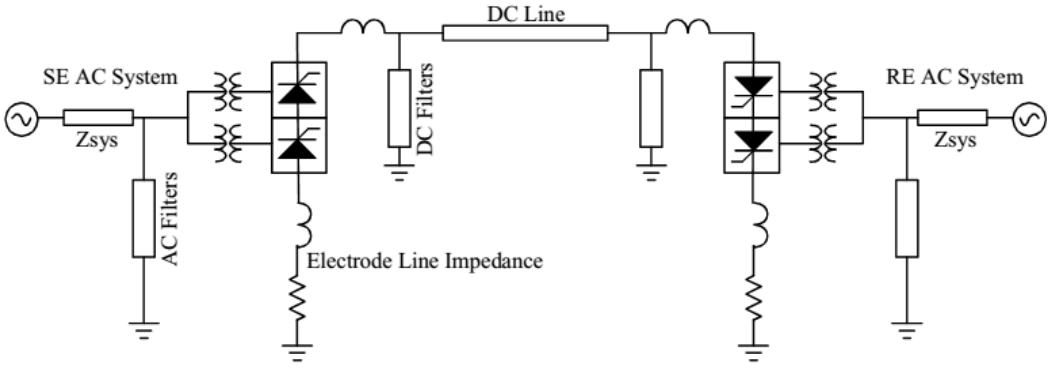

Figure 2:22 Monopole HVDC with Earth Return [23]

Monopole with a Dedicated Metallic Return

This type of system avoids the concerns raised due to permanent earth electrode current. In this case, a second conductor of the same current rating of the main conductor but at much lower dc voltage is needed as shown in Figure 2.23 The DC-line investment and operational cost of monopolar link with metallic return are higher than those of monopolar link with ground return, due to no direct current flowing through earth during operations, transformer magnetism saturation and electrochemistry corrosion can be avoided.

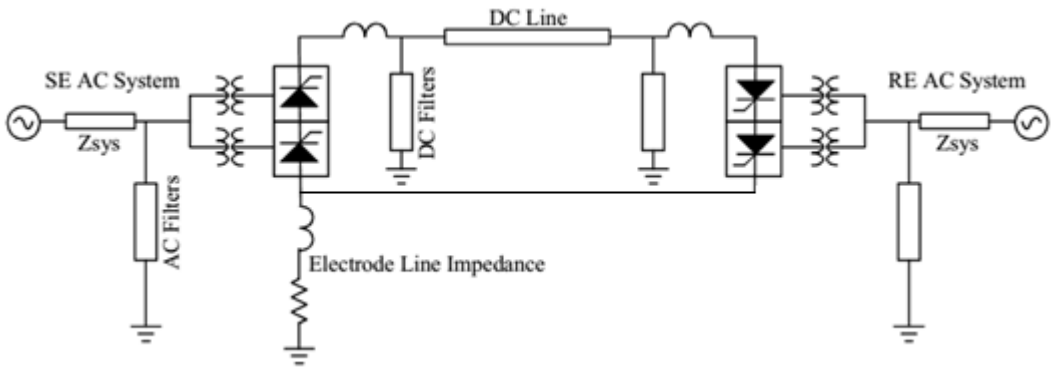

Figure 2:23Monopole with a Dedicated Metallic Return [23]

Bipolar system

In bipolar configuration, it consists of two poles, one positive polarity and the other negative polarity, and with their neutral points grounded. This configuration is used, if the required transmission capacity exceeds that of a single pole. In steady state operation, the current flowing in each pole is the same and hence no current flows in the grounded return. The two poles may be operated separately. It is also used if requirement to higher energy availability or lower load rejection power makes it necessary to split the capacity on two poles. If either pole malfunctions, then the other pole can transmit power by itself with ground return. In a bipole the amount of power transmission is increased by a factor of two compared to the monopolar case. This creates fewer harmonics in normal operation as compared to the monopolar case. Reverse power flow can be controlled by converting the polarities of the two poles.

During maintenance or outages of one pole, it is still possible to transmit part of the power. More than 50 % of the transmission capacity can be utilized, limited by the actual overload capacity of the remaining pole. The advantages of a bipolar solution over a solution with two monopoles are reduced cost due to one common or no return path and lower losses.

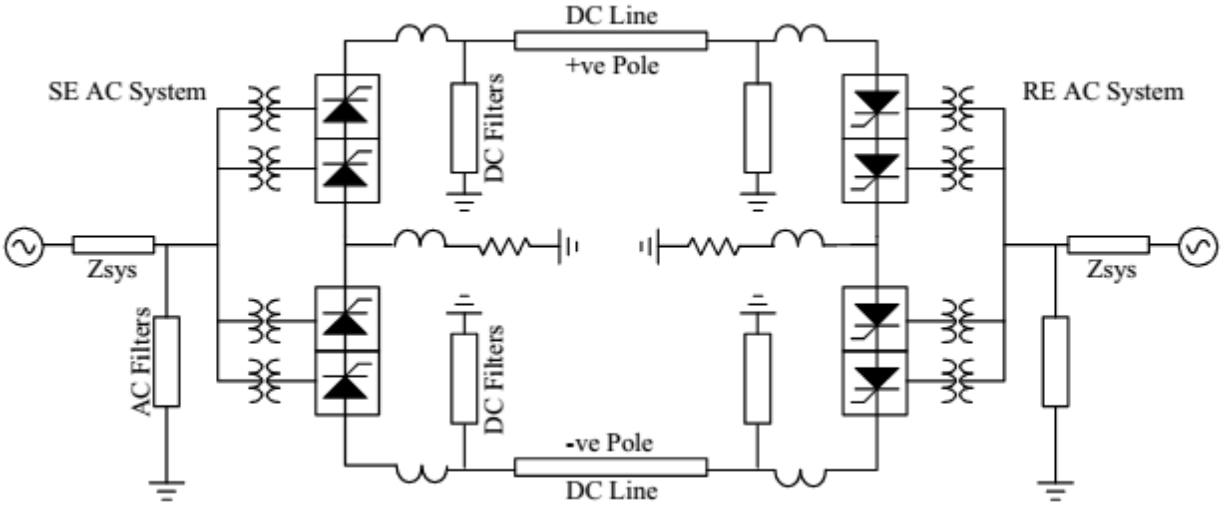

Figure 2:24 Bipolar system [23]

Hompolar link

The other HVDC transmission system is homopolar link, the system has two or more conductors including ground return, the main poles are with the same polarity either positive pole or negative pole. Technically a negative polarity is preferred from positive pole due to environment effect. For negative pole many of the electrons are concentrated in a region of lower potential-gradient due to this effect the radio interference is very small. The ground return is preferred for system which allows continuous ground return.

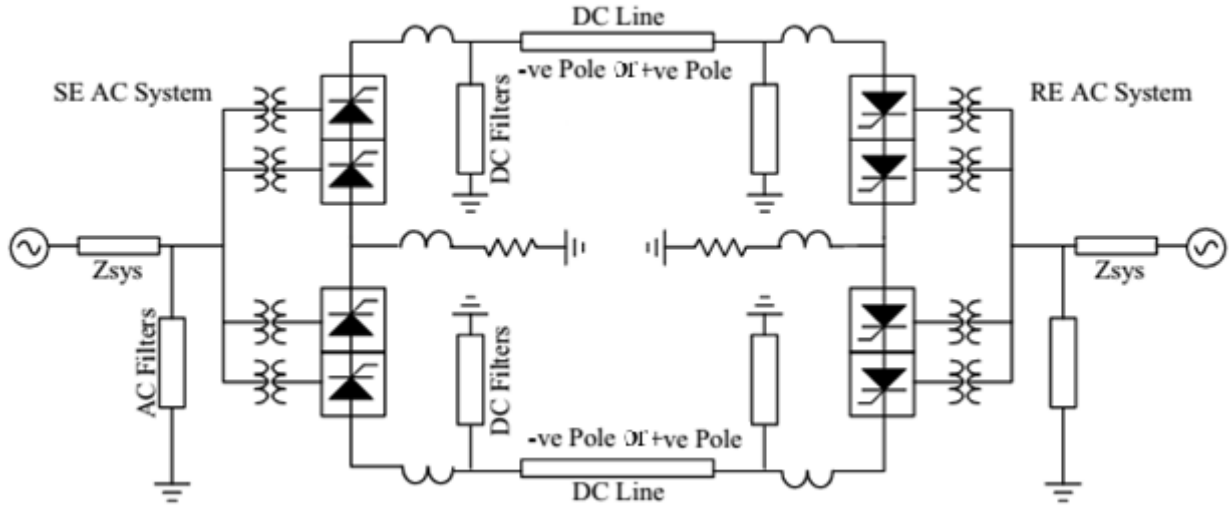

Figure 2:25 Homopolar system [23]

The advantage of Homoploar link is like bipolar link it can be operated at half rated power under faulty condition and also lower corona loss and radio interference at ground level due to negative poles.

Back -to –Back system

As the name indicates, Back-to-back systems are that have rectifier and inverter are located in the same station. Back-to-back systems are mainly used for power transmission between adjacent AC grids which cannot be synchronized. For this type of system, the amplitude of DC voltage is generally small, around150 kV to optimize the valve and installation cost.

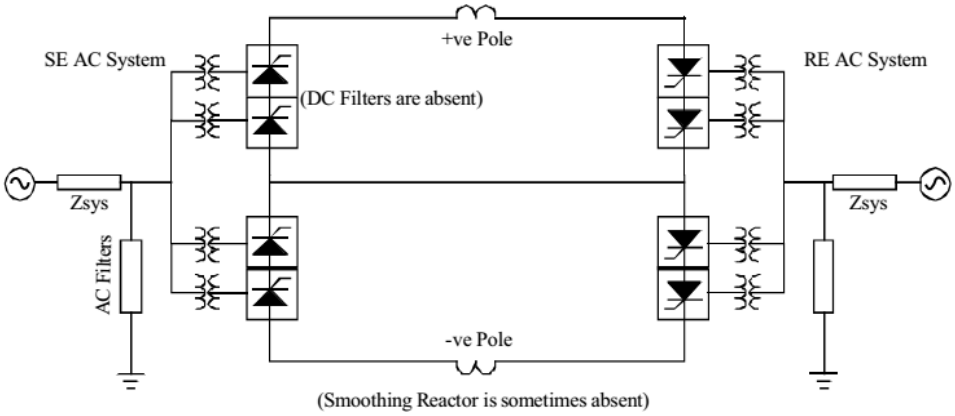

Figure 2:26 Back-to-back system [23]

Multi Terminal system

A multi-terminal HVDC transmission system is one of HVDC configuration able to connect two or more AC systems or to separate an entire AC system into different isolated subsystems. It is possible to connect multi-terminal HVDC transmission system, converter stations in series or in parallel.

In the series-connected HVDC scheme, the regulation and distribution of active power among converter stations mainly depend on the direct-voltage variation that is achieved by regulating the converter firing-angle or transformer tap-changer.

In the parallel-connected HVDC scheme, the regulation and distribution of active power among converter stations mainly depend on the direct-current variation that is achieved by regulating the converter firing angle or transformer tap-changer [18].

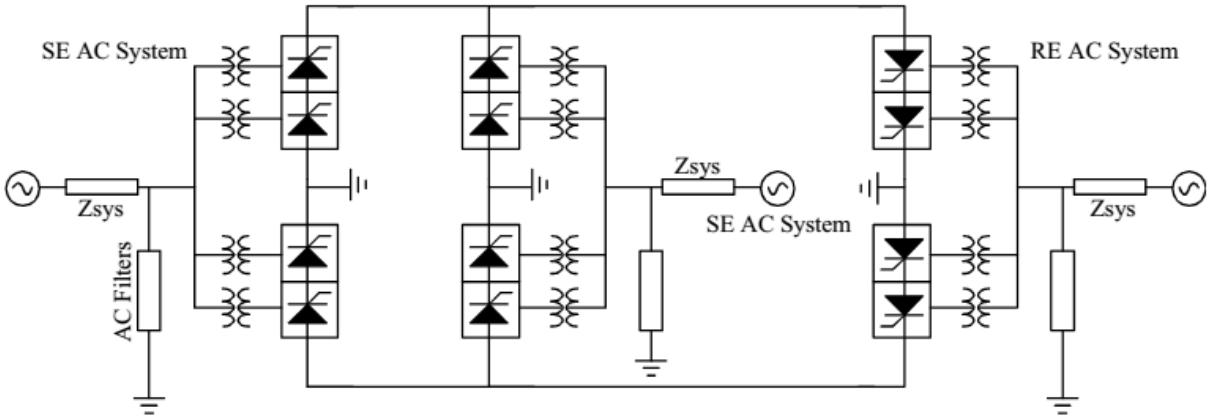

Figure 2:27 Multi terminal system [63]

HVDC transmission line

On HVDC systems with overhead lines are almost always bipolar systems. Monopolar systems, however, are conceivable as the initial stage of a system which, in the final stages, becomes a bipolar HVDC system, or as an overhead line section of a cable transmission system. Nevertheless, a wide variety of types of HVDC overhead lines have been constructed or at least been planned for high power transmission. In the decision to construct a certain type of HVDC line, both the reliability of the overall system and construction costs play important roles. Consideration of the effects of an overhead line on the environment is also becoming increasingly important

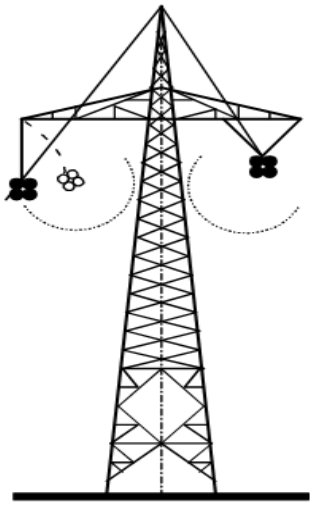

Figure 2:28 Over head bipolar HVDC line [39]

A typical tower structure for bipolar HVDC is shown on figure 2-28 During design taking account on minimum clearance is most important factor. In determining the minimum clearance against the tower structure, the swing width of the insulator strings under maximum wind load must be taken into consideration. This swing width can be reduced, and thus the cross arm can be kept shorter, if the conductor is suspended on V-strings. The required width of the right-of-way can be reduced by [39] means, but the reduced clearance between the conductors has the unfavorable influence of increasing the conductor surface gradient and the effects which are a function of it. HVDC overhead lines are conventionally protected against direct lightning strikes by means of an overhead ground wire over their length. Otherwise a steep-fronted overvoltage surge could enter both converter and inverter stations.

Terrain structure of a solid can cause different footing resistance during construction of towers. If the line runs through a topology with very high specific ground resistance, it may also be necessary under some conditions to connect the tower feet to one another by means of an uninsulated cable laid in the earth. The purpose of this cable is to lower the footing resistance and to prevent back flashovers between the tower and conductor in the event of a lightning strike which hits the tower or the surrounding earth.

2.4. Advantage of HVDC transmission over HVAC transmission

- For a bipolar HVDC overhead line transmission only two conductors with positive and negative polarities are required, as a result the tower structure is simple, low transmission line investment and less power loss.
- In HVDC transmission the capacitance of transmission line is never taken into account. Since capacitive current does not exist, direct voltage maintains the same along the transmission line and the transmission distance for DC cable is unlimited theoretically.
- For the HVAC and HVDC cables with the same insulation thickness and cross section, the transmission capability for HVDC cable is considerably higher than that for AC cable due to the absence of skin effect in HVDC.
- For Bipolar HVDC line, only two conductors are needed whereas for HVAC lines we need three cables, due to three-phase AC transmission. Therefore, the price for HVDC Conductor is substantially lower than the prices for AC cable lines.

- HVDC lines can be used to interconnect asynchronous HVAC systems with different frequency (50 Hz or 60 Hz) therefore, the short-circuit current level for each HVAC system interconnected will be minimized
- For a bipolar HVDC system, earth is usually used as a backup conductor. If either of the pole fails, the bipolar HVDC system can be changed into the monopolar system automatically and improves the reliability of HVDC system.

2.5. Disadvantage HVDC transmission over HVAC transmission

- For HVDC system with the same rating, the investment cost for a converter station is several times higher than the investment for a HVAC substation.
- A converter acts as not only a load or a source, but also a source of harmonic currents and voltages, therefore it will incur power quality problem by distorting current and voltage waveforms.
- Reactive power compensation ~~is~~ must be installed at converter station because in a conventional converter station, the reactive power demand is approximately 60% of the power transmitted at full load.
- With the absence of HVDC current zero crossing point, because of small inductance of HVDC side of the system the rate of rise of DC fault current is considerably high and it demands for very fast interruption technology, which is very expensive. [39]

2.6. Literature review:

Currently, many researchers have been doing various studies to explore the technical and economic feasibilities of hybrid HVAC/HVDC transmission lines but with knowledge of this authors the hybrid system not implemented anywhere in the world.

According to Jan Lundkvist , Igor Gutman and Lars Weimers *with their study entitled "Feasibility study for converting 380 kV AC lines to hybrid AC / DC lines",* existing HVAC parallel transmission line can be converted to hybrid system with several options. One of the proposed methods is without changing the existing arrangement of conductors and insulation ceramic to form bipolar DC line with a metallic-return conductor [3].

M. Kizilcay, A. Agdemir and M. Lösing with their paper entitled "*Interaction of a HVDC System with 400-kV AC Systems on the Same Tower"* presented a paper on HVDC/AC power transmission system interactions for the hybrid tower configuration. They have concluded that The AC and DC lines on the same tower can be effectively used to increase the power transmission capacity of an existing transmission corridor [2].

H.L. Nakra, Ly X. Bui and Isao Iyoda have done a study on "*system considerations in converting one circuit of a double circuit AC line to DC".* The paper presents the results of a study of the possible interaction between the AC and DC lines placed on the same tower and they have concluded that converting to HVAC to hybrid HVAC/HVDC model is feasible [40].

POVH, D. RETZMANN, E. TELTSCH U. KERIN, R. MIHALIC [4], in their paper entitled "*Advantages of Large AC/DC System Interconnections* developed a model of an interconnected system of existing and future systems. With this benchmark model, the application of HVDC, integrated into the AC system, has been studied

CHAPTER THREE

Modeling and Design of Hybrid HVAC/HVDC System

3.1 Modeling Hybrid HVAC/HVDC system

In the previous chapter, Introduction and literature review of power system component for Alternating current and Direct current were discussed. This chapter mainly deals with modeling and designing of hybrid HVDC/HVAC transmission system. The 400KV HVAC double circuit transmission line from Gilgel GibeIII to Akaki substation has been constructed with a total distance of 402 km. In this chapter, hybrid HVA/HVDC model will be discussed

3.1.1 Converter station model

On recent HVDC technology VSC transmission is limited to the power rating about 300 MW, due to the voltage limitations in the presently used PWM technology. Currently the maximum voltage capacity in operation found in the Caprivi Link, Namibia Interconnector, rated 300 MW at 350 kV[41]. LCC system despite their limited controllability, static LCCs of high reliability are now used extensively in the power transmission field. LCC system is superior to self-commutating VSC transmission in terms of capital cost, power losses and reliability for large-scale HVDC transmission. The main disadvantage of LCC converter is, it operates with lagging power factor consuming a reactive power of 40-50% of active power. For our study we have selected 3000 MVA LCC system.

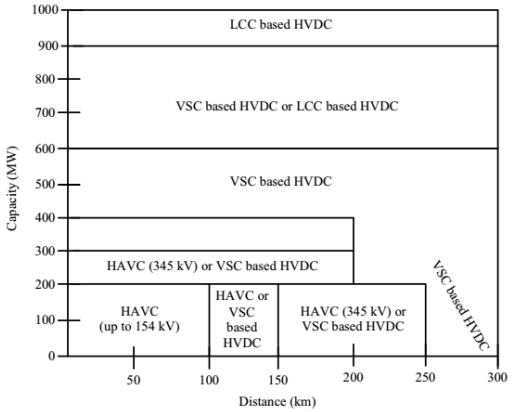

Figure 3:1 Converter model selection with respect to distance [19]

The converters can be installed at the GIBEE III switch yard and Akaki substation in Addis Ababa. Gibe III switch yard is located at the toe of river basin with the altitude of 1010 meter, with double 400KV bus bar. Both inverter and rectifiers are modeled with 12 – pulse circuit. This can be done by connecting in series two 6 pulse converter bridges with two 400KV three phase sources from bus bar which are spaced apart from each other by 30 electrical degrees. The phase difference effected to cancel out the 6-pulse harmonics on the AC and DC side.

There are two valve groups, each valve group is composed of two serially connected 6-pulse bridges that are supplied from two converter transformers. The transformers adopt Y/Y and Y/D connections providing the 3 phase shift necessary for12-pulse operation.

Two sets of harmonic filters are used at each end of the HVDC line. They consist of the 11^{th} and 13th harmonics filters and a high-pass filters. The harmonic filters must be designed for full bipolar power operation that includes continuous and short-time overload factors. A high-pass DC filter that is tuned to the 12th harmonic is also installed on the DC side. A current limiting resistors are used for the converter breakers installed in both of the stations (Gibe III switch yard and Akaki II substation) in order to limit inrush current and over-voltage occurring during energization of converter transformers.

Converter stations are equipped with different kinds of reactors.

- DC smoothing reactors are connected in series with outgoing HVDC poles of a transmission line which intended to reduce the harmonics on the DC side, to reduce the current rise caused by failures in the DC system and to improve the dynamic stability in the HVDC system.
- AC harmonic filters also used on the AC side. To reduce high frequency propagation and radio interferences, tuned filters are used. During light load operation to keep system voltage stable
- Double tuned AC filter is used to filter voltage and current harmonics at both the AC and DC sides. Such harmonics overheat the generator and disturb the communication system.
- Shunt capacitors are used as the reactive power sources such to provide the reactive power necessary for power conversion

- Shunt reactors can be used as a part of converter station to provide inductive compensation for AC harmonic filters, especially under light-load conditions

Other control and protection equipments are also used on both converter stations but this thesis does not go detail component design of converters as the scope is limited on technical feasibility of hybrid AC/DC transmission line. The single line diagram of 12-pulse converter station looks like as Fig 3.2.

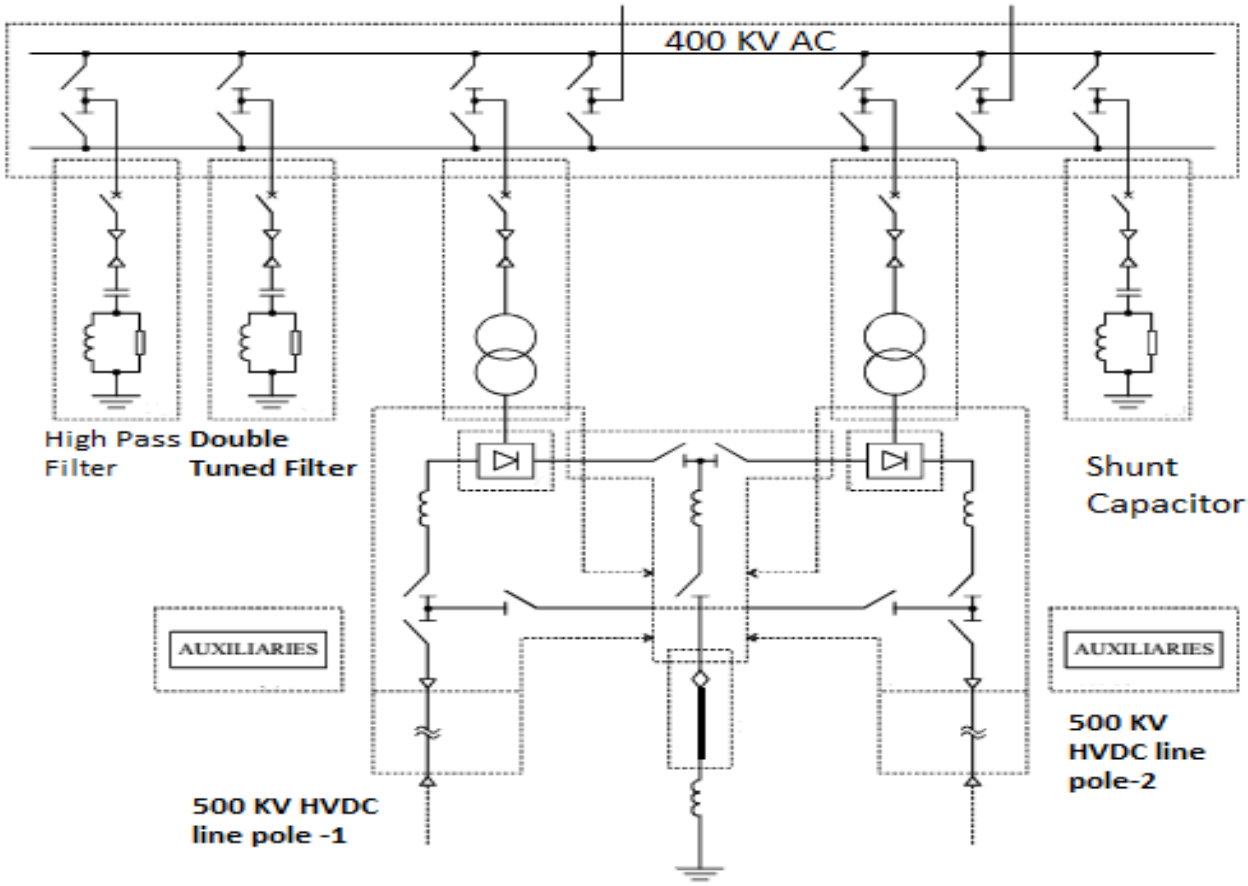

Figure 3:2 12-pulse converter station

3.1.2 Transmission Tower Re-configuration

When the contractor undertakes the 400kV double circuit tower the client, EEP demanded the design and installation be undertaken in compatible with international standard so that the system can sustain the adverse weather condition for long time. During the design of the transmission lines for Gibee III to Addis Ababa, the following climate condition has been considered. The average annual rain fall is of the region is over 100~400 mm for a month, which assure between July and September. The rest of the year is generally dry with occasional rains. The highest temperatures occur between December and February, lowest between June and August. The maximum temperature is 40 ^{0}c where the minimum is -5 ^{0}c. The mean annual humidity is between 60 - 90%. For design purpose, the wind load on the structure can be taken as 86 kg/m², on conductors & OPGW wire be 52 kg/m² and for single insulator rod, the wind load be 60 kg/m² . For design purpose a solar radiation value of 1.100 W/m² be considered.

Four types of towers have been used with respect to the basic-, wind-and weight-spans. All towers are designed to carry line conductors with the associated insulator sets, overhead optical fiber core and galvanized steel shield wires and all fittings under the conditions and within the factors of safety specified

Table 3-1 400 KV lattice tower types

400 kV Ruling Span: 400 m	Suspension Tower Types DS	Tension Tower Types DA	Tension Tower Types DT
Angle of deviation (deg.)	0º-2º	0º-30º	30º-60º
Max. sum of adjacent spans (m)	1000 (0º) 800 (2º)	1600 (20º) 800 (30º)	1200 (45º) 800 (60º)
Maximum span (m)	700	800	700
Maximum wind span (m)	500 (0º) 400 (2º)	800 (20º) 400 (30º)	600 (45º) 400 (60º)
Maximum weight span (m)	1000	1400	1000
Uplift weight span (m)		- 500	- 300

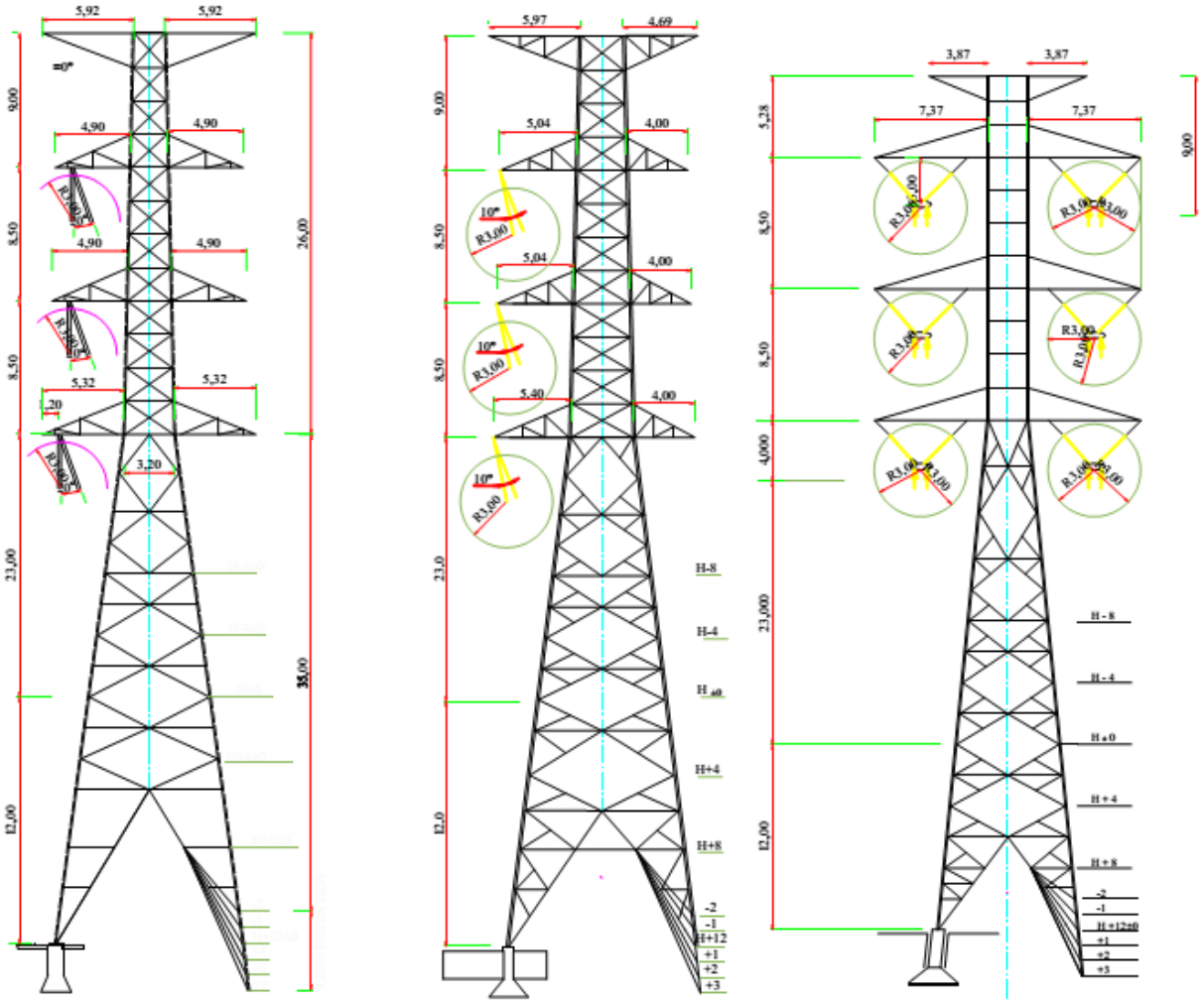

Figure 3:3 Gibe III – Akaki 400 KV transmission tower [EEP]

3.1.3 Conductor Re-arrangement

HVDC bipole transmission lines contain two separate pole conductors. Each pole conductor designed to use a bundle of three sub-conductors. Under normal operating circumstances, the positive pole is energized at +500 kV and the negative pole at -500 kV. When the fault occurs on one conductor, or a partial outage of the converter facilities, the line may be operated in monopolar mode, with one conductor energized at up to +/-500 kV and the current flow maintained by ground or earth return via the converter station ground electrodes.

There are several possible ways to convert the double-circuit, twin-conductor HVAC line into a hybrid line.

- One of the method would be to keep the existing HVAC conductors and insulators in their original positions to form a bipolar DC line with a metallic-return conductor. But this method will hinder the power transfer capacity of HVDC line and flexibility.
- The second and more efficient way of increasing the power transfer capacity would be to rearrange the available conductors by splitting the center twin-conductor bundle belonging to the other two phases to form a bipolar HVDC line with triple-conductor bundles. The advantage of the latter solution is that triple-conductor bundles allow a higher DC current rating and a higher DC service voltage with regard to the corona effects.

All Tower structures are the self-supporting lattice type steel frame with square bases. They have been designed for double circuits 400KV HVAC transmission. The members of the latticed structures are angle sections and all material are factory made and entirely galvanized by the hot-dip process.

The conductors that have been used for GIBEE III to Addis Ababa Project are twin AAAC "ASTER 851" conductor for each phase for both circuits. The outermost aluminum alloy layer is stranded with a right hand lay and there is no joints in its individual wires. The inner layer of aluminum alloy wires is covered with grease. The technical specification of the conductor is shown on Table 3-2

Table 3-2 Conductor specification

No	Technical Specification	value
1	Type	AAAC
2	Code Name	ASTER 851
3	Number x diameter (mm) of aluminum strands	91 x 3.45
4	Overall diameter (mm)	37.95
5	Aluminum alloy area (mm^2)	850.66
6	Total area (mm^2)	850.66
7	Weight (kg/km)	2,354
8	Ultimate strength (kN)	273.90
9	Maximum current carrying capacity (A)	1356
10	DC resistance at 20^0C (Ω/km)	0.0391
11	Maximum admissible stress (at -5°C and wind load) (%UTS)	24.8
12	Every day stress (EDS) (%UTS)	20
13	Modulus of elasticity, final (daN/mm^2)	5,250
14	Coefficient of linear expansion, (/°C)	0.000023
15	EDS temperature (°C)	20

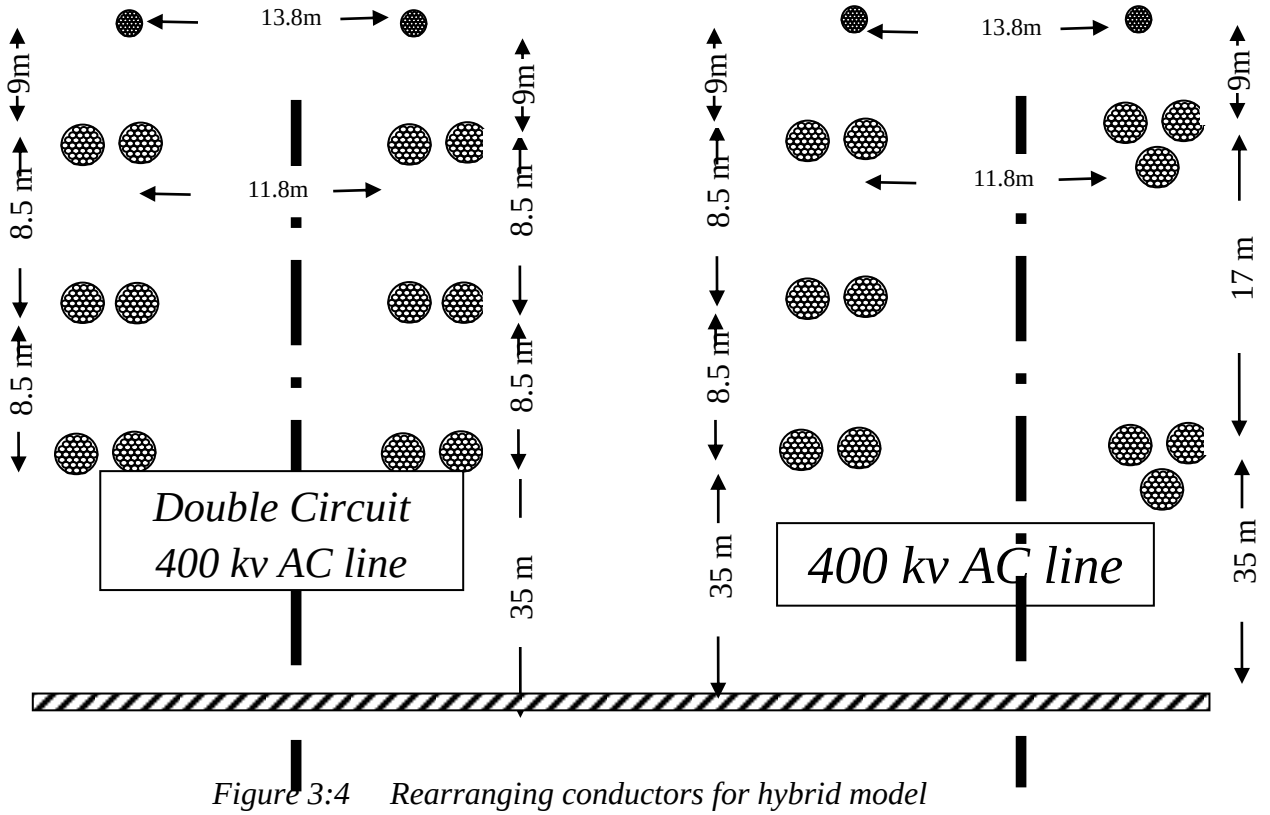

Figure 3:4 Rearranging conductors for hybrid model

3.1.4 Spacer dumper

A 400KV AC Phase conductors, arranged in a horizontal bundle be fitted with spacers in order to maintain a distance of 400mm between the two sub-conductors under all normal working conditions. The other part of circuit, 500 KV HVDC circuit uses three bundle conductors which is arranged with equilaterally spaced arrangement with a distance of 400 mm. Equilaterally custom designed spacer dumpers can be used for keeping the spacing and damping the oscillation. The custom designed Spacer dampers used to suppress bundle conductor sub span oscillations that could cause damage to multi-conductor bundle systems and it can be used to control Aeolian vibration as well as wake-induced oscillation.

The spacer damper designed to maintain 400mm space of the bundle system against loads. It must also restore the bundle to normal posture after experiencing severe loads due to short-circuit currents, and wind. The Spacer Damper combines the function of a spacer in maintaining conductor separation and the function of a damper in controlling aeolian vibration and oscillation.

Figure 3:5 spacer dumper [24]

The number of spacer dampers are distributed throughout the spans not exceeding 60m and not less than 2m away from any mid span joint or repair sleeve or any other -fitting attachment to the conductor, as a result Sub-conductors contacts under normal service conditions are excluded, Conductor bundle will have a satisfactory torsional stability. And damage of sub-conductors and of spacers themselves by short circuit will be excluded.

3.1.5 Insulator model

The insulator strings of HVDC transmission line consist, like those of HVAC transmission lines, of porcelain, glass insulators or composite insulators. For composite insulators there are proven advantages such as lower weight, pollution resistant, weather and explosion proof [42].

Under the effect of the HVDC voltage an ion migration dependent on, among other things, temperature, takes place in the insulating material. One zone becomes richer in ions, another poorer, and consequently the field strength distribution in the material changes. HVDC Composite insulator design must consider surges, contamination, and weathering because, composite insulators for HVDC lines can experience more problems when compared to AC lines, due to increased nonlinearity of voltage distribution, which also helps to increase the contamination on the insulator. [43]

On Gibee III - Addis 400 KV transmission line projects utilize composite insulator with double string for each phase. The suspension V-string for the 400 kV lines have 23 units and the tension string have 21 strings. The composite insulator has the following technical specification. Composite type of insulators is more significantly used for 500KV HVDC as well as 800KV HVDC in china [25].

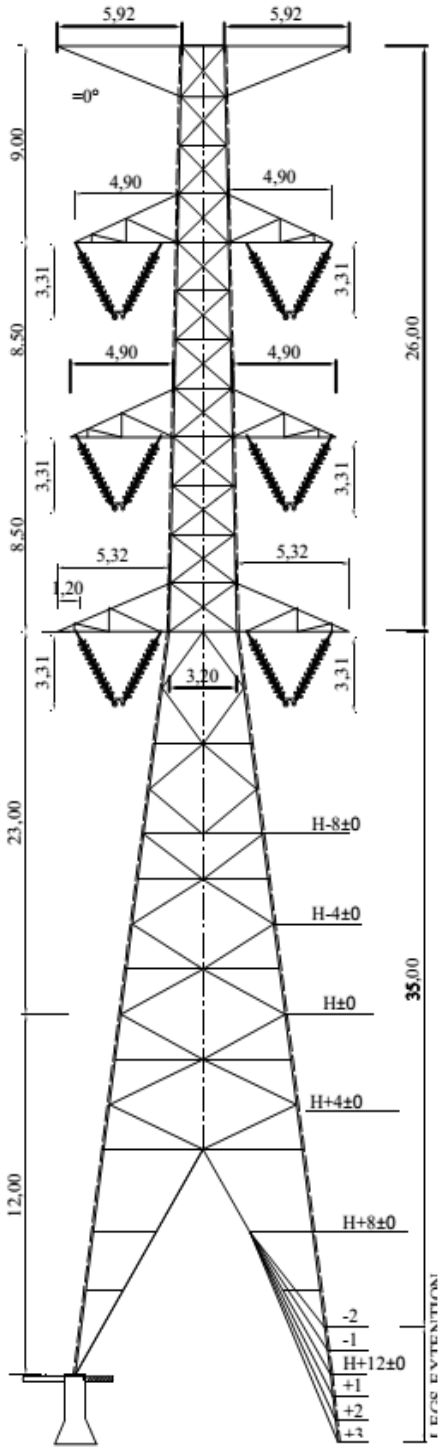

Figure 3:6 Existing 400KV suspension V-string composite insulator arrangement

Table 3-3 Existing insulator composite insulator

S/N	Parameter	unit	Suspension	Tension
1	Electromechanical strength	KN	120	210
2	Nominal Diameter (Disc)	mm	254	280
3	Nominal spacing	mm	146	170
4	Min creepage distance	mm	292	370
5	Ball and socket gage	mm	16	20
6	Minimum flashover voltage			
	6.1. Power frequency (Dry)	KV	78	80
	6.2. Power frequency (wet)	KV	45	47
	6.3. Impulse 50%, positive	KV	120	125
	6.4. Impulse 50%, negative	KV	125	130
7	Withstand voltage			
	7.1. Power frequency (Dry)	KV	70	75
	7.2. Power frequency (wet)	KV	40	45
	7.3. Impulse 50%	KV	110	115
	7.4. Power frequency puncture voltage	kV	110	125

3.2 Hybrid HVAC/HVDC System Design

3.2.1 Overhead line

Many HVDC projects in operation throughout the world like, India, china, Canada and Namibia uses AAAC conductors as overhead lines for HVDC system [44]. on Gibe III- Addis 400 KV HVAC project ASTER 851 AAAC has been used. On this section we can discuss the technical feasibility of existing HVAC line for hybrid HVAC/HVDC line.

3.2.2 Conductor current carrying capacity

On Hybrid HVAC/HVDC line, for HVDC circuit bipolar configuration has been considered. Bipolar line is a line with two conductors of different polarity without dedicated ground return, When the current in the two conductors is equal, a condition which can be achieved by current control, there is no ground current. If one of the conductors fails, the converter ground system serves as a standby conductor. The maximum load capacity of a long HVDC line is usually dictated by consideration of system stability, permissible voltage regulation or cost of energy losses.

The current carrying capability of Hybrid HVAC/HVDC conductors are calculated according to CIGRE recommendation [26]. It is known that the DC current has a lower heating effect than AC current due to the absence of the transformer and eddy current effects. On DC transmission the conductor can be loaded near to the thermal limit.

The thermal state of overhead conductors mainly depends on external parameters, like wind speed and direction, temperature and solar irradiance, as well as on the electrical load circulating through it. Assuming all these parameters remain fairly constant, the conductor can be considered as in a steady state, and its temperature stays reasonably constant. In this situation, the heat supplied due to electric current and the solar radiation is balanced by the heat dissipated by wind and radiation. The heat balance equation can then be written as:

$$\text{Heat gain} = \text{Heat loss}$$

$$P_{J+}P_M + P_S + P_i = P_c + P_r + P_w \qquad (3.1)$$

where P_J = Joule heating
P_M = magnetic heating
P_S = solar heating
P_i = corona heating
P_c = convective cooling
P_r = radiative cooling
P_w = evaporative cooling

Most of the time the heat gain due to corona and the heat loss due to evaporation may both be significant when there are precipitations, for rating purposes they are rarely relevant, and it is suggested that the terms Pi, P_M and P_w in Eqn. 3.2 be neglected [26]

$$P_J + P_S = P_c + P_r \quad (3.2)$$

Joule heating (Pj): Joule heating refers to the energy generated due the current flow through a resistive body. It takes into account the pure DC resistance and the skin effect when AC currents are used. The Joule heating, disregard the magnetic effects produced in AC currents due to cyclic magnetic flux, which may cause a non-neglible power loss at high current densities in certain conductors with a ferrous core.

For Direct current, the value of the Joule heat gain per unit length for conductors carrying direct current is found from the following equation:

$$P_J = I_{DC}^2 \cdot R_{dc}(1+\alpha(T_{av}-20) \quad (3.3)$$

where I_{DC} is the total direct current (A) and R_{dc} the direct current resistance per unit length Ω/m), which depends on the resistivity of the materials ρ (Ω·m) at the temperature considered, α temperature coefficient and the mean temperature T_{av} (°C).

With alternating current, the resistance of the conductors increases with increasing frequency due to skin effect, the increase of current density towards the surface. In this case the Joule heat gain is then given by the following equation:

$$P_J = k_{sk} \cdot I^2 \cdot R_{dc} \quad (3.4)$$

where k_{sk} is the skin effect factor, the average value is suggested 1.0123 [40] For aluminum – steel conductor with three layers and above aluminum wires, according to cigre' 207 [40]

$$I_{ac} = \frac{I_{DC}}{\sqrt{1.0123 + 2.319 * 10^{-5} I_{DC}}} A \quad (3.5)$$

$$I_{DC} = I_{ac}\sqrt{(1.0123 + 2.36 * 10^{-5} I_{ac})} A \quad (3.6)$$

Solar heating (*Ps*): The solar heat gain per unit length P_S by a conductor is directly proportional to the total diameter of the conductor, *D*, and the absorptivity of the surface of the conductor, α_s. It depends on the radiation intensities.

The solar heating using global solar radiation can be written as:

$$P_s = \alpha_s SD$$

Where: α_s = absorptivity of conductor surface

S = Global solar radiation

D = External diameter of the conductor

The value of α_s varies from 0.23 for stranded aluminum to 0.95 for weathered conductor for industrial purpose. It quite appropriate to αs = 0.5 for design purpose

convective cooling (P_c): Convection is usually the most important factor for cooling overhead conductors. Convention cooling taking place with two condition when the wind speed is zero, it is a natural convention and when the wind is low, forced convention. convention cooling for bare conductor to a fluid (air) dependent on convective heat transfer factor hc [W/K·m2].

In order to obtain empirical values that can be used in practical situations, the convective heat loss can be expressed as a function of the dimensionless Nusselt number (Nu = hc·D/λf). The convective heat loss is give by the following formula

$$Pc = \pi \lambda_f (Ts - Ta) Nu \quad (3.7)$$

Where: λ_f thermal conductivity

$Nu = B_l(R_e)^n$ [for forced convection cooling]

B1 and n are constants depending on Reynolds number [Annex D]

$Nu = A_2(G_r.Pr)^m$ [for natural convention cooling]

A_2 and m are constants for various ranges of the Rayleigh number [Annex D]

Radiative cooling (P_r): Radiative Cooling Calculation The radiative heat loss from a conductor is given by the following equation

$$P_r = \pi D \varepsilon \sigma_B [(T_s + 273)^4 - (T_a + 273)^4] \quad (3.8)$$

where D : is the outer diameter of the conductor (m),

ε: is the emissivity of the surface of the conductor varies from (0.23 - 0.9)

d_B : is the Stefan-Boltzmann constant

T_s: is the temperature of the surface of the conductor (˚C),

Ta: is the ambient temperature

For Gibee III, Addis 400 kV transmission line, the following climate data have been considered for design purpose.

Table 3-4 Gibee III- Addis Ababa Climate

No	Climate	Value
1	Rain Fall	100~400 mm for a month (Annual average)
2	Temperature	Mean max. temperature 35ºC Mean min. temperature 10ºC Minimum temperature -5ºC Maximum temperature 40^0C Loading temperature 70ºC
3	Humidity	60 to 90 %
4	Solar radiation	1100w/m^2

The proposed hybrid tower comprise both AC and DC circuits, depending on the parameter and arrangement of the conductors the current carrying capacity can be calculated based on the following design parameters.

Table 3-5 Hybrid Tower double circuit parameter

	Hybrid Tower double circuit parameter		
	Design Parameter	**400 KV AC**	**±500 KV DC**
	Conductor Type	ASTER 851 AAAC	ASTER 851 AAAC
	Over all conductor diameter (D)	38mm	38mm
	DC resistance (R_{DC})	0.0394 Ω/KM	0.0394 Ω/KM
	Solar radiation	1100 w/m^2	1100 w/m^2
	Wind speed (v)	2 m/s	2/ms
	Wind angle (δ)	45 ^{0}	45 ^{0}
	Number of Bundle	2	3
	Ambient Temperature (T_a)	20 ^{0}c	20 ^{0}c
	Maximum allowable Temperature (T_c)	70 ^{0}c	70 ^{0}c
	Height above sea level (h)	2000m	2000m

Considering the above design parameter, the maximum allowable current for DC and Ac can be calculated as follows.

From equation 3.3 Joule heating is $P_J = I_{DC}^2 \cdot R_{dc}(1+\alpha(T_{av}-20)$

Solar radiation is, $P_s = \alpha_s SD = 0.5*1100W/m^2*38*10^{-3}\ m = 20.9$ w/m

convective cooling is $Pc = \pi \lambda_f (Ts - Ta) Nu$

Where thermal conductivity is, $\lambda_f = 2.24*10^{-2} + 7.2*10^{-5}T_f$, $T_f = 0.5(T_c + T_a) = 45^0c$

$\lambda_f = 0.02744$

For forced convection cooling, $Nu = B_l(R_e)^n$

Where B_1 and n are constants depending on Reynolds number Re[Annex D]

$$R_e = \frac{\rho * V * D}{V_f} \qquad (3.9)$$

where $\rho = \exp(-1.16*10^{-4}*h) = 0.792$

h = Height above sea level.

V = wind speed

V_f = Kinematic Viscosity (m^2/s)

$V_f = 1.32*10^{-5}+9.5*10^{-8}*T_f = 1.747*10^{-5}\ m^2/s$

$$R_e = \frac{\rho * V * D}{V_f} = \frac{0.792 * 2m/s * 0.038m}{1.747 * 10^{-5} m^2/s} = 3445$$

Having Reynolds number from Annex- D $B_1 = 0.641$ n = 0.471

$Nu = B_l(R_e)^n = 0.641(3445)^{0.471} = 29.7$, considering the wind angle the Nuslet number can be calculated as follows

$N_{u45} = Nu\ (A_1 + B_2(Sin\delta)^{m1})$,

Where $A_1 = 0.42$, $B_2 = 0.58$, $m_1 = 0.9$ for wind angle $24^0 < \delta < 90^0$

$N_{u45} = 29.7\ (0.42 + 0.58(Sin45)^{0.9}) = 25.08$

Considering the wind angle we can take Nu=25.08 the convective cooling is calculated as follows

$$Pc = \pi \lambda_f (Ts - Ta) Nu$$

$Pc = 3.14*\ 0.02744*\ (70 - 20)\ *25.08 = 108$ w/m

The radiative heat loss from a conductor is given by the following equation

$$P_r = \pi D \varepsilon \sigma_B [(T_s + 273)^4 - (T_a + 273)^4] \quad (3.10)$$

where D: is the outer diameter of the conductor (m)=0.038,

ε : is the emissivity of the surface of the conductor varies from = 0.5

σ_B : is the Stefan-Boltzmann constant = $5.67*10^{-8}$ $wm^{-2}/k\text{-}4$

T_s : is the temperature of the surface of the conductor) = 70˚C,

Ta : is the ambient temperature =20˚C,

From the above value Pr = 14.34 w/m

The heat balance equation is calculated as

$$P_J + P_S = P_c + P_r$$

$$I_{DC}^2 \cdot R_{dc}(1+\alpha(T_{av}\text{-}20) + 20.9 \text{ w/m} = 108 \text{ w/m} + 14.34 \text{w/m}$$

$$I_{DC}^2 \cdot R_{dc} + 20.9 \text{ w/m} = 122.34 \text{ w/m}$$

$$I_{DC}^2 \cdot 3.94*10^{-5} = 101.44 \text{ w/m}$$

$$I_{DC} = 1604 \text{ A}$$

Now taking eqn 4.5for calculating the AC current.

$$I_{ac} = \frac{I_{DC}}{\sqrt{1.0123 + 2.319 *10^{-5} I_{DC}}} A$$

$$I_{ac} = \frac{1604}{\sqrt{1.0123 + 2.319 *10^{-5} 1604}} A$$

$$I_{ac} = 1565 A$$

From the above result, ASTER 851 AAAC conductor has a capacity of 1565A of AC current and 1604 A for DC current. From manufacturer catalogue [Annex A], the rated current carrying capacity of the conductor is 1751A. We can inject a DC current near to thermal limit of the conductor which is difficult for AC case due to HVAC overhead lines are intended to limit the temperature attained by the energized conductors and the resulting sag and loss of tensile strength. Considering the bundle arrangement, current carrying capacity of bundled conductor is derated by a factor of 0.8.

3.2.3 Short circuit level

For hybrid HVAC/HVDC line without proper design and installation of the capacitors on the DC side and AC filters on HVAC bus side the short circuit level of the system will be increased. All protection equipment on both converter and inverter side must be equipped enough to with stand the short circuit current. On HVDC part of hybrid line, since reactive power is not transmitted, the design must provide a means to extend the active power exchanged without increasing the short circuit level.

Regarding the different factors that are involved in determining the cross-section of conductors, short circuit current also must be considered as the main key aspect in proper selection of the conductors. Conductor cross section is determined according to the rated current, and then based on the level of short circuit test. The following equation is used to determine the area of the conductor based on the short circuit level. [38]

$$A = \frac{I_{SC} * \sqrt{t}}{K} \qquad (3.12)$$

$$where\ K = \sqrt{\frac{W.C.\Delta\theta}{0.24\rho}}$$

Where:

A: Cross section of conductor (mm)

I_{SC} : Standard short circuit current (A)

t: The persistence time of short circuit current (s)

k: Constant coefficient related to the conductor material

W: Specific weight of the conductor (gr/cm^3)

C: Specific heat of conductor metal (Calory/g-^{o}c)

ΔΘ: The conductor temperature rise (0c)

ρ: Specific resistance of the conductor (ohm.m/mm2).

K value for AAAC conductors is 68, Isc value for 500kV HVDC line is 55kA, and t is 0.5s. Inserting these values in Eqn 3.12 the required cross sections obtained to be 571mm^2which is able to withstand short circuit level compared to the three-wire bundled conductor.

3.2.4 Insulator Coordination

On this section we can verify technical feasibility of existing composite insulator for reusing for hybrid HVAC/HVDC transmission. Configuring composite insulators for HVDC part of the transmission line needs insulator coordination for evaluating the technical feasibility of the hybrid HVAC/HVDC system. On HVDC transmission, string design and insulator coordination require specific considerations. The string length and characteristics, such as leakage distance, have to be verified according to the relevant contamination conditions of the area crossed by the line.

3.2.5 String Dimensioning

There are several factors which should be taken in to consideration for HVDC insulator string. The following factors have been considered.

- Contamination conditions
- Altitude of the path of the line
- Maximum Voltage level of the line

On HVDC line, most of the time the string length is determined by contamination considerations than switching impulse requirements. For HVDC the contamination performance is the dominating factor determining the size (i.e. axial length) of the insulators. HVDC energized insulators tend to accumulate more pollution than do AC insulators, and it is found that with the same amount of pollution on the insulator, a DC energized insulator has a lower flashover voltage than an AC energized one [12]. Thus, any uncertainty in the estimation of the pollution severity may directly impact the required insulator length. This is fundamentally different to AC where insulator lengths are rarely impacted by the required contamination performance [12]. On HV composite insulator surface the contamination level is high, it can increases in the leakage distance on HVDC insulators than that of for HVAC.

The first step in dimensioning the insulation is to determine the reference site contamination severity. This is preferably done by measuring the contamination severity on DC energized insulators to obtain the most representative results. The measurements should include Equivalent Salt Deposit Density (ESDD) and Non-Soluble Deposit Density (NSDD) measurements, which are performed so that the top to bottom ratio and distribution of contamination along the insulators. For Gibee III – Addis line, considering the contamination level, the creepage distance

has been identifies as to be to 25mm/kv [20]. The transmission line route of existing line mostly dominated by agricultural areas. According to Table 3-6, the creepage distance of 20mm/ KV can be sufficient for the HVDC lines.

Table 3-6 Length of creepage distance for insulators in various contamination zone [28]

Zone	Description	Creepage Distance(cm/KV)
1	Agricultural areas, wood lands	2
2	Outskirt of industrial areas, some distance from sea	3
3	Industrial areas, coast	5
4	Certain chemical industries, thermal power station etc	7

The existing long rod composite insulator have the specification as given on Table 3.3. For V-string, 23 units of insulator has been selected for 400KV transmission line. Verification of creepage distance for HVDC should be done for re-using existing insulators. The creepage distance for V-string is 6716mm and for 7770mm for tension string. The overall string length is 3358mm and 3570mm for v-string and tension string respectively, refer Fig 3.7

For ±500 KV bipolar line the operating voltage can be considered as ±500 KV, for creepage distance of 25mm/kv 12875mm of leakage distance is required for insulation positive and negative pole of HVDC from the ground. The existing insulator is of a long-rod composite material and there is no option of disassembling the unit and reusing for HVDC, so for Hybrid HVAC/HVDC line, changing all the insulator with appropriate specification in needed. Line insulators for the HVDC circuit must be replaced with new composite long rod insulators.

Table 3-7 Proposed composite long rod insulator

Type of string	**Unit**	**V – string / tension String**
Number of shades	Qt	129
String Length	mm	3844
Creepage Distance	mm	11260
Dry Arching Distance	mm	3404
Low frequency flash over		
Dry	KV	1200
Wet	KV	1070
Critical Impulse withstand voltage		
Positive	KV	2145
negative	KV	2145
Net Weight	KG	21.5

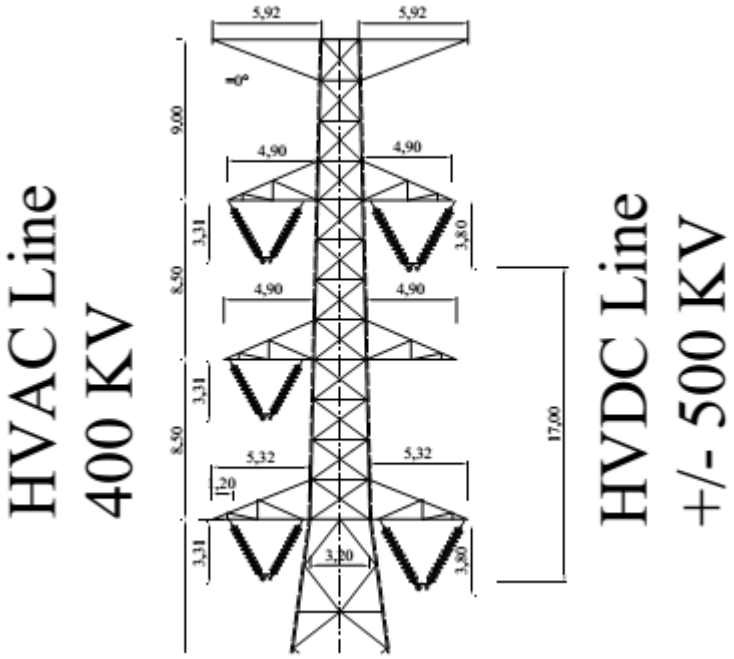

Figure 3:7 Hybrid HVAC/HVDC tower

Altitude can be considered as a sensitive issue on designing the insulator for HVDC overhead line. According to standard GB/T311.1 the insulation strength would decrease by one percent while the altitude increase by 100m due to atmospheric variation from sea level. The Corona loss is more on hilly areas where temperature is low and pressure is high. One of the most important to consider in this case being the positive switching impulse flashover value. A correction factor must be considered for transmission line passing through high altitude areas. For Gibee III – Addis Ababa project, the 400 KV transmission line route passes over an altitude which varies from 1500 – 2000 m above sea level. For ± 500 kV bipolar line the switching voltage at sea level measure up to 1.7pu, 850KV [27]. The correction factor is calculated according to IEC60071-2.

$$K_a = e^{(\frac{mH}{8150})} \qquad (3.13)$$

Where m: is 0.63 for switching flash over voltage.

H: Altitude in meter.

For Hybrid HVDC/HVAC line the HVDC line switching voltage is about 850 kV at sea level. For 2000 m altitude, the correction factor K_a calculated as 1.16.

$$U_{corr} = K_a * U_{sl}$$

Where: Ka – is correction factor

U_{corr} is – corrected switching voltage

U_{sl} - switching voltage at sea level.

Considering the correction factor the composite long rod insulator must be able to with stand the switching voltage of

$$U_{corr} = K_a * U_{sl}$$
$$U_{corr} = 1.16 * 850\,KV$$
$$U_{corr} = 975\,KV$$

Considering the fact that switching overvoltage and flash over creepage distance, the following long rod composite insulator is proposed for HVDC line as shown on Table 3-8

. Table 3-8 Proposed composite insulator specification

Type of string	Unit	V – string / tension String
Number of shades	Qt	129
String Length	mm	3844
Creepage Distance	mm	11260
Dry Arching Distance	mm	3404
Low frequency flash over		
Dry	KV	1200
Wet	KV	1070
Critical Impulse withstand voltage		
Positive	KV	2145
negative	KV	2145
Net Weight	KG	21.5

3.2.6 Pole Spacing

For AC lines carrying nominal voltages greater than 300 kV, the magnitude of the switching surge is the determining factor for the minimum clearance (flashover distances) which must be maintained in HVDC overhead lines as well. The pole spacing can be designed according to the insulator string arrangement. On Gibe III – Addis 400kV transmission line towers are designed

on tension and V string arrangement. For V string there is no swing angles due to wind at the towers and hence clearance requirements for switching surges - determine the pole spacing.

$$PS = 2(d_{\min} + R) + W \tag{3.14}$$

Where PS = pole spacing

d_{min}= Operating voltage clearance

R = Bundle radius, $R = \frac{m}{2 * \sin(\pi / n)}$

n = number of sub conductor on bundle

m = sub conductor spacing

w = Tower spacing

Considering the conductor arrangement of hybrid HVAC/ HVDC tower in Fig 3.7 tower spacing is not a design parameter, as since ±500KV DC poles are located on one part of double circuit. The existing 400KV transmission line conductor rearrange as shown on Fig 3.6. The HVDC part of a tower is a bipolar line each poles of a conductor are bundled with three sub conductors with 40cm spacing. According to [27] Standard of operating voltage considering switching and transient overvoltage minimum clearance are tabulated as Table 3-8. The overvoltage due to switching and transient of ± 500KV HVDC line can reach up to 1.8 pu the minimum clearance (d_{min}) can be taken as 2.2m

Table 3-9Minimum clearance in air as a function of the overvoltage factor

Over Voltage factor (PU)	Minimum Clearance in m at nominal voltage [kv]			
	250	400	500	750
≤ 1.5	0.91	1.37	1.83	3.35
1.6	0.91	1.37	1.98	3.66
1.7	0.91	1.52	2.13	4.11
1.8	1.07	1.62	2.2	4.57

$$PS = 2(d_{\min} + R) \tag{3.15}$$

$$PS = 2(d_{\min} + \frac{m}{2 * \sin(\pi / n)})$$

$$PS = 2(2.2 + \frac{0.40}{2 * \sin(\pi / 3)})$$

$$PS = 4.76\ m$$

For ±500KV the minimum pole spacing is calculated as 4.76m. Referring figure 3.7, the pole spacing for hybrid HVAC/HVDC line is 17m, therefore the hybrid HVAC/HVDC line satisfies the minimum requirement.

3.2.7 Conductor-Ground clearance

For Hybrid HVAC/HVDC tower, the line conductors will be suspended by V string and tension string insulator on lattice steel structures. To verify the existing tower height, calculating conductor sag on worst climate condition is necessary. Bare stranded overhead conductor is normally held clear of objects, people, and other conductors by periodic attachment to insulators. The elevation differences between the supporting structures affect the shape of the conductor catenary. The catenary's shape has a distinct effect on the sag and tension of the conductor, which can be determined using well-defined mathematical equations. The shape of a catenary is a function of the conductor weight per unit length w, the horizontal component of tension, H, the span length S, and the sag of the conductor D. Conductor sag and span length are illustrated in Fig. 3.8 for a level span. The exact catenary equation uses hyperbolic functions. Relative to the low point of the catenary curve shown in Fig. 3.8, the height of the conductor y(x) above this low point is given by the following equation:

$$Y(x) = \frac{H}{W}(\cosh(\frac{wx}{H}) - 1) \cong \frac{wx}{2H} \qquad (3.16)$$

For a level span, the low point is in the center and the sag D is found by substituting x= S/2 in equation 4.16. The exact centenary and approximate parabolic equations for sag calculated as

$$D = \frac{H}{W}(\cosh(\frac{ws}{2H}) - 1) \cong \frac{ws^2}{8H} \qquad (3.17)$$

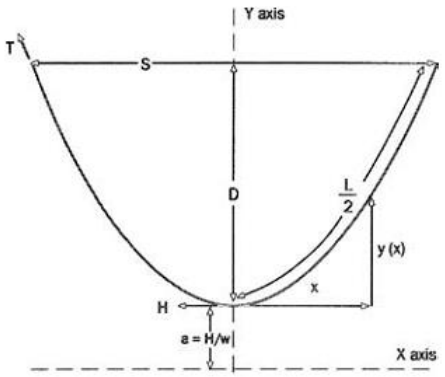

Figure 3:8 The centenary curve for level spans.

Referring a technical specification of Addis Ababa - Gibe III project [20] the ultimate tensile strength (H) taken as 50KN, the tower span taken as 450m from table 3.1 the conductor weight per unit length is 2354 Kg/km or 23 N/m. substituting the above parameters on equation 4.17 we can calculate sag as follows

$$D \cong \frac{ws^2}{8H} \tag{3.18}$$

$$D \cong \frac{23N/m*(450)^2}{8*50KN}$$

$$D \cong 11.6m$$

Practically the towers are not installed on the same height throughout length but on some geographical terrain the two consecutives towers are located on inclined span. The Sag and tension in inclined spans may be analyzed using essentially the same equation. The catenary equation for the conductor height above the low point in the span is the same. However, the span is considered to consist of two separate sections, one to the right of the low point and the other to the left as shown in Fig.3.9.

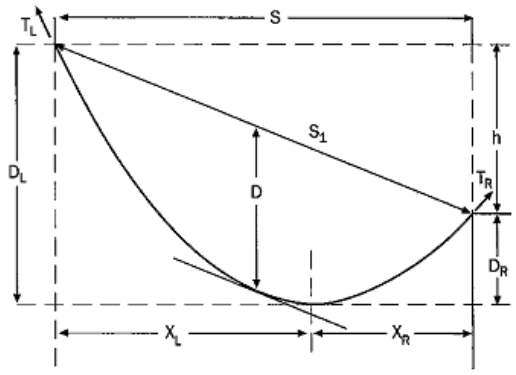

Figure 3:9 The centenary curve for inclined spans

DL and DR can be calculated as

$$D_L = D(1-\frac{h}{4D})^2 \quad , \quad D_R = D(1+\frac{h}{4D})^2 \tag{3.19}$$

Where D= midpoint sag for level span

D_R= sag in right subspan section

D_L = sag in left subspan section

h = vertical distance between support points

Assuming the minimum span length on technical document of the project 450m and allowable condition for 10m height variation on two consecutive conditions which is a practice on different HVDC transmission line project.

$$D_R = D(1-\frac{h}{4D})^2$$

$$D_R = 11.6(1-\frac{10}{4*11.6})^2$$

$$D_R = 7.13m$$

$$D_L = D(1+\frac{h}{4D})^2$$

$$D_L = 11.6(1+\frac{10}{4*11.6})^2$$

$$D_L = 17.13m$$

Sag and stress vary with temperature because of the thermal expansion and contraction of the conductor. Temperature rise of conductor increase the length of the conductor and hence sag increases and tension decreases. A fell in temperature causes opposite effect. Maximum stress occurs at the lowest temperature when the line has contracted and is also possibly covered with ice. As far as existing 400KV transmission line route concerned the minimum temperature considered as 10^0c, therefore ICE loading in negligible. Wind loading also another factor on sag and tension calculation of overhead conductors. Assuming that wind blows uniformly and horizontally across the projected area. Fig 3.10 shows the force of wind on overhead conductor. The horizontal force exerted on the line as a result of the pressure of the wind is calculated as follows.

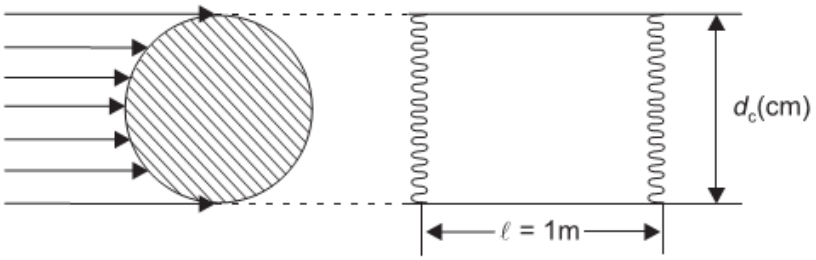

Figure 3:10 Force of wind on overhead conductor

$$F = \frac{d_c}{100} * P \quad Kg/m \qquad (3.20)$$

Where:

F= Horizontal force due to wind

P = wind pressure (kg/m)

During sag calculation the effective load (w_e) on the conductor can be calculated by considering the resultant value of weight of the conductor (w) and the horizontal force (F) due to wind as shown on the fig 3.11.

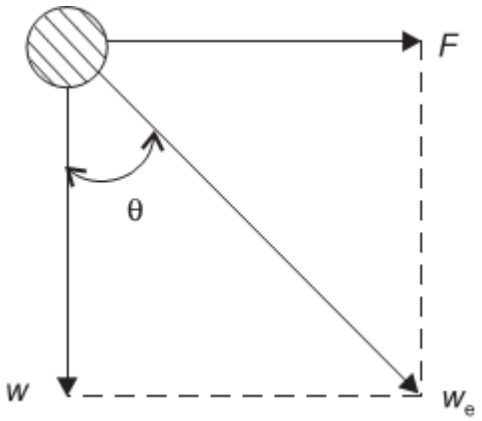

Figure 3:11 Horizontal and vertical force due to wind

$$w_e = \sqrt{w^2 + F^2} \tag{3.21}$$

Considering wind loading on the conductor same level tower sag equation can be re- written as equation 4.22

$$D \cong \frac{w_e s^2}{8H} \tag{3.22}$$

On technical specification document of Addis – GibeIII 400kv transmission line the wind load on conductor can be considered to be 52 kg/m². The horizontal force due to wind can be calculated as follows,

$$F = \frac{d_c}{100} * P \quad Kg/m$$
$$F = \frac{3.795}{100} * 52 \quad Kg/m$$
$$F = 1.97 Kg/m$$

Calculating the result and loading on the conductor by considering conductor weight per unit length and wind load.

$$w_e = \sqrt{w^2 + F^2}$$
$$w_e = \sqrt{2.354^2 + 1.97^2} kg/m$$
$$w_e = 3.08 \quad kg/m$$
$$w_e = 30.2 \quad N/m$$

the sag equation can be modified as eqn-4.22

$$D \cong \frac{w_e s^2}{8H}$$

$$D \cong \frac{30.2N/m*(450)^2}{8*50KN}$$

$$D \cong 15.2m$$

Substituting D=15.2m for consecutive inclined tower configuration in Eqn 3.19, the new sag value of DR and DL are 6.86m and 26.8m respectively. The minimum ground clearance of the conductor HVDC pole can be calculated by using equation 3-23

$$H_p = Cs + D + Ext + R \quad (3.23)$$

3.

Where - H_p = distance from the center of the bundle conductor to the ground

Cs = clearance to ground at mid-span

D = conductor sag

Ext = tower extensions up to 2 x 2 m = 4 m

R = bundle radius

From technical specification document of Addis – GibeIII 400kv transmission line clearance from the ground is set to be 10m. The bundle radius calculated as 0.23m, the minimum clearance from the ground can be calculated as:

$$H_p = Cs + D + Ext + R \quad (3.24)$$

$$H_p = 10 + 15.2 + 4 + 0.23$$

$$H_p = 29.43 \ m$$

Referring Fig 3.6, The existing transmission tower of 400 kV double circuit line (DS, DA and DT) have the minimum clearance value of 35m which satisfies the calculated value.

3.2.8 Loading of Hybrid HVAC/HVDC lattice tower

The loads in power line lattice towers categorized into three types: Environmental loads, construction and maintenance loads and security loads. Environmental loads consist of wind, temperature changes and snow, construction and maintenance loads which relate to personnel safety. Security loads consist of accidental occurrences such as broken conductors or adjacent structure failure due to tornados.

The existing 400 kV lattice tower structural stresses in members and connections for the structural design calculation, based on the design loading and design unbalanced loading (broken wire conditions) multiplied by safety factor according British standard. All the Connections are designed for the same member forces according to British standards. All the towers are designed with an overload capacity (factor of safety) for the unbalanced design loading [20].

When we rearrange the conductors for hybrid HVDC/HVAC system, the existing 400 KV tower arranged as shown on [Fig 3.7]. The wind load on the modified conductors and conductor load on the hybrid HVAC/HVDC tower are verified as below:

Wind load on a conductor

The wind load on existing 400 KV transmission line tower structure is related to the wind speed in accordance with the code of practice applicable to the country. For Gibe III – Addis Ababa project Wind loads on conductors and earth wires are 52 kg/m2 and wind load on a single insulator 60 kg/m2 are considered for design purpose. The basic wind pressure on structures are taken as 86 kg/m2. [20].

The wind loading on the conductor is determined from the formula [14]

$$wind\ load = l * D * q * C_f \qquad (3.25)$$

Where:

l=length of conductor (m)
D=diameter of conductor (m)
q = wind pressure
C_f = force coefficient

The length of the conductor between two adjacent towers is 450m; the diameter of the three bundle conductor is calculated as 46.18cm in Equation 3.29. Wind pressure is calculated from design wind speed, 20m/s under worst condition and topography factor. For Gibe III – Addis Ababa project topography factor can be taken as 1.0 from dynamic wind pressure table [49]. Wind pressure is $(0.613*(20m/s)^2 = 0.25\ KN/m^2$, where 0.613 a factor considering the altitude. The force coefficient C_f is determined from flow regime = $D*V_s$, where D=46.18cm and Vs=20m/s. Flow regime= $0.46*20= 9.2m^2/s$. Referring force coefficient table, C_f =0.7. The wind load calculated as:

$$wind\ load = l * D * q * C_f$$
$$wind\ load = 450m * 0.46m * 0.25KN/m^2 * 0.7$$
$$wind\ load = 36\ KN$$

Conductor load

The conductor load is considered as a Vertical load generally come from the weight of the conductors suspended on the cross arms and the self-weight of the structure. Ice and snow loads must also be superimposed where towers are routed in such areas. For Gibee III – Addis Project we neglect the Ice and snow loading.

The vertical weight of the conductor calculated as the vertical conductor weight span multiplied by conductor weight, including weight of insulator strings and fixings

$$condcutor\ load = (n * sp * W + I) * g \qquad (3.26)$$

Where:

Sp= weight span in m

n= number of bundle conductors

W= conductor weight in Kg/m

I= insulator string and fixing weight

g = gravity ($10m/s^2$)

From Table 3-2 the net weight of the conductor is 2354 Kg/km and the proposed insulator and fitting weight is 42.5kg. We have used three bundle conductors for each phase with the span of 450m. The conductor load calculates as

$$condcutor\ load = (3 * 450m * 2.354kg/m + 41.5kg) * 10m/s^2$$
$$condcutor\ load = 32.2KN$$

The combined load due to wind load on the conductor, conductor weight including insulators with accessories, sag and tension load of hybrid HVAC/HVDC conductor calculated as the summation of all loads on the cross arm of the lattice tower under worst condition.

$$Combined\ load = A + B + C$$

Where:

A= Wind load on conductor in KN

B= Conductor load with insulators and accessories in KN

C= Longitudinal force due to conductor tension KN

$$Combined\ load = 36KN + 32.2KN + 50KN$$
$$Combined\ load = 36KN + 32.2KN + 50KN$$
$$Combined\ load = 118.2KN$$

The foundation of 400 kV lattice structure for Gibee III – Addis Ababa project designed to with stand the ultimate load of 5000 KN and the designed composite insulator also withstand 180KN load at any condition, therefore the existing 400 KV tower can withstand all the combined load after conversion to hybrid HVAC/HVDC tower.

3.2.9 Earth Electrode Design

On Existing 400kVsystem the tower Structures are grounded. The connection of ground electrodes to the stub angle are made with compression lugs, fixed to the stub angles by 2 bolts with 16 mm diameter. To accommodate eventual additional grounding, every stub angle feature two pair of holes, one for compulsory grounding rod and the other for additional grounding.

For hybrid HVAC/HVDC line, the electrode at converter and inverter stations must have reducing effect on earth currents and as well on the environment. The appropriate selection of electrode site and electrode size can enhance the system safety and reliability. On most HVDC system, two types of electrodes namely, horizontal and vertical electrodes are used as shown in Figure 3.12-The earth electrode resistance and electrode line resistance must be restricted within a 10 -20Ω range.

For hybrid HVAC/HVDC model the vertical electrode system is advisable due to the location of ground electrode is fairly close to the converter station. The design of HVDC ground electrode involves many fundamental parameters like, the electrode configuration, the soil structure and characteristics.

Unlike the grounding system of HVAC line which only considers fault conditions, HVDC grounding electrodes are designed for normal, emergency and fault conditions. [45] HVDC

grounding electrode is must capable of handling ground return circuit for bipolar operation which permit a current to flow through earth during monopolar operation.

The following formula is used by [45] to design ground electrode by conventional simplified method.

$$R_e = \frac{\rho}{2\pi l}(\ln\frac{4l}{d} - 1).....for\ l >> d \qquad (3.27)$$

Where:

R_e= Ground electrode resistance in Ω

ρ = soil resistivity Ω – m

l = total length of the conductor in m

d – diameter of the conductor in m

According to [20] the soil resistivity of both Akaki and Gibee III substation varies from 100 Ω-m 36 Ω-m to the depth level of 1.5m – 53m. To achieve minimum earth resistance of 10Ω at burial depth of 5 meter, by using Eqn 3.28 the minimum electrode diameter is calculated as 0.013m.

$$d = \frac{4l}{e^{(1+\frac{R_e 2\pi l}{\rho})}} \qquad (3.28)$$

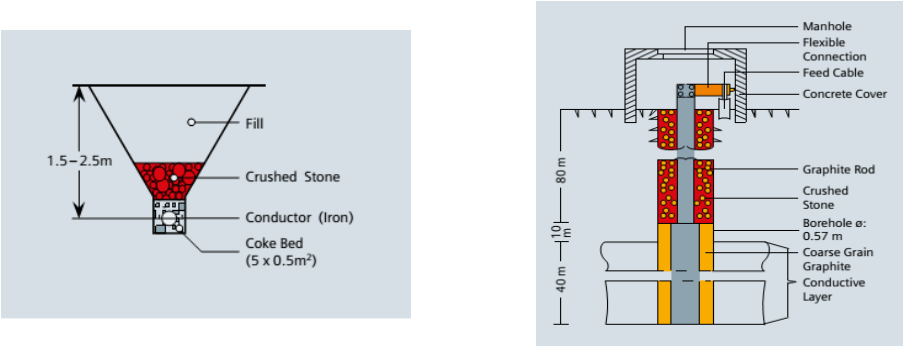

Figure 3:12a) Cross section through a horizontal land electrode b) Vertical electrode at Apollo, the Southern Cahora Bassa HVDC station [28]

3.2.10 Fundamental Frequency Coupling

The main issue on hybrid HVAC/HVDC line can be the magnetic coupling effect of HVAC line with HVDC line due to both lines are running on the same tower. HVDC line running in the same tower with an HVAC line, the HVDC line will be exposed to fundamental frequency

coupling. A steady state fundamental frequency current will be superimposed on the DC current in the HVDC line due to inductive and capacitive coupling from AC lines on the same line. The induced fundamental frequency current is converted into a DC current and a series of harmonic currents of the sidebands of the converter transformer valve side current [36]. The DC component causes an unsymmetrical magnetization and could lead to converter transformer core saturation during a fraction of the cycle. This causes the non-characteristic current harmonic, increased noise and transformer heating.

When the converter transformer saturation occurs, undesirable effects are emerging on the system, such as core saturation which leads to an increased noise level and increased heating in the transformer due to unsymmetrical magnetization. The life of the transformer will be decreased due to the localized stray flux heating and possible deterioration of interlamination insulation caused by the increased magnetostrictive forces. The second effect could be the harmonic generation and injection to both AC and DC sides due to the saturation. High harmonic content is present also in the neutral current of the transformer, which is of primary importance to filter design, because it causes a much higher level of telephone interference than the same amount of current flowing in a balanced mode of the transmission line [29].

To minimize the fundamental coupling effect of hybrid HVAC/HDC system, a tuned fundamental frequency filter must be installed on both the inverter and converter stations. The tuned filter will give a better filtering capacity on the system. The tuned filter filters at a fixed fundamental frequency (in general, low order characteristic harmonics). Its impedance is calculated by using Equation 3.29. The impedance at the resonance frequency consists of a low resistance:

$$Z_f = R + j\left(\omega L - \frac{1}{\omega C}\right) \tag{3.29}$$

The advantage of tuned filter is the investment cost and provides efficient suppression of individually selected harmonics but provide little damping at other harmonics.

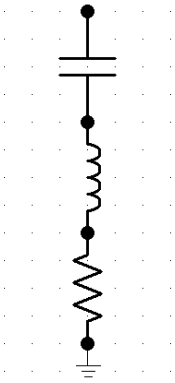

Figure 3:13 Single tuned filter

During design of single- tuned filter before selecting the values of R, L, and C the quality factor and relative frequency deviation must be determined. Quality factor (Q) determines the sharpness of tuning of the filter. Depending on order of filtering the values of Q varies. At resonant frequency, the reactance of both inductor and capacitor is calculated as

$$X_o = \omega_n L = \frac{1}{\omega_n C} = \sqrt{\frac{L}{C}} \qquad (3.30)$$

The quality Q is defined as

$$Q = \frac{X_o}{R}$$

Assuming the inductance value of 10mH, at resonant frequency the capacitor will be 1000μF.

$$\omega_n = \frac{1}{\sqrt{LC}}$$

$$C = \frac{1}{\omega_n{}^2 * L}$$

The fundamental frequency is 50HZ and $w_n=2\pi f$ the value of c will be 1000 μf. considering the series resistance of 10 Ω, Q will be 0.316. (Which harmonic frequency is the severe one for such arrangement? It is not mentioned. If this is not known, how do you design a filter?

3.2.11 Corona Effects

Corona considerations in the design of HVDC transmission lines have been discussed by different researchers [1], [2]. The performance of HVAC or HVDC transmission lines have always been measured on corona losses (CL), radio interference (RI) and audible noise (AN

Conductor Surface Gradient

The parameter that has the most important influence on corona performance is the conductor surface gradient. Electrostatic principles are used to calculate the electric field on the conductors of a transmission line [15]. If a single conductor is used on each pole of the line, the electric field is distributed almost uniformly around the conductor surface. When bundled conductors are used, the electric field around the sub-conductors of the bundle is distributed non-uniformly, with maximum and minimum gradients occurring at diametrically opposite points and the average gradient at a point in between [15]. The degree of non-uniformity increases as the number of sub-conductors in the bundle as well as the ratio of the sub-conductor radius to the bundle radius increase. For hybrid HVAC/HVDC tower surface gradient has been calculated using the method known as Markt and Mengele's method, the average and maximum bundle gradients [30] of a bipolar HVDC line, with n-conductor bundles on each pole, are given as

$$E = \frac{\frac{V_{DC}}{r}}{\ln\frac{2H}{r} + (m-1)\ln(\frac{2H}{s'}) + x\frac{m}{2}\ln\left[1+(\frac{2H}{A})^2\right]} \qquad (3.31)$$

Where:

r= Conductor radiusin cm

s'=s(for m=2, m=3) , 1.123*s (for m = 4)

x= -1 for bipolar

V_{DC} = Line to ground voltage

m= number of strands per bundle

s= distance of the strands within the bundle

H= average height above the ground 35m

A= pole – to - pole distance

The maximum conductor surface gradient of bundle conductors is found to be

$$E_{\max} = E\left[1+(m-1)\frac{r}{R}\right]$$

where: R = Bundle radius, $R = \frac{s}{2*\sin(\pi/m)}$

m = number of sub conductor on bundle

s = sub conductor spacing

For calculating the surface gradient,

$$E = \frac{\frac{V_{DC}}{r}}{\ln\frac{2H}{r}+(m-1)\ln(\frac{2H}{s'})+x\frac{m}{2}\ln\left[1+(\frac{2H}{A})^2\right]}$$

Where :

r = 1.897 cm

s' = s = 40cm

x = -1 for bipolar

VDC = 500kv

m = 3

H = 3500cm

A = 1700cm

$$E = \frac{\frac{500}{1.89}}{\ln\frac{2*3500}{1.897}+(3-1)\ln(\frac{2*3500}{40})+(-1)\frac{3}{2}\ln\left[1+(\frac{2*3500}{1700})^2\right]}$$

$$E = 18.55\ \frac{KV}{cm}$$

The maximum conductor surface gradient on 500 KV HVDC line is found to be:

$$E_{\max} = E\left[1+(m-1)\frac{r}{R}\right]$$

$$R = \frac{s}{2*\sin(\pi/m)}$$

$$R = \frac{40}{2*\sin(\pi/3)}$$

$$R = 23.09\ cm$$

$$E_{max} = 18.55\left[1 + (3-1)\frac{1.897}{23.09}\right]$$
$$E_{max} = 21.55\ KV/cm$$

From the above calculation, the DC conductor gradient determined to be 21.55 KV/ cm. which is quite below on 500 kV HVDC projects in the world at this stage [19]. The main reason for surface gradient value is below existing HVDC lines in the world is, the pole spacing is high, 17m and we have used three sub conductors as a bundle for each pole.

Electrostatic Field

Up to know there is no practically implemented hybrid HVAC/HVDC transmission line implemented throughout the world. There is no field measurement data regarding electrostatic field from a lateral distance from the center of the ground. The electrostatic filed distribution for Hybrid tower has been studied with different authors [31] [32]. The electrostatic field is formed in the space between the live conductor and the ground when there is no interference from charge carriers. From eqn 3.32, the field strength at 20 m lateral distance to the left of the tower center level is calculated as 2.9KV/m

$$E = \frac{V_{DC}}{H}\frac{2}{(1-k)\ln(\frac{2H}{R})}\left[\frac{H^2}{H^2+X^2} - \frac{H^2}{H^2+(X-S)^2}\right] \qquad (3.32)$$

Where: V_{DC}= conductor – Ground voltage in KV

H= Height of the Conductor above the Ground in meter (35m)

R= Equivalent conductor bundle radius in meter

X= lateral distance from the conductor in meter

S = distance between poles

R= Equivalent bundle radius

K= Coupling factor

D = Distance of bundle

d= conductor diameter

$$K = \frac{\ln\left[\sqrt{\frac{2H + S^2}{S}}\right]}{\ln(\frac{2H}{R})} \tag{3.33}$$

$$R = \frac{D}{2} n \sqrt{\frac{nxd}{D}}$$

Magnetic Field

In a power system installation, a common value for the exposure limit value for AC fields is 100 μT and for DC fields 40 mT [33]. The magnetic fields generated by the DC line are well below the exposure limit value and are not treated further. According to [33], after converting the existing HVAC line to hybrid HVAC/HVDC the magnetic field value has no significant variation from the existing double circuit. Therefore, for hybrid HVAC/HVDC system the magnetic field distribution on the lateral distance above 1m from ground is within acceptable range.

HVDC Corona Loss

Corona inherently affects both the design and operation of overhead transmission lines. Although corona plays an important role in the protection of high-voltage equipment by attenuating the steepness of surge over voltages travelling along the line, it causes undesirable effects. On HVAC and HVDC transmission corona losses occur due to the movement of ions positive and negative created by corona. There are basic differences between HVAC and HVDC coronal loss. On AC lines, the positive and negative ions created by corona are subject to an oscillatory movement in the alternating electric field present near the conductors and therefore, confined to a very narrow region around the conductors. On DC lines, however, ions having the same polarity as the conductor move away from it, while ions of opposite polarity are attracted towards the conductor and are neutralized on contact with it. Thus, the positive conductor in corona acts as a source of positive ions which fill the entire space between the conductor and ground, and vice-versa, for the negative conductor.

The theoretical calculation of corona losses for HVDC transmission lines demands – the evaluation of the electric field and space charge in the environment [19]. Such calculation determines in the first step the electric field and ion current distributions on the surface of the conductors and ground plane.

Considering the complexity of theoretical calculations and factors influencing corona on hybrid HVDC transmission lines, it is often preferable to use empirical formulas derived from a large amount of data on long-term corona loss measurements made on experimental lines with different conductor bundles and under different weather conditions [21].

The following empirical formulas derived from intense laboratory experiment from different research for evaluating fair and foul weather corona losses of bipolar HVDC transmission lines

$$P_{fair} = p_0 + 50\log(\frac{g}{g_0}) + 30\log(\frac{d}{d_0}) + 20\log(\frac{n}{n_0}) - 10\log(\frac{HS}{H_0 S_0}) \qquad (3.34)$$

$$P_{foul} = p_0 + 40\log(\frac{g}{g_0}) + 20\log(\frac{d}{d_0}) + 15g(\frac{n}{n_0}) - 10\log(\frac{HS}{H_0 S_0}) \qquad (3.35)$$

Where P : Bipole corona loss in dB above 1W/m,

d : conductor diameter in centimeter

g : conductor surface gradient

n : number of conductors

H : height

S : pole spacing

The following reference values are assumed :0

g_0= 25kV/cm,

$d_{0=}$ 3.05 cm,

n_0= 3,

H_0= 15 m and

S_0= 15 m.

The values obtained from regression analysis

P0= 2.9 dB for fair weather and

P0= 11 dB for foul weather.

To convert bipole losses from dB above 1w/m to watt/m Eqn 3.33 is used

$$p(kwatt/m) = 10^{P_{dB}/10} \tag{3.36}$$

For hybrid HVAC/HVDC line the coronal loss for both fair and foul weather can be calculated by considering the following parameters as a given data [38]

d=0.38cm

g= 21.5kv/cm

n= 3

H=35m

s=17m

$$P_{fair} = p_0 + 50\log(\frac{g}{g_0}) + 30\log(\frac{d}{d_0}) + 20\log(\frac{n}{n_0}) - 10\log(\frac{HS}{H_0 S_0})$$

$$P_{fair} = 2.9 + 50\log(\frac{21.5}{25}) + 30\log(\frac{3.8}{3.05}) + 20\log(\frac{3}{3}) - 10\log(\frac{35*17}{15*15})$$

$$P_{fair} = -1.78\ dB\ over\ 1w/m$$

By eqn 3.33 corona power loss on fair weather is

$$P_{fair} = 10^{P_{dB}/10} = 0.663 kw/km$$

For bipolar line the total corona loss would be twice of fair corona loss multiplied by 402 km

$$P_{total} = 2*402km*0.663kw/km = 533\ kW$$

On foul weather, the corona loss can be calculated by using equation 3.34

$$P_{foul} = p_0 + 40\log(\frac{g}{g_0}) + 20\log(\frac{d}{d_0}) + 15g(\frac{n}{n_0}) - 10\log(\frac{HS}{H_0 S_0})$$

$$P_{foul} = 11 + 40\log(\frac{21.5}{25}) + 20\log(\frac{3.8}{3.05}) + 15\log(\frac{3}{3}) - 10\log(\frac{35*17}{15*15})$$

$$P_{foul} = 6.03\ dB\ over\ 1w/m$$

When we convert the above value to

$$P_{foul} = 10^{P_{dB}/10} = 4kw/km$$

For bipolar line the total corona loss would be twice of fair corona loss multiplied by 400 km.

$$P_{total} = 2 * 402km * 4kw/km = 3.22Mw$$

In normal fair weather condition, the corona loss per phase per km for both HVAC and HVDC is 6 kW/km [45]. Considering worst case scenario the corona loss is calculated as 4 kW/km which is below the standard.

Audible Noise

On hybrid HVAC/HVDC model, the largest corona activities like corona loss occur in foul weather [36]. Thus, the ion currents under DC-lines are largest during heavy rain season. Considering the environment condition, the corona discharge is quite different in fair and foul weather. In contrary with AC corona effect, RI and AN are reduced from fair to foul weather in the case of DC [36]. Therefore, changing from fair to foul weather, AC AN is increased and DC AN decreased.

On bipolar line the high impulsive corona discharge occurs on positive pole of the conductor therefore the negative pole effect on corona effect actually neglected in the case of bipolar lines [36]. The main reason for dc corona excels on fair weather than foul weather is due to airborne particles, prevailing and insects. Naturally due to tribo-electricity insects are charged negatively and attracted to positive pole, corona activity increases due to this.

Hybrid HVAC/HVDC is the emerging technology in power system field. As a result, it is difficult to find many publications on this regard. As far as Audible noise prediction is concerned, verified method for calculation is rare in the field. The common result is that the corona activities of pure AC and DC lines are not changed fundamentally when combined in a hybrid line [36]. For AC AN formulas used to calculated according to [27]. According to [36], the heavy rain level L5 in [dB(A)] per phase calculated as

$$L_5 = 20\log(n) + 44\log(d) + 67.9 - \frac{665}{E} + 22.9(n-1)\frac{d}{D} - 10\log(R) - 0.02R \qquad (3.37)$$

where:

n: number of sub conductors per bundle

d: diameter of the conductors [cm]

E: conductor surface gradient in [KV/cm]

D: bundle diameter [cm]

R: radial distance from the phase to the point of observation [m].

According to [36] the wet conductor level [L_{50}] is calculated from heavy rain level by considering a correction factor

$$L_{50} = L_5 + \Delta A_{wc}$$

Where

$$\Delta A_{wc} = 10.4 - \frac{14.2E_c}{E} + 8(n-1)\frac{d}{D} \qquad (3.38)$$

$$E_c = \frac{24.4}{d^{0.24}}$$

For three phase case the three AN noise is calculated individually and take the average values as in Eqn.3.36

$$L_5 = 10\log[10^{L_{5A}/10} + 10^{L_{5B}/10} + 10^{L_{5C}/10}] \qquad (3.39)$$

Where $L_{5A,}$ L_{5B} and L_{5C} are AN level on heavy rain for phase A, Phase B and Phase C respectively. The conductor surface gradient (E) as for AC three phase line is calculated using equation 4.35 [27]

$$E = E_{av}(1 + \frac{d}{D}(n-1)\cos\theta \qquad (3.40)$$

$$E = \frac{q}{2\pi\varepsilon nr}(1 + \frac{d}{D}(n-1)\cos\theta$$

$$E = \frac{CV}{2\pi\varepsilon nr}(1 + \frac{d}{D}(n-1)\cos\theta \quad KV/m$$

Where: $C = \frac{2\pi\varepsilon_0}{\ln(\frac{D}{GMR})} F/m$

V= Phase voltage in KV

d= conductor diameter

D= Bundle spacing

$$GMR = \sqrt{r * d}$$

Table 3-10 400 KV transmission line conductor specification

Items	Unit	Values
Nominal Voltage	KV	400
Capacitance c	f/m	$8x10^{-12}$
Radius of the conductor(r)	cm	1.9
Distance between Component conductor centers	cm	40
Bundle diameter (D)	cm	32.4
Height of conductor above ground (h)	cm	3500
Number of component conductors in bundle (n)	pc	2

Using the above Table 3.10 the conductor surface gradient is E=16.94KV/cm.

Taking the configuration of Fig 3.4, the three phase audible noise calculated at 10 meter from the phase. Observation distance for phase A is 36.4m, phase B is 44.6m and phase C is 52.9m.

$$L_{5A} = 20\log(n) + 44\log(d) + 67.9 - \frac{665}{E} + 22.9(n-1)\frac{d}{D} - 10\log(R) - 0.02R$$

$$L_{5A} = 20\log(2) + 44\log(3.8) + 67.9 - \frac{665}{16.9} + 22.9(2-1)\frac{3.8}{32.4} - 10\log(36.4) - 0.02*36.4$$

$$L_{5A} = 47.02\ dB$$

With the same method

$$L_{5B} = 45.48 \text{ db and } L_{5B} = 44.49 \text{ db}$$

AN contribution due to three is calculated as shown below

$$L_5 = 10\log[10^{L_{5A}/10} + 10^{L_{5B}/10} + 10^{L_{5C}/10}]$$

$$L_5 = 10\log[10^{47.02/10} + 10^{45.48/10} + 10^{44.9/10}]$$

$$L_5 = 50.55\ \ dB$$

For DC AN case, it is calculated by means of the formulas indicated on [36]. The exceedance level L50 of the positive pole during fair weather is calculated by

$$L_{50} = 56.9 + 124\log(\frac{E}{25}) + 25\log(\frac{d}{4.45}) + 18\log(\frac{n}{2}) - 10\log(R) - 0.02R$$

$$L_{50} = 56.9 + 124\log(\frac{21.5}{25}) + 25\log(\frac{3.8}{4.45}) + 18\log(\frac{2}{2}) - 10\log(36.4) - 0.02 * 36.4$$

$$L_{50} = 30.74 dB$$

The difference between L_{50} and $L_5$is quantified to be $L_{50} - L_5 = 6\,dB$.

For hybrid model AN level can be calculated with combination of AC and DC levels. According to [36], the equivalent AN for hybrid model can be calculated as:

$$L_{eq} = L_{50} + 0.115 * \sigma^2$$

$$\sigma = (\frac{L_5 - L_{50}}{1.64})$$

$$L_{eq} = L_{50} + 0.115 * \sigma^2$$

$$L_{eq} = 30.74 + 0.115 * \frac{6^2}{1.64}$$

$$L_{eq} = 33.26 \;\; dB$$

According to [46] the national regulations for AN is limited to with level limited (50...60) dB for AC (foul weather) and (40...50) dB for DC (fair weather) is made. For both HVAC and HVDC contribution, the calculated value is below the standard.

Radio Interference

Radio interference (RI)results from Corona discharges, which generate high frequency currents in the conductors producing electromagnetic radiation, in the vicinity of the lines. RI measurements have shown that radio noise from a DC line is considerably lower than from AC lines of similar capacity. The corona effect causes a wide-band electromagnetic radiation which can lead to interference, particularly with AM radio transmission. The sources of these radiations are widely different. On the negative conductor, there are Trichel pulses which are distributed approximately in a uniform manner over the surface of the conductor and contribute every little to the radio interference measured. On the positive conductor, there are several mechanisms which can be observed. The major contribution to the high frequency interference Generated by a bipolar line is from ‘streamers’, which are distributed more randomly.

For hybrid HVAC/HVDC model, according to [25], the RI level behaves very much like the AN level with regard to weather conditions, which means that the fair weather RI level may be higher for the hybrid AC/DC line due to the RI contribution from the DC line. However, in rainy conditions, the RI contribution of the AC will increase by about 15-20 dB, while the RI contribution of the DC line will decrease. This means that the maximum RI level of the line, which occur in rainy conditions, will be somewhat influenced by the "hybrid effect", i.e. the increase in surface voltage gradients on the AC line caused by the presence of the DC line. However, the RI level is not regarded as a principal environmental effect and the RI levels will not be considered further in this thesis

For HVAC case the radio interference is calculated according the fowling formula

$$RI = 120 \log E_{av} + 40 \log d + 20 \log(\frac{h}{D_2}) + 10[1 - \log(10 f))^2] - 150.4 \quad (3.41)$$

Where, Eav : the average conductor surface gradient in kV/cm,

d: the conductor diameter in mm,

D: the aerial distance from phases to the measuring point in meters,

h: the conductor height in meters

f : the frequency in MHz

For HVDC the radio interference can be calculated as

$$RI = 25 + 10 \log m + 20 \log r + 1.5(E_{\max} - 22) \quad (3.42)$$

In most literatures the radio interference is defined as the field strength, F0, measured in a horizontal distance from the nearest conductor of 30 m, at a frequency of 1 MHz with a band width of 9 kHz. RI is obtained in dB over 1mV/m. The reference point of this equation which was empirically determined in field tests is a maximum conductor surface gradient, E_{max} =22 kV/cm.

CHAPTER FOUR

Technical and Economical Comparison HVAC and Hybrid HVDC/HVAC

This chapter is dedicated to discuss on technical and economical comparison between hybrid HVAC/HVDC in comparison with the existing 400KV HVAC line.

4.1 Introduction

There are many advantages for hybrid HVAC/ HVDC system over existing 400kV HVAC system systems. Most of hybrid system advantage matches with HVDC system advantages over HVAC systems. The first factor is that there is no technical limit to the length of transmission distance connection over the same tower. it is also possible to connect to asynchronous system together. The main benefit of Hybrid system is the significant increase of the power transferring capacity from existing system.

On implementation of hybrid HVAC/HVDC system, since we are using existing infrastructure like conductor, steel structure tower, and OPGW cable the installation cost is reduced to big scale. The only additional item that must be changed is the insulator, the capacity of the insulator cannot withstand wet and dry power frequency overvoltage. A three bundle vibration dumber must be used on every 400 m of the transmission length

4.2 Technical aspect

Power transferring capacity

For ASTER 851 bare aluminum conductor the current carrying capacity of single conductor has been calculated as 1604A. Considering the dynamic performance and thermal limit of the conductor it is advisable to load 75% of the total carrying capacity of the line. Since we are using 3 bundle conductor we can take the grouping factor of 0.8 when we calculate the total current carrying capacity of one pole of bipolar line.

The total power carrying capacity of the line is calculated as:

$$P_{DC} = n * V_{DC} * I_{DC} * C * m \quad (4.1)$$

Where:

n= number of bundle conductors (3)
V_{DC}: Direct current voltage (500kV)
I_{DC}: Current carrying capacity of the conductor (1604A)
c: correcting factor (0.75)
m= grouping factor for bundle conductor (0.8)

Substituting the above values, the total power carrying capacity of the single pole line is:

For Bipolar HVDC line the overall power transferring capacity is twice of the single pole which is 2.88GW. The converter station is selected with a capacity of 3000 MVA, considering the reactive power consumption of LCC converter which is 40 -50 % of the active power [19]. The optimum capacity of hybrid HVAC/HVDC system is of 2.5GW'. According to [20] a 400 kV transmission line is designed to transmit a power of 1500MA. A Bipolar HVDC model can transmit a total power of 2.5GW.

The HVDC section of hybrid HVAC/HVDC line has is a capability to operate as monopolar link when a fault or technical disconnection happened on either of the poles, the healthy pole can supply a 50 % of the capacity. For HVAC case if fault happens on one of the three phases, the the protection relay will disconnect the system, there is no possibility to supply power under fault condition.

2.6.1.1. Power efficiency

HVAC Corona Loss

Assuming the 400 KV HVAC conductors are arranged with two sub conductors per phase.
The voltage gradient for HVAC is calculated by using equation 4.2.

$$E = \frac{V}{\sqrt{3}} \frac{\beta}{r \ln((\frac{a}{R_e})(\frac{2h}{\sqrt{4h^2 + a^2}}))} \quad (4.2)$$

Where:

$$\beta = \frac{(1+(n-1))}{n} \qquad (4.3)$$

$$R_e = Rn\sqrt{\frac{nr}{R}}$$

$$R = R\frac{s}{2\sin\frac{\pi}{n}}$$

Where

E = Conductor Surface Voltage Gradient (kV/cm)

V = Rated Voltage (400kV)

β= Factor for Multiple Conductors (0.5475)

r = Radius of Conductor (1.9cm)

R = Outside radius of bundle (20cm)

Re = Equivalent Radius of bundle conductor (17.43cm)

S = Distance between Component conductor centers (40cm)

A = Phase Spacing (850cm)

H = Height of conductor above ground (3500cm)

n = Number of component conductors in bundle (2)

The conductor surface gradient calculated is 16.5 kv/cm.

For corona loss for HVAC different formulas are proposed with different authors based on voltages and voltage gradients. For calcuationg HVAC corona loss a formula by Anderson, Baretsky, McCarthy Formula is used [50]

$$p = P_{FW} + 0.36068 * K * V * r^2 \ln(1+10\rho)E^5 \qquad (4.4)$$

Where:

P_{FW}= total fair-weather loss 3kW/km (1 to 5 kW/km for 500 kV, and 3 to 20 kW/km for 700kV),

K= $5.35 \times 10^{-10}$for 500 to 700 kV lines, = $7.04 \times 10^{-10}$for 400 kV lines (based on Rheinau results),

V= conductor voltage in kV, line-line, r.m.s., (400KV)

E= surface voltage gradient on the underside of the conductor, kV/cm, peak, (√2*16.5 KV/rms)

ρ= rain rate in mm/hour, [3.5mm/hr assuming moderate rainfall)

r= conductor radius in cm, (1.9cm)

N= number of conductors in bundle of each phase (2)

Substituting the above values Eqn 4. we get 9.7 kw/km – phase. Overall length of the transmission line the total loss can be

$$p = 3 * 9.7 kw/km * 402 km = 11.7 MW$$

The bipolar HVDC line the coronal loss under foul weather (rainy season) is about 6MW which is very minimum compared to HVAC case 11.7KW.

Active power loss

On any transmission line configuration three will be the active power loss due to the resistance of the conductor throughout the route. It is obvious that the resistance value of the conductor is directly proportional to the length of the route.

For 400KV HVAC system assuming 1500MVA power transferring capacity, the line current is 2165A per phase. The resistance of the conductor is 0.0391 Ω/km, since it is bundled with 2 sub conductors its effective resistance amounts to 0.0195Ω. The active power loss will be:

$$p = 3 * I^2 * R * distance = 3 * 2165^2 * 0.0195 \Omega/km * 400 km = 109.68 MW$$

For Bipolar HVDC case, with transmission capacity of 1.25GW per pole the current rating is 2500A. The effective resistance for 3 bundle sub conductor is 0.0130 Ω/km. Therefore, the active power loss is calculated as :

$$p = 2 * I^2 * R * distance = 3 * 2500^2 * 0.0130 \Omega/km * 400 km = 65 MW$$

The total power loss due to corona and I^2R are calculated above. For 400KV HVAC system the corona loss is 11.7 MW and for ±500 KV HVDC is 6MW. For the same transmission length, the HVAC corona loss is almost 2 times that of HVDC. On this regard HVDC system is more economical compared to HVAC. HVDC system also has an advantage over HVAC system regarding to I^2R loss, HVAC I^2R loss is 1.6 times of that of HVDC.

Table 4-1 HVAC and hybrid HVAC/HVDC comparison

	Line capacity	Corona loss	Active power loss	Line Efficiency
Existing 400KV HVAC Line	1500 MVA	11.6MW	109.6MW	90.1 %
Converted Bipolar ± 500KV line	2500MW	6MW	65 MW	97.2%

4.3 Economic aspect

During feasibility study of new transmission line construction, transmission utilities companies gives a greater attention towards performing life cycle costing studies for cost management and decision making.

The existing double circuit transmission line is designed to transmit power from Gibee III to Addis Gelan with a capacity of 3000MVA. The hybrid HVAC/HVDC system is designed to upgrade the transmission capacity of the system. Now the comparison lies between the Hybrid HVAC/HVDC line investment cost with the new-and HVAC line which able to transmit 1500 MVA.

On hybrid system the bipolar HVDC line designed to transfer 2500 MW power by converting one part of the circuit to HVDC. The existing 400KV AC line designed to accommodate 1500MVA per circuit, assuming the power factor of 0.9, one circuit able to evacuate 1350 MW to Addis Ababa. The power upgrading factor is about 1.8 times of the existing capacity and 1100MW extra power is supplied through HVDC line from Gibee III to Gelan Subsation.

The investment comparison is done between new single circuit 400KV HVAC line construction and the hybrid HVAC/HVDC line.

4.3.1 HVAC investment cost

The engineering investment cost for single line 400 KV line is calculated in Annex E. The cost includes all design, supply and installation cost of substation upgrading at Gelan and GibeIII switch yard including 402 km length of transmission line. During calculation different assumption from local and international 400KV AC transmission line project has been taken [35].

During investment cost study it is a mandatory to study resettlement cost for construction. The total resettlement implementation cost for the construction of Gibe III-Sodo HVTL is studied by [37]. The total budget required for compensation payment, i.e. for loss of crops, trees and residential houses due to ROW, tower foundation, access roads and substation will be23,939,240.60 Birr 2,242,278.75 (USD). This Budget includes compensation cost for environmental monitoring [37].

The assessment of electric transmission line is done by [35] in 2009. For this project we have taken EPC estimation for 400KV single circuit. For 500KV single circuit transmission line (approximate with 400KV line) the study estimates 1,350,000 CAD/km and 33,658,000.00 CAD/ per KM. We have taken the price estimate by considering inflation from 2009 and local engineering estimate for 400KV HVAC line.

Table 4-2 400KV single circuit HVAC investment cost

S/n	***Item***	***Total Cost [USD]***
1	Gibee III switchyard upgrading	42,976,120.00
2	Gelan Substation upgrading 4.1.1.	37,816,720.00
3	Transmission line cost from GibeeIII – wolyita - Gelan 4.1.2. 4.1.3.	562,800,000.00
Total cost		643,592,840.00
EIA and RAP costs (8%)		51,487,427.20
Contingency (25%)		160,898,210.00
Grand total		855,978,477.20
Grand total [Birr 20.94 @ Sep 2015]		17,958,428,451.66

Comparing HVAC or HVDC transmission line project the investment cost includes of the capital investment required for the actual infrastructure (i.e. Right of Way (RoW), towers, conductors, insulators and terminal equipment), substation/ Converter cost and costs incurred electrical power losses. For HVDC transmission is, the converter cost is very expensive compared to that that HVAC. Because the technology is new few manufacturers patented the technology and the price looks expensive for several years. According to ABB (pioneer on HVDC technologies) the

price of converter will go down for the coming 10 years due to recent technologies on controlling and power electronics technologies. [28]

We took the study of assessment of electric transmission technologies [35] for estimating bipolar ±500KV HVDC transmission line. For bipolar line with three bundle conductors the engineering estimate be 762,000.00 CAD/KM and the 2500MW converter station costs about 300,0000,000 CAD. We have considered the inflation as well as the countries experience to estimate the cost. The following table illustrates the investment cost for bipolar 500 kV HVDC transmission line.

Table 4-3 HVDC Bilpolar line cost estimation

Cost item	±500kV 2.5 GW Bipolar line estimation			
	unit		Unit price	Total price
Bipolar transmission line cost	km	402 KM	876,000.00 USD/km	352,152,000.00
Converter cost for 2500MW	pc	1	345,000,000.00USD	345,000,000.00
Total				697,152,000.00
EIA and RAP costs (8%)				55,772,160.00
Contingency (25%)				174,288,000.00
Grand Total [USD]				**927,212,160.00**
Grand total [Birr 20.94 @ Sep 2015]				**19,425,094,752.00**

4.3.2 Hybrid HVAC/ HVDC investment cost

For Hybrid HVAC/HVDC cost the cost estimation depends on the existing transmission line. On a power transmission project almost 8% of the project is EIA and RAP costs [37]. Since we are using existing tower, conductor and ROW. Since dry and wet power frequency withstand capacity of existing 400KV composite insulator is below the standard for ±500 kV HVDC line. All the insulators must be changed with proper withstand capacity. The other equipment which must be changed in a thee bundle spacer dumber to accommodate a three bundle conductor on every 400m of the length. The contribution of Insulator and spacer damper investment on overhead line is almost 1.8%

The investment cost for constructing new single circuit 400KV HVAC line about 855,978,477.20 USD. (17,958,428,451.66 Birr) The Hybrid HVAC/HVDC line with a power transferring capacity of 2.5GW costs 439,173,420.00 USD. The price reduction is about 416,805,057.20 USD. Investment point of view the total reduction of cost is about 49%.

Table 4-4 Hybrid HVAC/HVDC line estimation

Cost item	***Hybrid HVAC/HVDC line estimation***			
	unit		Unit price	Total price
Insulator and spacer damper	km	402 KM	15,768 USD/km	6,338,736.00
Converter cost for 3000MVA	pc	1	345,000,000.00USD	345,000,000.00
Total				351,338,736.00
EIA and RAP costs (8%)				0.00
Contingency (25%)				87,834,684.00
Grand Total [USD]				**439,173,420.00**
Grand total [Birr 20.94 @ Sep 2015]				**9,200,683,149.00**

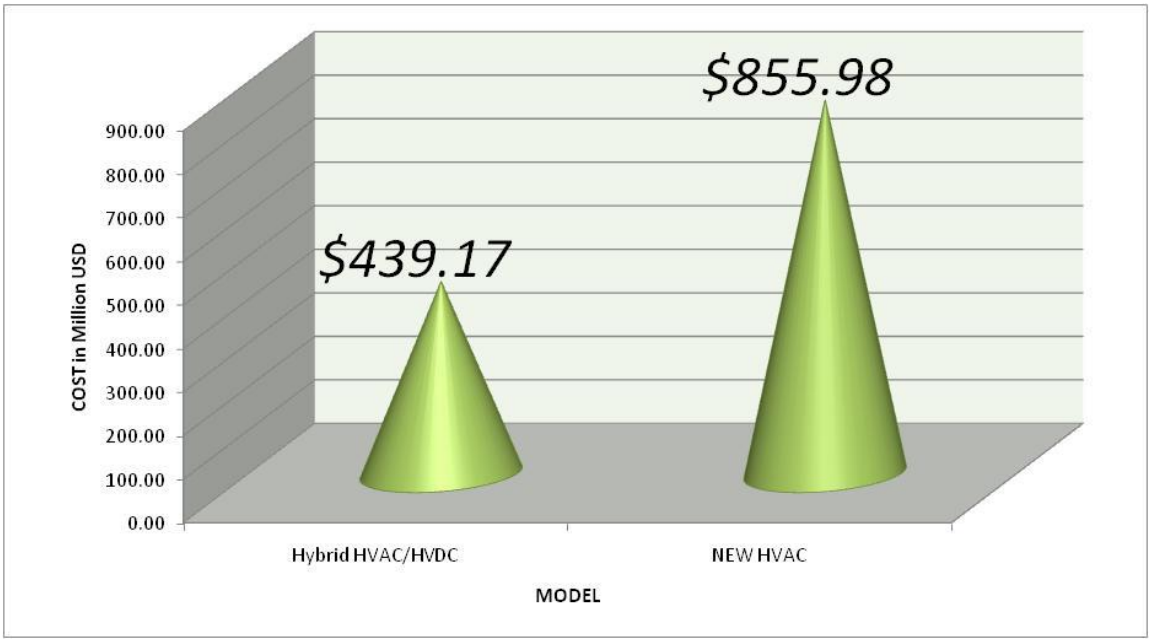

Figure 4:1 Investment cost comparison

4.3.3 Transmission life cost

In a transmission line electrical losses are an avoidable phenomenon, the loss always there where ever the line is energized with any load. The power loss is mainly directly proportional with the product a square of the current with the transmission line resistance

For new power system project costs are expressed in terms of long run marginal costs. For cost calculation the levelized costs for the planned system additions are used to estimate the system long run marginal costs. In Ethiopia the average levelized system generation cost for the planned expansion is 0.0455 USD per kWh [37]. For hydropower the generation cost is 0.0402. The levelized cost for transmission is estimated to be 0.007 USD per kWh and 0.014 USD per kWh for distribution. Therefore, the levelized cost of power supply for the planed GTP period expansion is estimated at 0.067 USD per kWh, one of the lowest in the World. We can use 0.067 USD per KWh for our calculation.

Table 4-5 Data used for lost cost analysis

No	Description	Unit	
1	Life of transmission line	Years	35
2	Energy cost [Sep 2015]	$/kwh	0.0291
3	Energy generation cost	$/kwh	0.067
4	Load factor	--	0.57
5	Loss factor	-	0.38
6	Annual Load growth	-	1.2%
6	Discount rate	-	10%

Load factor: is defined as the ration over average power and peak power on a given period of time

Loss factor: is the ratio of average and peak losses during certain period of time

The discount rate: The interest rate used in discounted cash flow analysis to determine the present value of future cash flows.

Annual cost of losses: The annual cot losses is determined by the following equation [22]

$$LC = \frac{3Ir^2 * 8760 * L_D{}^2}{1000}(L_o E_C + EGC)$$

where

L_C = cost of losses ($/km/year)

r = conductor resistance (ohms/phase/km)

I = annual average current (amps)

L_D = annual load factor

L_0 = annual loss factor

E_c = annual average cost of energy ($/kWh)

EGC = annual average cost of generation ($/kWh)

The annual loss of cost is calculated using table xxx data for HVAC and HDVC line. For HVAC case the average current assumed to be near to thermal limit which is 1353A per phase and 2500A per pole for HVDC. The DC resistance of ASTER 851 AAAC conductor is 0.0394 Ω/km. For HVAC case since the conductors are bundled with 2 sub conductors the effective resistance is 0.0197 Ω/km per phase. The bipolar HVDC line contains 3 sub conductors per pole, effective resistance 0.0131 Ω/km per pole.

Annual cost of losses

To calculate the present value equation 4.5 is used.

$$PV = LC\frac{(1+d)^N - 1}{d(1+d)^N}. \qquad (4.5)$$

Where: PV = is the Present value of an annually recurring loss cost

LC= Loss cost

d= Discount rate

N= Economic life time of the transmission line

Considering a 35-year project life cost analysis calculation is performed [Annex F] for both new 400KV HVAC line and hybrid HVAC/HVDC line. From [Annex F], it is observed that the life cycle cost of new 400KV HVAC is 6,806,581.75 USD/km and 5,005,620.81 USD/km for hybrid HVAC/HVDC line.

The life cycle loss of new 400 KV HVAC is about 74% higher than that of hybrid HVAC/HVDC. When we compare the loss cost still the new HVAC line is 48% higher than hybrid HVAC/HVDC line. The IRR value for hybrid line is 74% and 24% for new HVAC line. By considering all economic cost comparison, hybrid HVAC/HVDC investments is more advantageous.

Table 4-6 Loss cost

	Loss cost unit price USD/km
Hybrid HVAC/HVDC line	6,806,581.75
New HVAC line	5,005,620.81

CHAPTER FIVE

Simulation Studies and Result Analysis

5.1 Introduction

The hybrid HVAC/HVDC system has been simulated by using ATP EMTP software and quick field analyzer. On the simulation different characteristics of hybrid HVAC/HVDC transmission line has been studied, among this power transferring capacity both circuits, fundamental frequency coupling, light and heavy loading of both system, transient disturbance and electric field distribution at ground level. The main purpose of the simulation is to verify hybrid HVAC/HVDC line power carrying capacity, electric field at the ground and system performance during disturbance.

5.2 Simulation Model

The simulation has been done by using ATP-EMTP software. The hybrid HVAC/HVDC transmission line is configured on LCC model of ATP-EMTP software (fig5.1). On the model all pole to pole distances and phase to phase distances with technical specification of the conductors are specified. A three phase 400KV AC source is used for one circuit and for converter section 12 pulse Cigre HVDC source is used for both +500KV and -500KV poles.

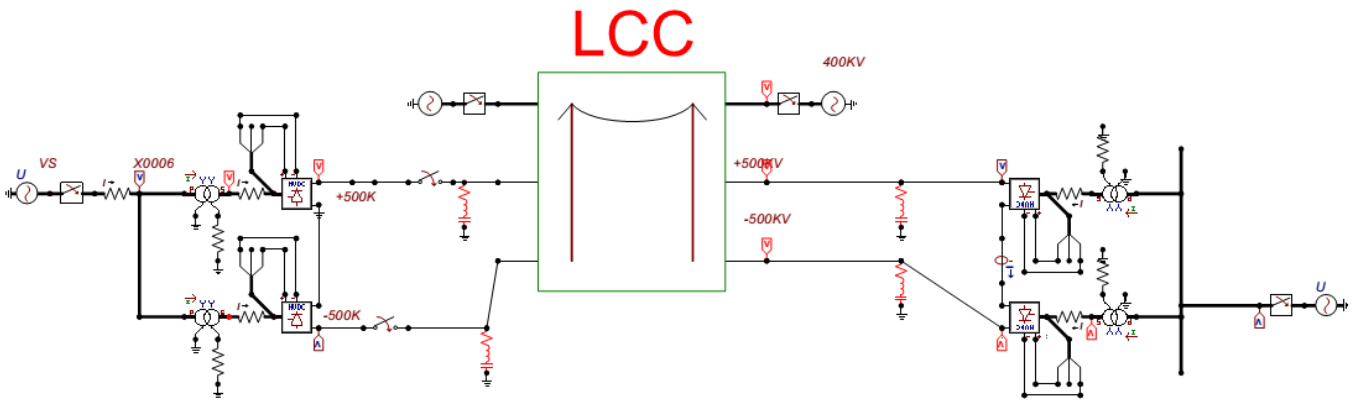

Figure 5:1Hybrid HVAC/HVDC model

5.3 Hybrid HVAC/HVDC line model

The line model is configured according to the existing HVAC 400KV transmission tower configuration. Each parameters of ASTER 851 AAAC conductor parameters are fed to the LCC model. The total length from GibeeIII to Gelan substation is assumed to be 402km. As an input to the model, the inside and outside diameter of the conductor, dc resistance of the the transmission line per km, number of bundle conductors per phase or per pole, separation distance from the tower and poles /phases are fed to LCC model.

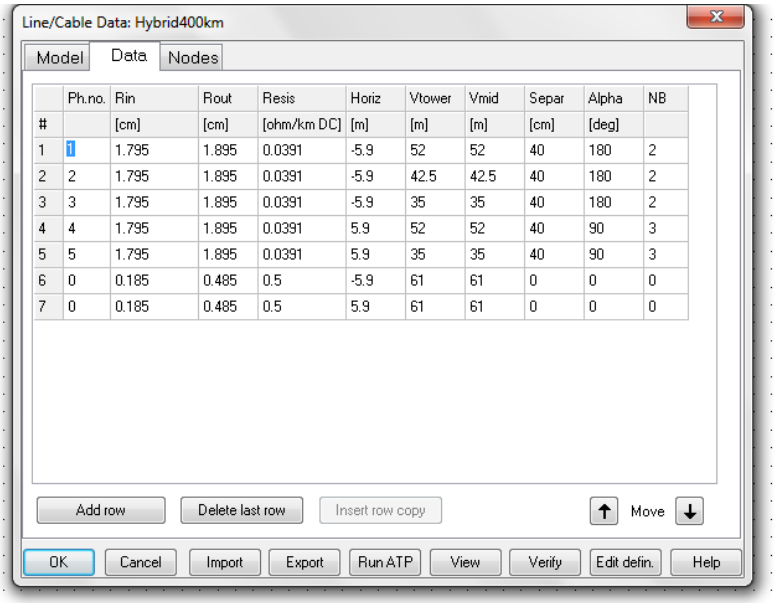

#	Ph.no.	Rin [cm]	Rout [cm]	Resis [ohm/km DC]	Horiz [m]	Vtower [m]	Vmid [m]	Separ [cm]	Alpha [deg]	NB
1	1	1.795	1.895	0.0391	-5.9	52	52	40	180	2
2	2	1.795	1.895	0.0391	-5.9	42.5	42.5	40	180	2
3	3	1.795	1.895	0.0391	-5.9	35	35	40	180	2
4	4	1.795	1.895	0.0391	5.9	52	52	40	90	3
5	5	1.795	1.895	0.0391	5.9	35	35	40	90	3
6	0	0.185	0.485	0.5	-5.9	61	61	0	0	0
7	0	0.185	0.485	0.5	5.9	61	61	0	0	0

Figure 5:2 Hybrid HVAC/HVDC line model

5.4 Electric field simulation model

The electric field simulation is done by quick field analyzer. The hybrid HVAC/HVDC tower with lateral distance of 60m to the left and right is considered. For proper simulation the mesh analysis is done by finite element method. Since the system is with both AC and DC fields, on a quick field analyzer a transient electric model is used to study the field distribution in the transmission line which is subjected to induced overvoltage's.

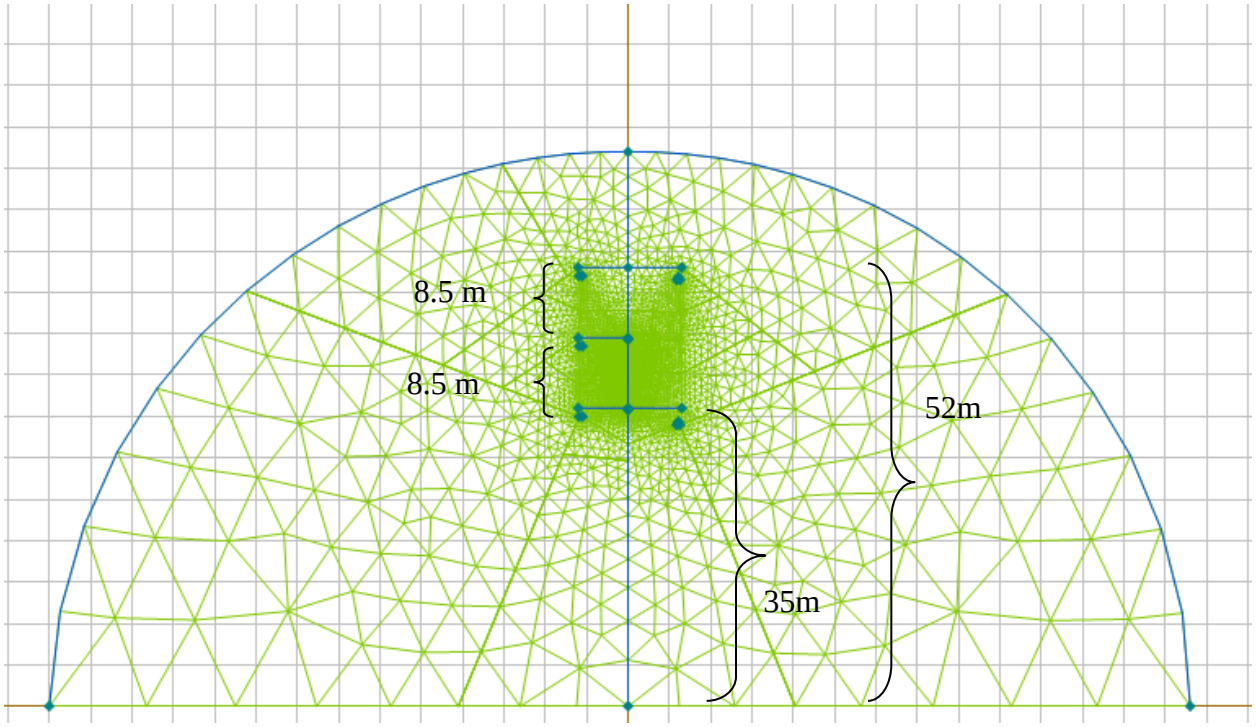

Figure 5:3 Electric field simulation model

5.5 Hybrid HVAC/HVDC System Simulation

5.5.1 Voltage disturbance

The HVAC source is a three phase 400KV rms voltage with energization time of 0.02 sec. For HVDC section a bipolar cigre 12 pulse HVDC model is used with +500KV volt and -500KV volt considered. Three different stages are realized on the simulation.

- When both circuits energized without tuned RLC filter, the disturbance for 0.02 sec experiences a voltage spike about ± 654KV on both bipolar line.
- When HVAC is off and bipolar HVDC line energized after 0.04sec, the dynamic disturbance voltage induced on HVAC line measures to the magnitude of 36 kv but decays to zero in 0.036sec fig 5.4(c).
- After installing a single tuned RLC filter the HVDC output looks smooth but the disadvantage is a ± 753KV on the poles of for 0.0351 sec as shown on fig 5.4(b).

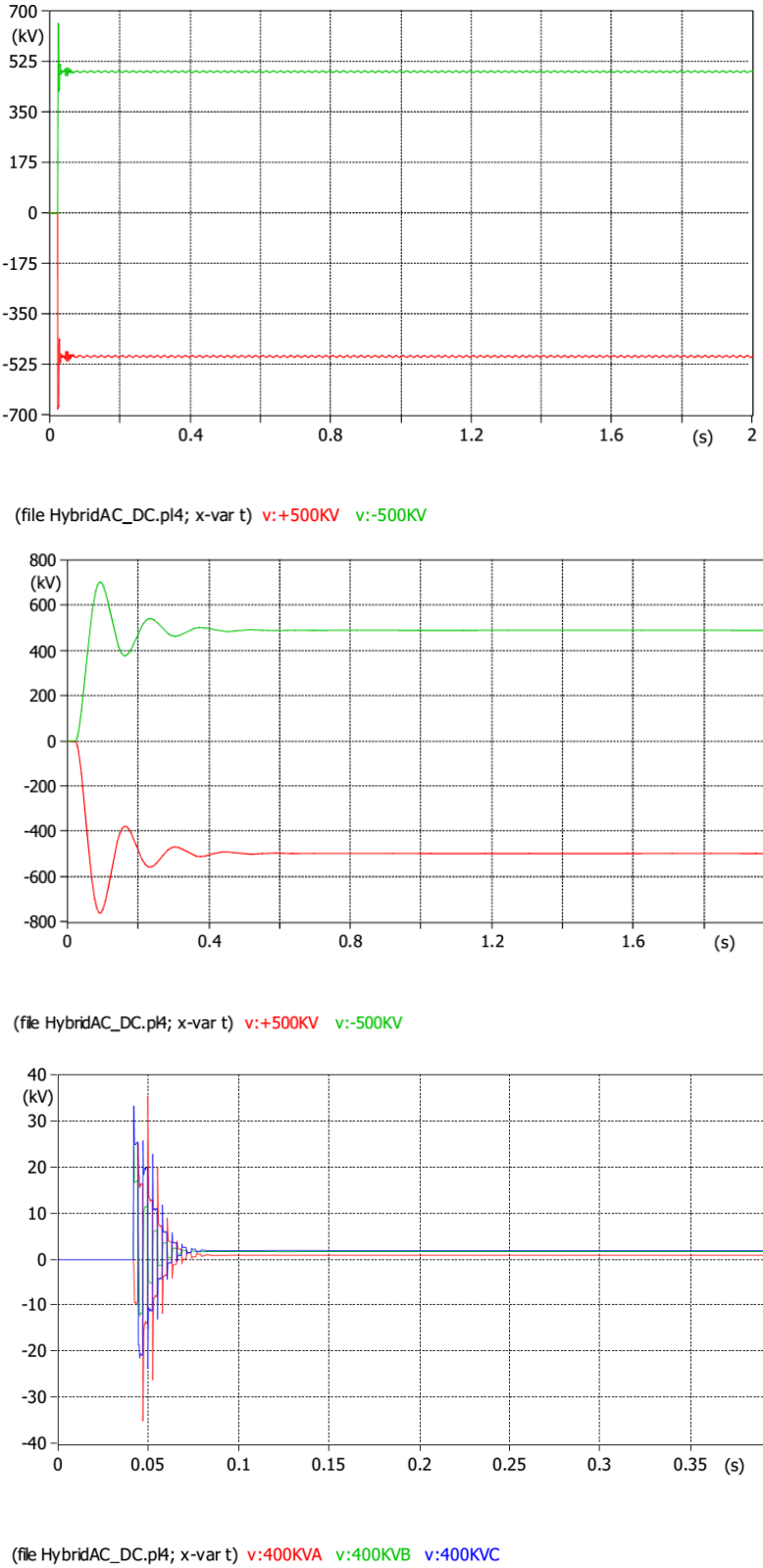

Figure 5:4 Energization disturbances

5.5.2 Fundamental frequency coupling

To study a fundamental frequency coupling on HVDC line, the hybrid HVAC/HVDC is simulated after and before single tuned RLC filer installation

- Without single tuned RLC filter and the HVDC system is de-energized and only HVAC is energized, fundamental frequency is coupling induces a voltage of 89KV on two poles of HVDC line as shown on fig 5.5 (a). This voltage can able to saturate both converter transformers unless properly filtered.
- The voltage can be filtered by using single tuned RLC filter. After properly installed a filter at both converter stations the fundamental frequency coupling will decrease to the value of 84V (fig 5.5 (b)).

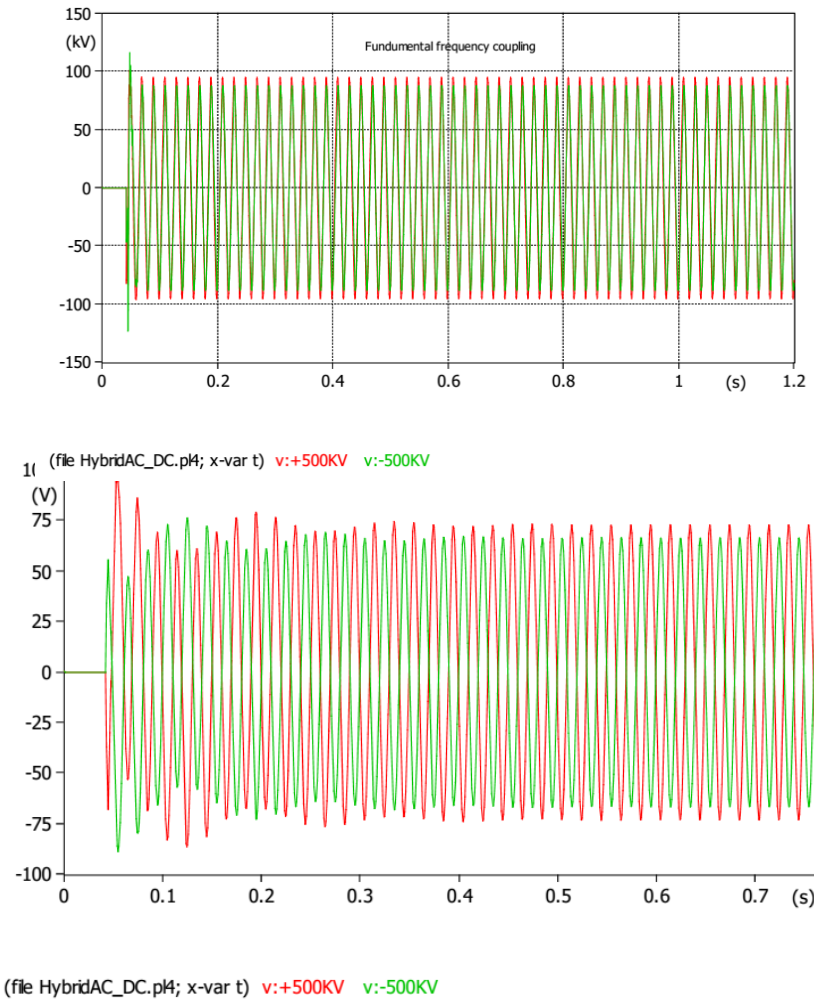

Figure 5:5 Fundamental frequency coupling

5.5.3 Power transferring capacity

The power carrying capacity of the hybrid HVAC/HVDC model simulated by using ATP-EMTP program. The simulation has been conducted for various scenarios. The Hybrid HVAC/HVDC system simulated under light load and heavy load conditions.

The HVAC source is a three phase 400KV rms voltage with energization time of 0.02 sec.For HVDC section cigre 12 pulse HVDC model is used with +500KV volt and -500KV volt. According to [20], the existing 400 KV transmission line has the following network parameters.

Table 5-1 Transmission line parameter

Nominal Voltage (KV)	400
R(Ω/KM) X_L=ωL(Ω/KM) Bc= ωC(s/KM)	0.039 0.161 1.31
Z_C (Ω) SIL(MW)	350 457
Charging MVA/Km	0.76

- At no load condition the 400KV AC output looks like fig 5.6 without shunt reactor, the terminal voltage peak value is rises to 359KV which is 1.1pu. The rise in the receiving end on no load condition is due to the flow of line charging (capacitive) current through line inductance. This is effect first noted by Ferranti, the effect called Ferranti effect.
- As shown on fig 5.6-line capacitance do not have a contribution voltage rise in the case of HDVC line after 0.4sec, the output terminal is flat to ±500KV.

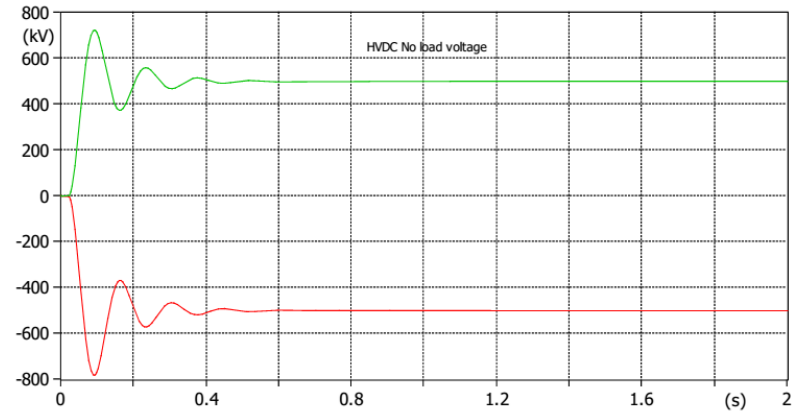

(a)

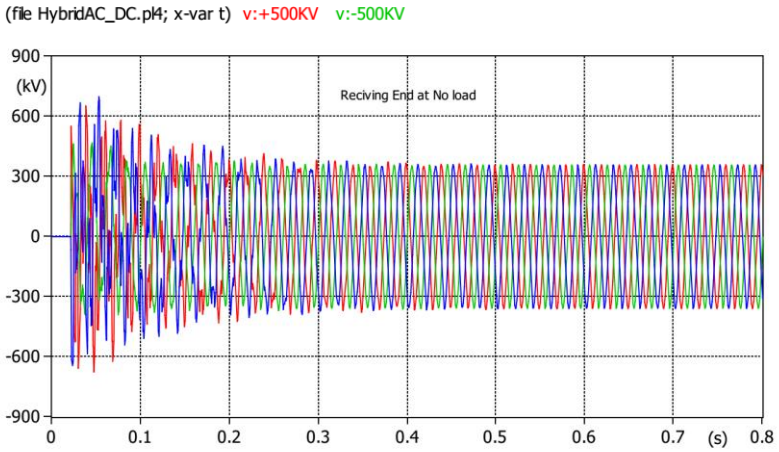

(b)

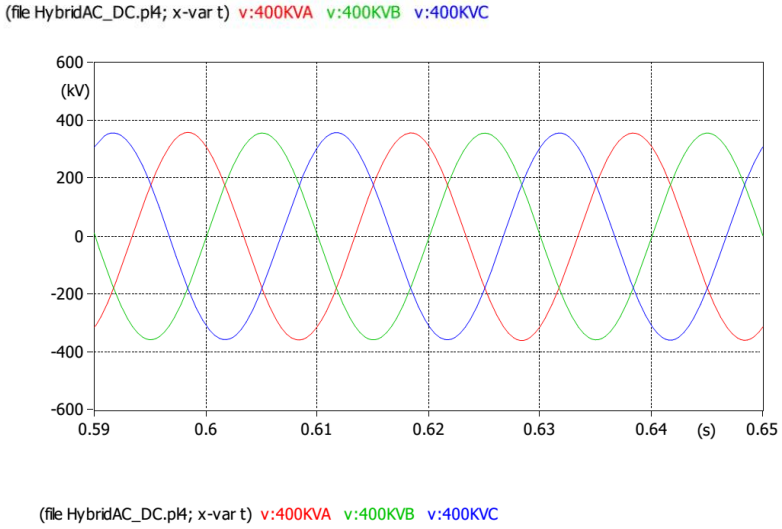

(c)

Figure 5:6 Power transfer at no load condition

- The Hybrid HVAC/HVDC system of simulated under light load, surge impedance loading (SIL) and heavy load. During SIL the system peak voltage about 326 kv and the surge impendence loading goes to about 455MW which is approximated with technical data

- During light load condition the system peak voltage increases up to 356 KV and for heavy load is up to 311 KV. For all simulation both HVAC and HVDC sources are energized.

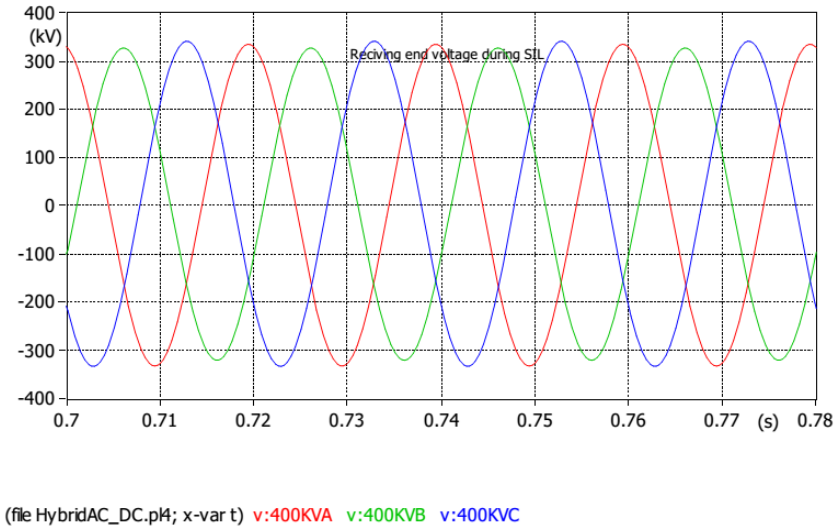

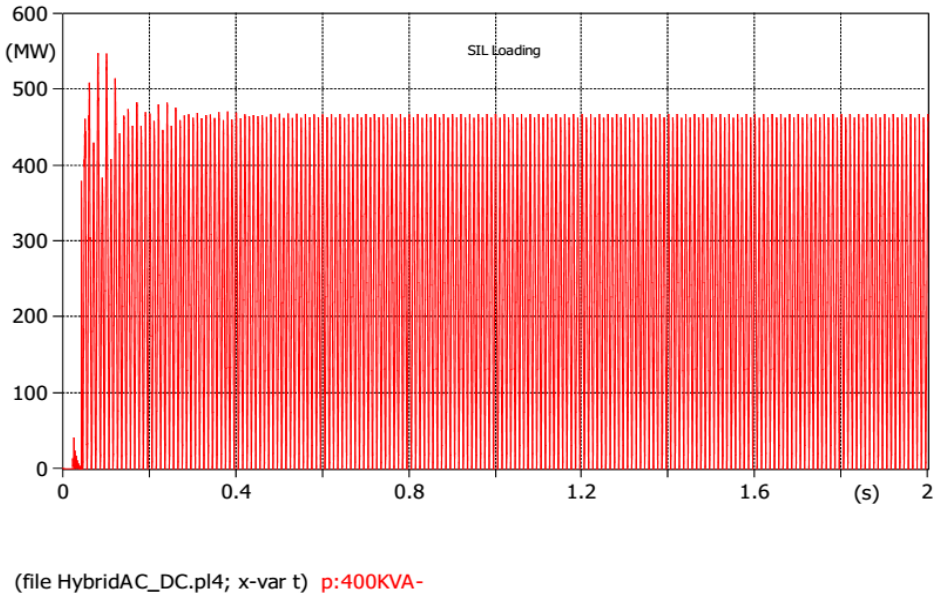

Figure 5:7 SIL loading

The existing Gibee III switch yard equipped with three single phase 110MVA shunt reactor are used when we consider the shunt reactor to the system the terminal voltage compensated during light load. When the hybrid system operating both circuits HVAC and HVDC evacuate power with a rated value of 2.34GW and both the 3 bundle bipolar lines loaded to the 1634A. The HVAC system can transfer a 585MW per phase without exceeding the operational limits of receiving end voltage 400KV± 10% and δ_{max}= 30^{o}

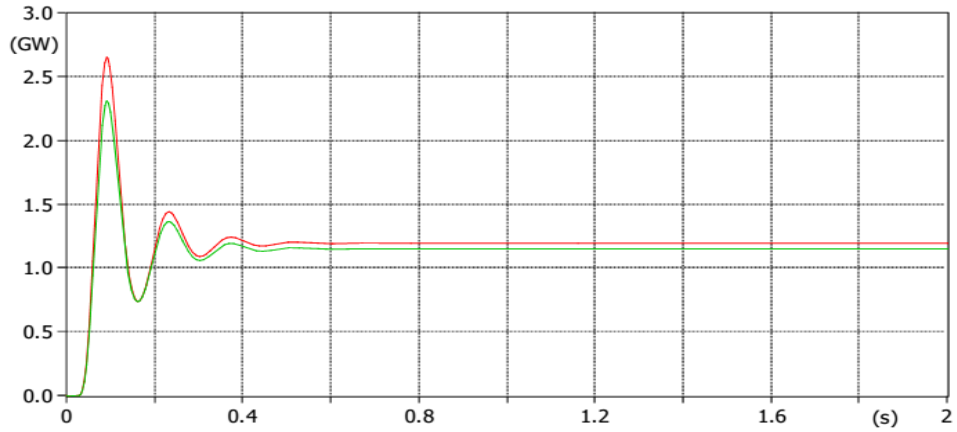

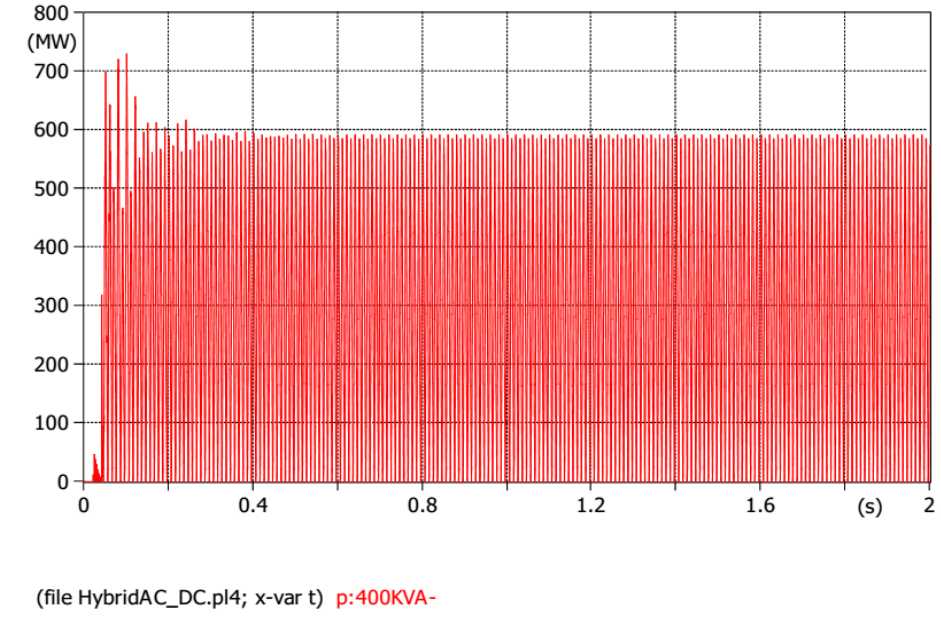

Figure 5:8 Hybrid HVAC/HVDC loading

5.5.4 Power transfer when one pole fails

The main advantage of hybrid HVAC/HVDC system is that the system can supply power even if either of the poles of a hybrid system fails. This simulation has been done to study the characteristics of the system if one of the poles fails.

- If the fault (pole –to ground or pole to phase fault) happened on hybrid HVAC/HVDC line at 0.4 sec, the hybrid system faces a disturbance for 0.2 sec and stays stable after that. The negative terminal voltage deeps to -225KV after 0.046sec and return back to -492KV. The fault also has the effect on 400KV AC system, the voltage experience a disturbance for 0.2 sec then keep working at normal condition [Fig 5:9].

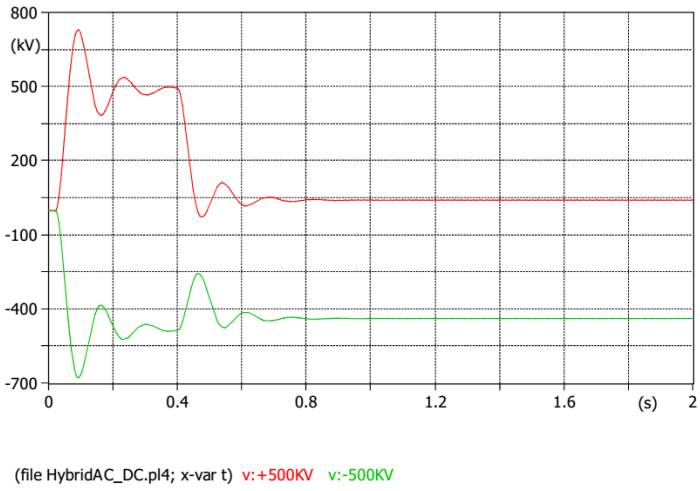

Figure 5:9 power transfer when positive pole fails

- If the fault (pole to ground or pole to phase fault) happened on hybrid HVAC/HVDC line at 0.4 sec the positive pole experiences the voltage dip after 0.062sec and stays for 0.12sec to the magnitude of 264KV. The positive pole operates on stable condition after 0.2 sec from fault occurrence with magnitude of 496KV. The loss of negative pole also has a significant disturbance for 0.2 sec on 400KV HVAC line as shown in fig 5:10

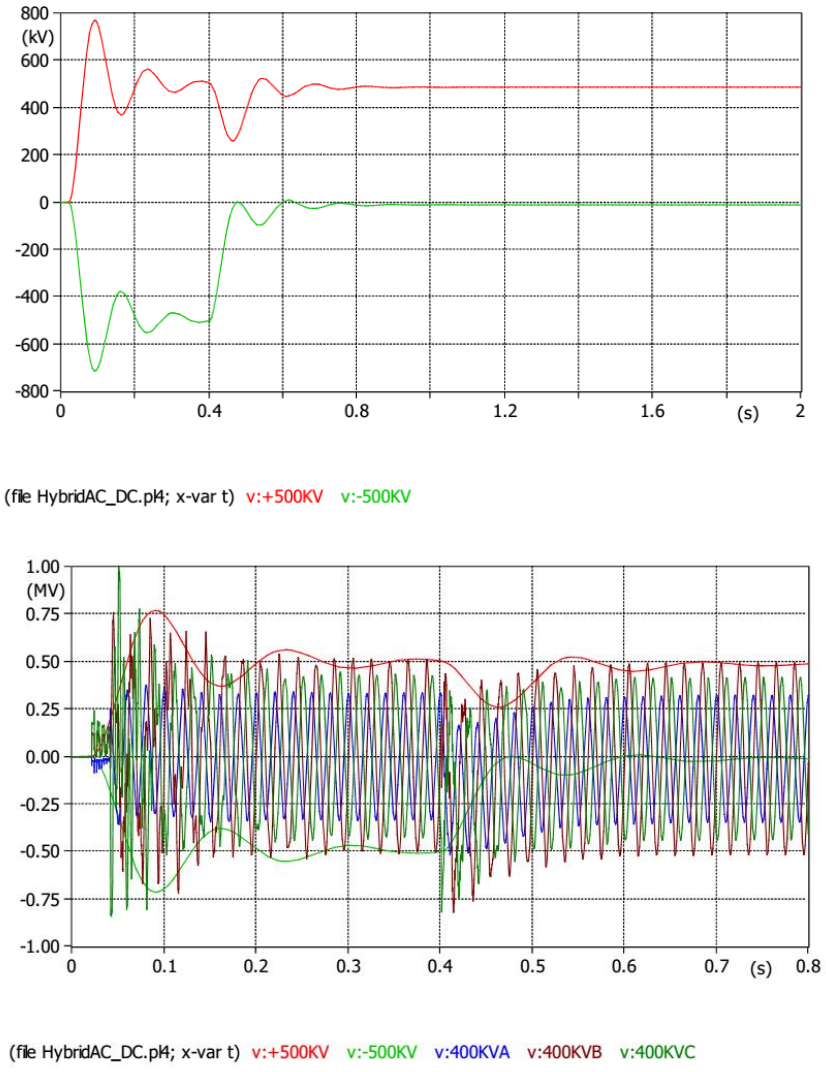

Figure 5:10 power transfer when Negative pole fails

5.6 Electric Field to the ground level.

To simulate the electric field configuration of hybrid HVAC/HVDC line quick filed Transient Electric module is used to study the field distribution between the conductors. The hybrid tower is configured according to the proposed line with pole spacing is 17m and phase spacing is 8.5m. The last conductor ground clearance is 35m. Two model of configuration has been simulated for electric field simulation. The first one is when the positive pole of bipolar HVDC line on top of negative pole the second option is vice versa.

During simulation measurement is taken 1m above the ground with lateral distance configuration of 60 m to the left and right of the tower center is used. The highest electric-field strength occurs directly under the overhead conductor, and the lowest electric-field strength normally occurs far away from conductor. The maximum electric field is measured when the positive pole is above the negative pole (configuration-2) with the magnitude of 3.8kv/m at the center (below the tower) and the minimum value is measured 0.3kv/m about 50m from left and right of the tower. When negative pole is above positive pole (configuration – 1), the maximum electric field measured 1m above the ground is about 1.95KV/m. The field measurement is lies on the standard [15], on international standard for high voltages (320-500KV) under the line is 3-5kv/m and the minimum filed values can be from 0.2 -0.5 kv/m at 25m from the tower[15].

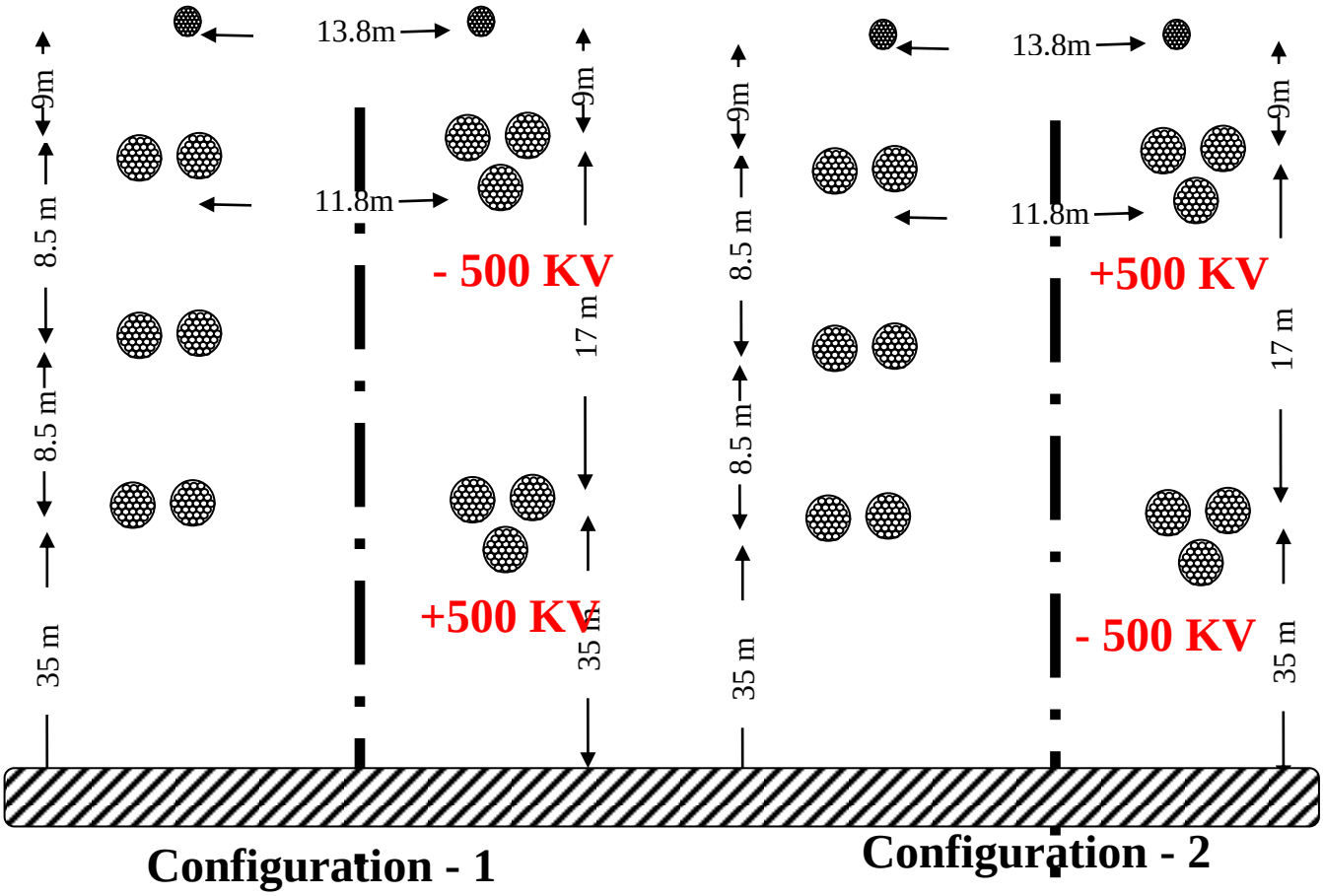

Figure 5:11 *Hybrid HVAC/HVDC model configuration option*

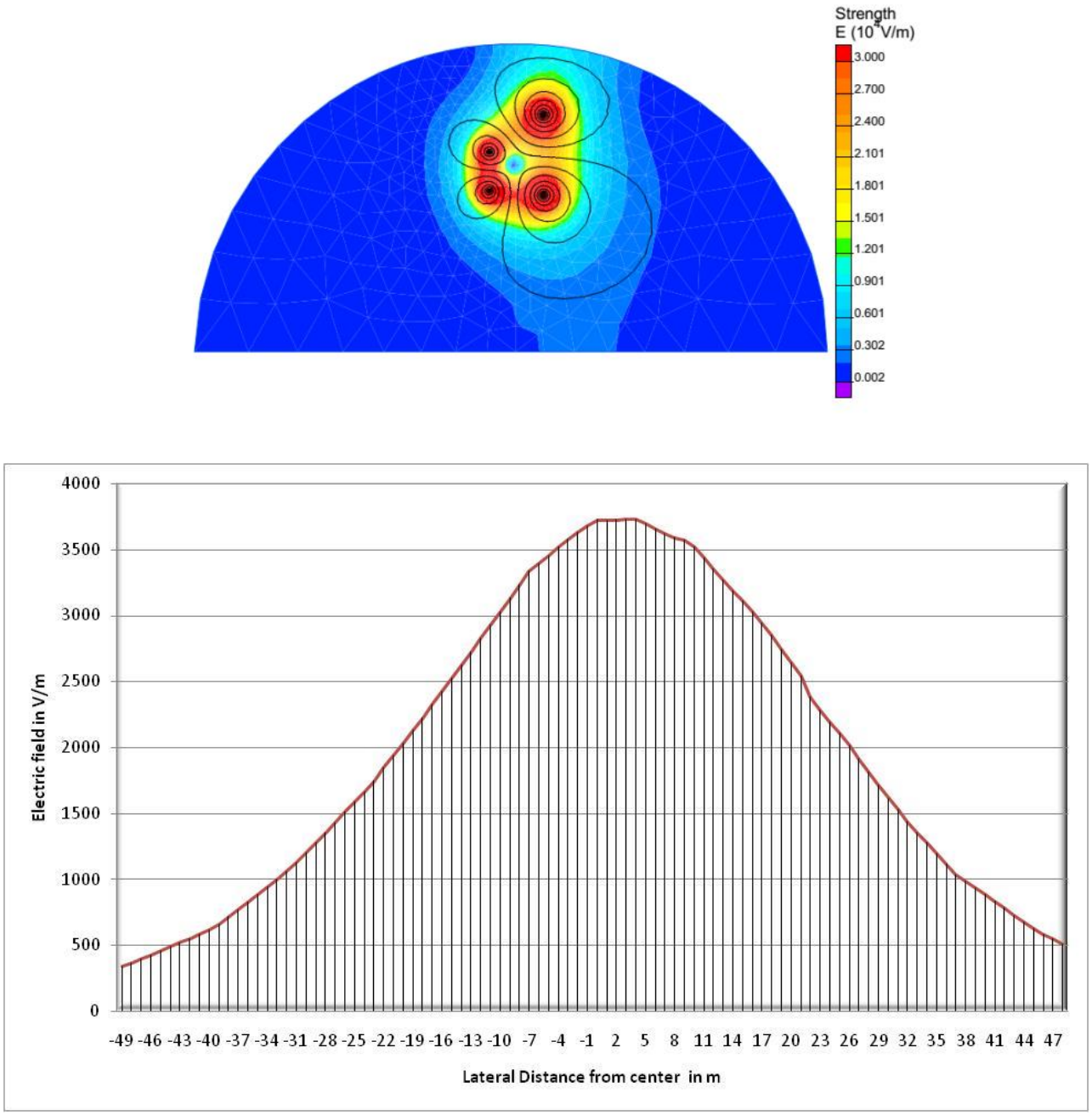

Figure 5:12 Electric field at 1m from ground level (Confuguartion-1)

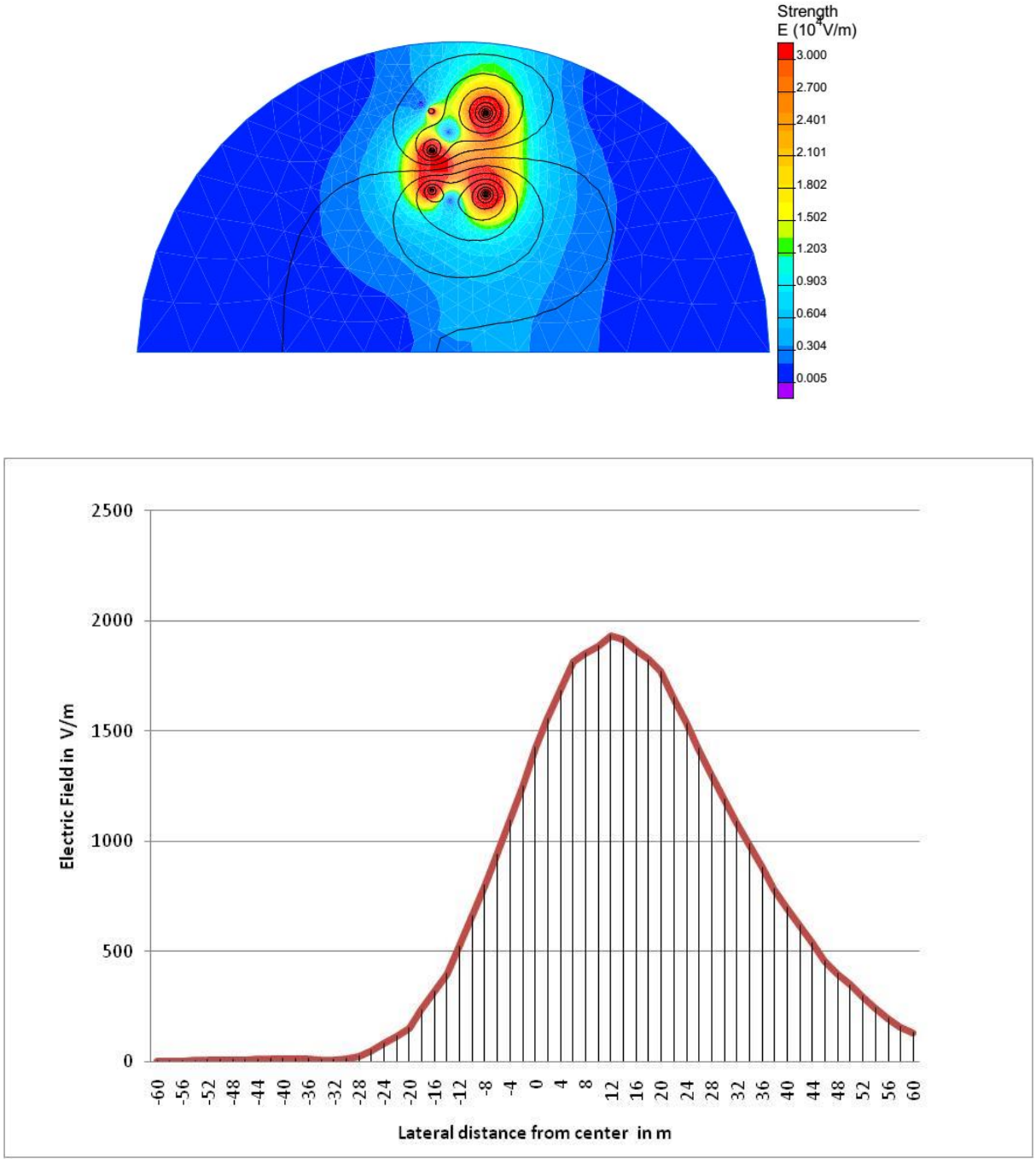

Figure 5:13 Electric field at 1m from ground level (Confuguartion-2)

CHAPTER SIX

Conclusion, Recommendation and Future Work

In this chapter conclusion based on the simulation studies carried out in the previous chapter are presented, recommendation is made and topics for further research in this area are suggested

6.1 Conclusion

Form this thesis work the following conclusion are made:

- It has been seen that the hybrid HVAC/HVDC model can increase the power carrying capacity of one part of double circuit tower from 1.5MVA to 2.5GW. This huge amount of power can be achieved with a minimum investment cost by reusing the existing tower, conductor and right of way.
- The power loss for existing 400KV HVAC line both due to corona and I^2R is greater than for that of the hybrid HVAC/HVDC line. The total active power loss is calculated as 167MW for 400KV AC and 71MW for Hybrid HVAC/HVDC line. HVAC line efficiency is about 91% and 97% for hybrid HVAC/HVDC line. This figure quite significant for utility company.
- Regarding to reliability again the hybrid HVAC/HVDC line is superior over existing line. If one pole of HVDC system affected by fault and disconnected from system, the bipolar line acts as a monoplar line and supplies 50% of the total power. For HVAC case, ifone of the phases fails due to fault, the overall power will be interrupted.
- On the economic point of view, it is known that HVDC Converter stations are expensive compared to HVAC substation with the same capacity. But for this project, since we have used the existing tower and conductor, the investment cost has been significantly lowered. On socio-economic point of view, as we know Gibee III- Addis Ababa 400 KV route is densely populated area and covered by different type of crops and vegetation, as a result EIA and RAP costs will be high for new transmission line project

- The investment cost for constructing new single circuit 400KV HVAC line to accommodate 1500MVA is about 855,978,477.20 USD for 402KM (17,958,428,451.66 Birr). The Hybrid HVAC/HVDC line with a power transferring capacity of 2.5GW costs 439,173,420.00 USD (9,200,683,149.00 Birr) The price reduction is about 416,805,057.20 USD (8,732,065,948.34 Birr). From the investment point of view, the total cost reduction is about 49%. It has been also verified that the investment cost is almost half of the new single circuit 400 KV HVAC line.
- Considering both technical and economical aspect, we can conclude that Hybrid HVAC/HVDC system is more economical and efficient for upgrading transmission line capacity.

6.2 Recommendation

Based on the result of the studies carried out in this thesis, we strongly recommend that EEP must consider the option of using hybrid HVAC/HVDC system. By doing so, the utility company can save cost, increase transmission efficiency and reduce socio-economic problem maintain from resettlement programs.

6.3 Suggestion for future work

For the future, it is suggested to perform experimental research and produce prototype in the laboratory to verify simulated results and gain more practical knowledge in this area.

REFERENCES

[1] Lei Chen, Kan-Jun Zhang, Yong-Jun Xia, and Gang Hu Hybrid Simulation of ±500 kV *"HVDC Power Transmission Project Based on Advanced Digital Power System Simulator",* JOURNAL OF LECTRONIC SCIENCE AND TECHNOLOGY, VOL. 11, NO. 1, MARCH 2013

[2] M. Kizilcay, A. Agdemir, M. Lösing *"Interaction of a HVDC System with 400-kV AC*
Systems on the Same Tower International Conference on Power Systems Transients" (IPST2009) in Kyoto, Japan June 3-6, 2009

[3] Jan Lundkvist Igor Gutman Lars Weimers "*Feasibility study for converting 380 kV AC lines to hybrid AC / DC lines EPRI High-Voltage Direct Current & Flexible AC Transmission Systems Conference"*, November 5 – 6 , 2009, Westminster, CO, USA

[4] POVH*, D. RETZMANN, E. TELTSCH U. KERIN, R. MIHALIC *"Advantages of Large AC/DC System Interconnections"*, 21 rue d'Artois, F-75008 PARIS

[5] Dr. Michael Häusler ,Gernot Schlayer and Gerd Fitterer *"Converting AC power lines to DC for higher transmission ratings'* ABB Review 1997

[6] Wenping Cao, Ying Xie and Zheng Tan , *"Wind Turbine Generator Technologies"* ,InTech 2012

[7] http://www.mpoweruk.com/index.htm, Solar Power Technology and Economics

[8] Wenping Cao, Ying Xie and Zheng Tan , *"Wind Turbine Generator Technologies"* ,InTech 2012

[9] Leonard L. Grigsby , "Electric Power Engineering Handbook", Taylor & Francis Group, LLC, 2006

[10] H.M. Ryan , *"High voltage engineering and testing"*, 2nd ed, London , united kingdom, the institute of of electrical engineers , UK, 2011

[11] Juho Yli-Hannuksela, "*The Transmission Line Cost Calculation*", 2011

[12] http://skm-system.com.

[13] Mohd junaize mohd Noor, "*application of knowledge –based fuzzy interference system on high voltage transmission line maintenance "* , 2004

[14] C. Bayliss, "transmission and Distribution engineering" , 2nd ed, Manchester, 2011

[15] *"ACSR aluminum conductor bare"* 2003

[16] Konstantin O. Papailiou Frank Schmuck, *"Silicone Composite Insulators",*Springer-Verlag Berlin Heidelberg 2013

[17] Dr.-Ing. Tekn. dr.h.c. Erich Uhlmann ,"*Power Transmission by Direct Current"*Springer-Verlag,1975

[18] D.G. Roice, R.J. Gursky, and Z. E. Trad, "*Cost of Electrical Power Losses for use in Economic Evaluations",* IEEE Transactions on Power Systems, Vol. 4, No. 2, May 1989

[19] Chan-Ki Kim , Vijay K. Sood , Gil-Soo Jang , Seong-Joo Lim and Seok-Jin Lee "HVDC TRANSMISSION Power Conversion Applications in Power Systems", John Wiley & Sons (Asia) Pte Ltd, 2009

[20] Ethiopian Electric corporation, "Gibee III hydro power plant feasibity study "

[21] J. Arrillaga, Y.H. Liu,N.R. Watson "Flexible Power Transmission The HVDC Options", John Wiley & Sons Inc,2007

[22] ACRES International Corporation, *"Life-Cycle Cost Studies for Overhead and Underground Electric Transmission Lines",* New York, July 1996.

[23] George G. Karady and F. Mike Carson *"SITKA-KAKE-PETERSBURG HVDC INTERTIE STUDY",*2011

[24] ACA conductor accessories, *"spacer damper"*,2012

[25] JM GEORGE Z. LODI*, "Design and selection criteria for HVDC overhead transmission lines insulators"*,CIGRÉ Canada, Conference on Power Systems, 2009

[26] Working group 22.12, 207 *"Thermal behavior of overhead conductor"*, August 2012

[27] EPRI "Transmission Line Reference Book HVDC to 600 kV", EPRI Report 1977

[28] Siemens AG Energy Sector, "*High Voltage Direct Current Transmission-Proven Technology for Power Exchange",* 2011

[29] Johan Ulleryd Ming Ye Gérard Moreau, *"Fundamental frequency coupling between HVAC and HVDC lines in the QuebecNew England multiterminal system - Comparison between field measurements and EMTDC simulations",*ABB Power Systems &Hydro-Québec

[30] B. Qin, J. Sheng, Z. Yan, and G. Gela, *"Accurate calculation of ion flowfield under HVDC bipolar transmission lines,*"IEEE Trans. Power Del., vol. 3, no. 1, pp. 368–376, Jan. 1988

[31] Dennis Woodford, Lionel Barthold, Liliana Oprea, Stefan Ulrich, Andreas Fuchs, Nikolaos Papadopoulos, Markus Bornowski *"Determination of Voltage Stress in Case of Operation of a Hybrid HVAC/HVDC Transmission Line",* International Conference on Power Systems Transients (IPST2015) in Cavtat, Croatia June 15-18, 2015

[32] M. Kizilcay, A. Agdemir, M. Lösing , *"Interaction of a HVDC System with 400-kV AC Systems on the Same Tower"* International Conference on Power Systems Transients (IPST2009) in Kyoto, Japan June 3-6, 2009

[33] Jan Lundkvist Igor Gutman Lars Weimers, *"Feasibility study for converting 380 kV AC lines to hybrid AC / DC lines",* EPRI's High-Voltage Direct Current & Flexible AC Transmission Systems Conference , November 5 – 6 , 2009, Westminster, CO, USA

[34] Task Force JWG-B2/B4/C1.17 *,"Impacts of HVDC Lines on the Economics of HVDC Projects"*,June 2008

[35] Alberta Energy, *"Assessment and Analysis of the State-Of-the-Art Electric Transmission Systems with Specific Focus on High-Voltage Direct Current (HVDC), Underground or Other New or Developing Technologies"*, 2009

[36] U. STRAUMANN and C.M. FRANCK, *"Discussion of Converting a Double-Circuit AC Overhead Line to an AC/DC Hybrid Line with Regard to Audible Noise",* High Voltage Laboratory, ETH Zürich

[37] EEPCo, *"Environmental Monitoring Unit (EMU) Gibe III-Sodo 400 kV Power Transmission Lines Project RESETTLEMENT ACTION PLAN",* 2009

[38] Aydin Sakhavati, Mostafa Yaltagiani, Shirin Saleh Ahari, Seyed Mahdi Mahaei *"765 kV Transmission Line Design",* International Journal of Electrical and Computer Engineering (IJECE) , October 2012, pp. 698~707

[39] Ataollah Mokhberdoran, Adriano Carvalho, Helder Leite, Nuno Silva *"A Review on HVDC Circuit Breakers"* IET Renewable Power Generation Conference, RPG2014, At Naples, Italy

[40] H.L. Nakra, Ly X. Bui and Isao Iyoda "*system considerations in converting one circuit of a double circuit AC line to DC". IEEE Transaction on Power Apparatus and Systems, Vol. PAS-103, No. 10, October 1984*

[41] B. JACOBSON, B. WESTMAN, M. P. BAHRMAN, *"500 kV VSC Transmission System for lines and cables",* cigre, 2012 San Francisco Colloquium

[42] Dan Wikström and Carl Öhlen *"Composite Insulation for Reliability Centered Design of compact HVAC & HVDC",* STRI

[43] H. EI-Kishky and R. S. Gorur, *"Electric field computation on an insulating surface with Discrete water droplets,"* IEEE Trans. Dielectrics and Electrical Insulation, vol. 3, pp. 450-456, June. 1996.

[44] http://www.apar.com/html/conductors.html

[45] Lars Weimers, *"Bulk power transmission at extra high voltages, a comparison between transmission lines for HVDC at voltages above 600 kV DC and 800 kV AC.",* ABB Power Technologies AB, 2012

[46] G. Gela, J.J. LaForest and L.E. Zaffanella, "HVDC Transmission Line Reference Book", Electric Power Research Institute, 3412 Hillview Avenue, Palo Alto, California, 1993, section 3, pages 1-188

[47] *nigdha sharma, Kanika Goel, Anmol Gupta, and Hemant Kumar "CORONA EFFECTS ON EHV AC TRANSMISSION LINES", IJSRET, August 2012*

APPENDICES

Appendix A: AAAC Aster 850 conductor specification

Conductoare din aliaj de aluminiu, conform EN 50182 (aliaj din aluminiu, tip AL4), utilizate in Franta
AAAC, All aluminium alloy conductors, acording to EN 50182 (aluminium alloy, type AL4), designed to be used in France

Cod		Sectiune	Numar sarme	Diametru sarma	Diametru conductor	Masa conductor	Forta de rupere nominala	Rezistenta in curent continuu	Capacitatea de transport a curentului
Code		*Cross section* mm^2	*No. of wires*	*Wires diameter* mm	*Overall diameter* mm	*AAAC weight* kg/km	*Breaking Load* N	*Resistance at 20°C* Ohm/km	*Current carrying capacity* A
22-AL4	ASTER 22	22.0	7	2.00	6.00	60.0	7.52	1.4989	166
34-AL4	ASTER 34.4	34.4	7	2.50	7.50	93.8	11.75	0.9593	221
55-AL4	ASTER 54.6	54.6	7	3.15	9.45	148.9	18.66	0.6042	297
76-AL4	ASTER 75.5	75.5	19	2.25	11.3	207.4	25.84	0.4388	367
117-AL4	ASTER 117	117.0	19	2.80	14.0	321.2	40.01	0.2833	486
148-AL4	ASTER 148	148.1	19	3.15	15.8	406.5	50.64	0.2239	567
182-AL4	ASTER 181.6	181.6	37	2.50	17.5	500.3	62.12	0.1831	646
228-AL4	ASTER 228	227.8	37	2.80	19.6	627.6	77.92	0.1460	748
288-AL4	ASTER 288	288.3	37	3.15	22.1	794.3	98.61	0.1154	871
366-AL4	ASTER 366	366.2	37	3.55	24.9	1008.9	120.85	0.0908	1018
570-AL4	ASTER 570	570.2	61	3.45	31.1	1576.0	195.02	0.0585	1356
851-AL4	ASTER 851	850.7	91	3.45	38.0	2360.7	290.93	0.0394	1756
1144-AL4	ASTER 1144	1143.5	91	4.00	44.0	3173.4	377.37	0.0293	2131
1596-AL4	ASTER 1600	1595.9	127	4.00	52.0	4427.5	526.66	0.0210	2650

Appendix B: Electric field simulation result for configuration -2

L (m)	x (m)	y (m)	Nx	Ny	U (V)	E (V/m)	Ex (V/m)	Ey (V/m)
0.00000	-60.0000	1.00000	0.00000		-1.00000	307.311	35.5077	-35.4899
2.00000	-58.0000	1.00000	0.00000		-1.00000	370.927	36.5660	-36.5526
4.00000	-56.0000	1.00000	0.00000		-1.00000	453.785	39.2297	-39.2121
6.00000	-54.0000	1.00000	0.00000		-1.00000	539.821	42.1643	-42.1480
8.00000	-52.0000	1.00000	0.00000		-1.00000	625.857	45.0991	-45.0839
10.0000	-50.0000	1.00000	0.00000		-1.00000	711.892	48.0341	-48.0198
12.0389	-47.9611	1.00000	0.00000		-1.00000	799.601	51.0262	-51.0128
14.0000	-46.0000	1.00000	0.00000		-1.00000	902.510	55.8123	-55.7170
16.0000	-44.0000	1.00000	0.00000		-1.00000	1032.75	63.5334	-63.4497
18.0000	-42.0000	1.00000	0.00000		-1.00000	1163.00	71.2570	-71.1824
20.0000	-40.0000	1.00000	0.00000		-1.00000	1293.24	78.9824	-78.9151
22.0234	-37.9766	1.00000	0.00000		-1.00000	1425.01	86.7994	-86.7381
24.0000	-36.0000	1.00000	0.00000		-1.00000	1621.48	100.659	-100.326
26.0000	-34.0000	1.00000	0.00000		-1.00000	1853.02	116.087	-115.799
28.0000	-32.0000	1.00000	0.00000		-1.00000	2084.56	131.526	-131.272
30.0000	-30.0000	1.00000	0.00000		-1.00000	2316.10	146.972	-146.745
32.0000	-28.0000	1.00000	0.00000		-1.00000	2600.25	167.460	-166.977
34.0000	-26.0000	1.00000	0.00000		-1.00000	3003.35	185.900	-185.465
36.0000	-24.0000	1.00000	0.00000		-1.00000	3406.46	204.350	-203.954
38.0000	-22.0000	1.00000	0.00000		-1.00000	3809.56	222.806	-222.443
40.0000	-20.0000	1.00000	0.00000		-1.00000	4280.05	248.965	-248.804
42.0000	-18.0000	1.00000	0.00000		-1.00000	4786.08	241.582	-241.416
44.0000	-16.0000	1.00000	0.00000		-1.00000	5292.11	234.200	-234.029
46.0000	-14.0000	1.00000	0.00000		-1.00000	5798.14	226.818	-226.642
48.0000	-12.0000	1.00000	0.00000		-1.00000	6409.06	217.857	-199.128
50.0000	-10.0000	1.00000	0.00000		-1.00000	6656.10	133.088	-15.8568
52.0000	-8.00000	1.00000	0.00000		-1.00000	6821.01	236.330	195.936
54.0000	-6.00000	1.00000	0.00000		-1.00000	6814.82	409.386	387.474
56.0000	-4.00000	1.00000	0.00000		-1.00000	4694.11	354.263	328.696
58.0000	-2.00000	1.00000	0.00000		-1.00000	2573.40	300.528	269.919
60.0000	0.00000	1.00000	0.00000		-1.00000	1677.24	362.068	224.989
62.0000	2.00000	1.00000	0.00000		-1.00000	1919.94	681.144	184.192
64.0000	4.00000	1.00000	0.00000		-1.00000	1919.94	1281.30	76.5197
66.0000	6.00000	1.00000	0.00000		-1.00000	1919.94	1902.51	-31.1529
68.0000	8.00000	1.00000	0.00000		-1.00000	1919.94	1943.11	-32.6528
70.0000	10.0000	1.00000	0.00000		-1.00000	1919.94	1959.35	-29.7276
72.0000	12.0000	1.00000	0.00000		-1.00000	1983.96	1988.40	-7.17409
74.0000	14.0000	1.00000	0.00000		-1.00000	1885.08	1962.75	51.9075
76.0000	16.0000	1.00000	0.00000		-1.00000	1885.08	1909.03	49.2244
78.0000	18.0000	1.00000	0.00000		-1.00000	1885.08	1855.31	46.5412
80.0000	20.0000	1.00000	0.00000		-1.00000	1814.91	1794.33	47.7153
82.0000	22.0000	1.00000	0.00000		-1.00000	1550.91	1673.08	73.3280
84.0000	24.0000	1.00000	0.00000		-1.00000	1550.91	1553.47	93.2874

86.0000	26.0000	1.00000	0.00000	-1.00000	1550.91	1434.34	113.247
88.0000	28.0000	1.00000	0.00000	-1.00000	1340.68	1313.03	129.255
90.0000	30.0000	1.00000	0.00000	-1.00000	1105.17	1201.51	128.242
92.0000	32.0000	1.00000	0.00000	-1.00000	1105.17	1097.08	125.029
94.0000	34.0000	1.00000	0.00000	-1.00000	1105.17	992.728	121.816
96.0000	36.0000	1.00000	0.00000	-1.00000	1105.17	888.467	118.602
98.0000	38.0000	1.00000	0.00000	-1.00000	650.332	787.350	102.931
100.000	40.0000	1.00000	0.00000	-1.00000	650.332	704.622	99.7349
102.000	42.0000	1.00000	0.00000	-1.00000	650.332	622.001	96.5392
104.000	44.0000	1.00000	0.00000	-1.00000	650.332	539.534	93.3434
106.000	46.0000	1.00000	0.00000	-1.00000	579.855	458.928	86.8208
108.000	48.0000	1.00000	0.00000	-1.00000	287.301	401.566	69.3049
110.000	50.0000	1.00000	0.00000	-1.00000	287.301	350.078	65.2354
112.000	52.0000	1.00000	0.00000	-1.00000	287.301	298.682	61.1660
114.000	54.0000	1.00000	0.00000	-1.00000	287.301	247.436	57.0965
116.000	56.0000	1.00000	0.00000	-1.00000	287.301	196.456	53.0270
118.000	58.0000	1.00000	0.00000	-1.00000	92.1372	160.843	41.9501
120.000	60.0000	1.00000	0.00000	-1.00000	92.1372	134.590	39.9874

Appendix C: Electric field simulation result for configuration -1

L (m)	x (m)	y (m)	Nx	Ny	U (V)	E (V/m)	Ex (V/m)	Ey (V/m)
0.00000	-60.0000	1.00000	0.00000		-1.00000	307.311	35.5077	-35.4899
2.00000	-58.0000	1.00000	0.00000		-1.00000	370.927	36.5660	-36.5526
4.00000	-56.0000	1.00000	0.00000		-1.00000	453.785	39.2297	-39.2121
6.00000	-54.0000	1.00000	0.00000		-1.00000	539.821	42.1643	-42.1480
8.00000	-52.0000	1.00000	0.00000		-1.00000	625.857	45.0991	-45.0839
10.0000	-50.0000	1.00000	0.00000		-1.00000	711.892	48.0341	-48.0198
12.0389	-47.9611	1.00000	0.00000		-1.00000	799.601	51.0262	-51.0128
14.0000	-46.0000	1.00000	0.00000		-1.00000	902.510	55.8123	-55.7170
16.0000	-44.0000	1.00000	0.00000		-1.00000	1032.75	63.5334	-63.4497
18.0000	-42.0000	1.00000	0.00000		-1.00000	1163.00	71.2570	-71.1824
20.0000	-40.0000	1.00000	0.00000		-1.00000	1293.24	78.9824	-78.9151
22.0234	-37.9766	1.00000	0.00000		-1.00000	1425.01	86.7994	-86.7381
24.0000	-36.0000	1.00000	0.00000		-1.00000	1621.48	100.659	-100.326
26.0000	-34.0000	1.00000	0.00000		-1.00000	1853.02	116.087	-115.799
28.0000	-32.0000	1.00000	0.00000		-1.00000	2084.56	131.526	-131.272
30.0000	-30.0000	1.00000	0.00000		-1.00000	2316.10	146.972	-146.745
32.0000	-28.0000	1.00000	0.00000		-1.00000	2600.25	167.460	-166.977
34.0000	-26.0000	1.00000	0.00000		-1.00000	3003.35	185.900	-185.465
36.0000	-24.0000	1.00000	0.00000		-1.00000	3406.46	204.350	-203.954
38.0000	-22.0000	1.00000	0.00000		-1.00000	3809.56	222.806	-222.443
40.0000	-20.0000	1.00000	0.00000		-1.00000	4280.05	248.965	-248.804
42.0000	-18.0000	1.00000	0.00000		-1.00000	4786.08	241.582	-241.416
44.0000	-16.0000	1.00000	0.00000		-1.00000	5292.11	234.200	-234.029
46.0000	-14.0000	1.00000	0.00000		-1.00000	5798.14	226.818	-226.642
48.0000	-12.0000	1.00000	0.00000		-1.00000	6409.06	217.857	-199.128
50.0000	-10.0000	1.00000	0.00000		-1.00000	6656.10	133.088	-15.8568
52.0000	-8.00000	1.00000	0.00000		-1.00000	6821.01	236.330	195.936
54.0000	-6.00000	1.00000	0.00000		-1.00000	6814.82	409.386	387.474
56.0000	-4.00000	1.00000	0.00000		-1.00000	4694.11	354.263	328.696
58.0000	-2.00000	1.00000	0.00000		-1.00000	2573.40	300.528	269.919
60.0000	0.00000	1.00000	0.00000		-1.00000	1677.24	362.068	224.989
62.0000	2.00000	1.00000	0.00000		-1.00000	1919.94	681.144	184.192
64.0000	4.00000	1.00000	0.00000		-1.00000	1919.94	1281.30	76.5197
66.0000	6.00000	1.00000	0.00000		-1.00000	1919.94	1902.51	-31.1529
68.0000	8.00000	1.00000	0.00000		-1.00000	1919.94	1943.11	-32.6528
70.0000	10.0000	1.00000	0.00000		-1.00000	1919.94	1959.35	-29.7276
72.0000	12.0000	1.00000	0.00000		-1.00000	1983.96	1988.40	-7.17409
74.0000	14.0000	1.00000	0.00000		-1.00000	1885.08	1962.75	51.9075
76.0000	16.0000	1.00000	0.00000		-1.00000	1885.08	1909.03	49.2244
78.0000	18.0000	1.00000	0.00000		-1.00000	1885.08	1855.31	46.5412
80.0000	20.0000	1.00000	0.00000		-1.00000	1814.91	1794.33	47.7153
82.0000	22.0000	1.00000	0.00000		-1.00000	1550.91	1673.08	73.3280
84.0000	24.0000	1.00000	0.00000		-1.00000	1550.91	1553.47	93.2874

48.0000	-1.10443	5.42970	-0.00807728	-0.999967	-19183.0	3675.15	219.045	3668.61
49.0000	-0.104458	5.42163	-0.00807728	-0.999967	-19395.4	3724.68	171.415	3720.74
50.0000	0.895509	5.41355	-0.00807728	-0.999967	-19435.4	3723.80	126.433	3721.65
51.0000	1.89548	5.40547	-0.00807728	-0.999967	-19507.9	3724.63	69.5946	3723.98

52.0000	2.89544	5.39739	-0.00807728	-0.999967	-19580.4	3726.33	12.7559	3726.31
53.0000	3.89541	5.38932	-0.00807728	-0.999967	-19652.9	3728.89	-44.0829	3728.63
54.0000	4.89538	5.38124	-0.00807728	-0.999967	-19424.3	3694.26	-95.2017	3693.03
55.0000	5.89535	5.37316	-0.00807728	-0.999967	-19167.3	3656.75	-145.780	3653.85
56.0000	6.89531	5.36509	-0.00807728	-0.999967	-18910.3	3619.99	-196.357	3614.66
57.0000	7.89528	5.35701	-0.00807728	-0.999967	-18689.1	3590.26	-244.751	3581.91
58.0000	8.89525	5.34893	-0.00807728	-0.999967	-18525.6	3571.26	-289.633	3559.50
59.0000	9.89522	5.34085	-0.00807728	-0.999967	-18434.0	3517.93	-306.244	3504.58
60.0000	10.8952	5.33278	-0.00807728	-0.999967	-17923.8	3434.36	-341.029	3417.39
61.0000	11.8952	5.32470	-0.00807728	-0.999967	-17413.6	3351.33	-375.814	3330.19
62.0000	12.8951	5.31662	-0.00807728	-0.999967	-16903.4	3268.89	-410.600	3243.00
63.0000	13.8951	5.30854	-0.00807728	-0.999967	-16393.1	3187.08	-445.385	3155.81
64.0000	14.8951	5.30047	-0.00807728	-0.999967	-15882.9	3105.95	-480.170	3068.61
65.0000	15.8950	5.29239	-0.00807728	-0.999967	-15372.7	3025.56	-514.955	2981.42
66.0000	16.8950	5.28431	-0.00807728	-0.999967	-15163.1	2941.34	-529.958	2893.21
67.0000	17.8950	5.27624	-0.00807728	-0.999967	-14808.4	2846.64	-531.249	2796.63
68.0000	18.8949	5.26816	-0.00807728	-0.999967	-14143.0	2744.68	-531.184	2692.79
69.0000	19.8949	5.26008	-0.00807728	-0.999967	-13477.7	2642.88	-531.119	2588.96
70.0000	20.8949	5.25200	-0.00807728	-0.999967	-12812.3	2541.23	-531.054	2485.13
71.0000	21.8948	5.24393	-0.00807728	-0.999967	-12146.9	2439.78	-530.989	2381.29
72.0000	22.8948	5.23585	-0.00807728	-0.999967	-11481.5	2338.53	-530.924	2277.46
73.0000	23.8948	5.22777	-0.00807728	-0.999967	-11246.6	2249.13	-519.933	2188.21
74.0000	24.8947	5.21969	-0.00807728	-0.999967	-11229.2	2165.65	-503.418	2106.32
75.0000	25.8947	5.21162	-0.00807728	-0.999967	-10672.6	2070.04	-493.153	2010.44
76.0000	26.8947	5.20354	-0.00807728	-0.999967	-10015.2	1972.27	-484.058	1911.94
77.0000	27.8946	5.19546	-0.00807728	-0.999967	-9357.71	1874.61	-474.962	1813.44
78.0000	28.8946	5.18738	-0.00807728	-0.999967	-8700.24	1777.09	-465.866	1714.94
79.0000	29.8946	5.17931	-0.00807728	-0.999967	-8042.78	1679.74	-456.771	1616.44
80.0000	30.8945	5.17123	-0.00807728	-0.999967	-7833.25	1594.49	-464.036	1525.47
81.0000	31.8945	5.16315	-0.00807728	-0.999967	-7821.01	1515.36	-478.507	1437.83
82.0000	32.8945	5.15508	-0.00807728	-0.999967	-7646.56	1435.82	-480.975	1352.86
83.0000	33.8944	5.14700	-0.00807728	-0.999967	-7117.75	1353.33	-457.225	1273.76
84.0000	34.8944	5.13892	-0.00807728	-0.999967	-6588.94	1270.86	-433.474	1194.65
85.0000	35.8944	5.13084	-0.00807728	-0.999967	-6060.13	1188.41	-409.724	1115.54
86.0000	36.8943	5.12277	-0.00807728	-0.999967	-5531.32	1105.97	-385.973	1036.44
87.0000	37.8943	5.11469	-0.00807728	-0.999967	-5120.09	1050.03	-365.318	984.434
88.0000	38.8943	5.10661	-0.00807728	-0.999967	-4715.04	995.484	-344.825	933.855
89.0000	39.8942	5.09853	-0.00807728	-0.999967	-4309.99	940.939	-324.332	883.275
90.0000	40.8942	5.09046	-0.00807728	-0.999967	-3904.94	886.397	-303.839	832.695
91.0000	41.8942	5.08238	-0.00807728	-0.999967	-3644.76	832.249	-288.170	780.766
92.0000	42.8941	5.07430	-0.00807728	-0.999967	-3638.97	778.908	-280.971	726.466
93.0000	43.8941	5.06623	-0.00807728	-0.999967	-3633.18	725.781	-273.772	672.166
94.0000	44.8941	5.05815	-0.00807728	-0.999967	-3536.09	676.626	-263.761	623.100
95.0000	45.8940	5.05007	-0.00807728	-0.999967	-3255.40	635.027	-248.098	584.557
96.0000	46.8940	5.04199	-0.00807728	-0.999967	-2974.71	593.428	-232.434	546.014
97.0000	47.8940	5.03392	-0.00807728	-0.999967	-2694.02	551.830	-216.770	507.471

Appendix D: – Composite suspension insulator specification

Sediver composite suspension insulators

40 kip - (180 kN)

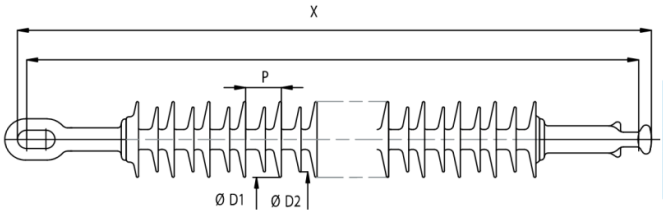

Section length adjustments

Ground fitting	Line fitting	Type letters	Adjustments inches	Adjustments mm
Socket	Ball	SB	-0.2	-5
Y-clevis	Ball	YB	+0.7	+19
Y-clevis	Tongue	YT	+1.7	+43
Clevis	Tongue	CT	+1.3	+34
Eye	Eye	EE	+1.1	+29

Typical Line Voltage	Sediver Catalog Designation	Number of Sheds	Section Length Inches (mm)	Leakage Distance Inches (mm)	Dry Arcing* Distance Inches (mm)	Low Frequency* Flashover - ANSI Dry kV	Low Frequency* Flashover - ANSI Wet kV	Critical Impulse* Flashover - ANSI Pos. kV	Critical Impulse* Flashover - ANSI Neg. kV	Approx. Net Wt Lbs. (kg)
345 kV with grading ring*	SEDNEB180XF81S1	81	99.4 *2524*	246 *6249*	85.6 *2175*	795	720	1420	1440	23.4 *10.6*
	SEDNEB180XM81S1			277.9 *7060*	85.8 *2180*	795	720	1420	1445	25.9 *11.7*
	SEDNEB180XL81S1			365 *9270*	86.5 *2197*	805	725	1430	1455	36.5 *16.6*
	SEDNEB180XF87S1	87	105.9 *2689*	264.3 *6714*	92.1 *2340*	850	770	1520	1540	24.3 *11*
	SEDNEB180XM87S1			298.6 *7585*	92.3 *2345*	850	770	1520	1540	27 *12.2*
	SEDNEB180XL87S1			392.1 *9959*	93 *2362*	860	775	15305	1550	38.4 *17.4*
	SEDNEB180XF93S1	93	112.4 *2854*	282.6 *7179*	98.6 *2505*	905	820	1615	1635	25.1 *11.4*
	SEDNEB180XM93S1			319.3 *8110*	98.8 *2510*	905	820	1620	1635	28 *12.7*
	SEDNEB180XL93S1			419.2 *10647*	99.5 *2527*	915	825	1630	1645	40.2 *18.2*
	SEDNEB180XF99S1	99	118.9 *3019*	300.9 *7644*	105.1 *2670*	960	865	1715	1730	26 *11.8*
	SEDNEB180XM99S1			339.9 *8635*	105.3 *2675*	960	870	1720	1730	29.1 *13.2*
	SEDNEB180XL99S1			446.3 *11336*	106 *2692*	965	870	1730	1740	42.1 *19.1*
500 kV with grading rings*	SEDNEB180XF119S5	119	140.5 *3569*	361.9 *9194*	123.2 *3129*	1110	995	1985	1990	42 *19*
	SEDNEB180XM119S5			408.8 *10385*	123.2 *3129*	1110	995	1985	1990	45.7 *20.7*
	SEDNEB180XL119S5			536.6 *13631*	123.2 *3129*	1110	995	1985	1990	61.3 *27.8*
	SEDNEB180XF129S5	129	151.3 *3844*	392.5 *9969*	134 *3404*	1200	1070	2145	2145	43.4 *19.7*
	SEDNEB180XM129S5			443.3 *11260*	134 *3404*	1200	1070	2145	2145	47.4 *21.5*
	SEDNEB180XL129S5			581.8 *14778*	134 *3404*	1200	1070	2145	2145	64.4 *29.2*

Table shows typical models. Higher voltages and other dimensions or fittings combinations are available on request. Tests complying with ANSI C29.11

*When grading rings are included in the designation, the electrical values and dry arcing distance are given accordingly

SED	N	Y B	120	XM	25	S	0
	ANSI Standard	End fitting type	SML in kN	Shed profile	Number of sheds	Material S for Silicon E for EPDM	Number/type of grading rings

Appendix E: – Constants for thermal rating calculation

Table I. Constants for calculation of forced convective heat transfer from conductors with steady crossflow of air

Surface	*Re*		B_1	n
	from	to		
Stranded all surfaces	10^2	$2.65 \cdot 10^3$	0.641	0.471
Stranded $R_f \leq 0.05$	$> 2.65 \cdot 10^3$	$5 \cdot 10^4$	0.178	0.633
Stranded $R_f > 0.05$	$> 2.65 \cdot 10^3$	$5 \cdot 10^4$	0.048	0.800

Table II. Constants for calculation of natural convective heat transfer from conductors in air

Gr·Pr		A_2	m_2
from	to		
10^2	10^4	0.850	0.188
10^4	10^6	0.480	0.250

Appendix F: life cost analysis

Hybrid HVAC/HVDC line

Economic analysis

Interest rate	10%	IRR	74%
Energy cost [Sep 2015]	0.0291 $/KWh	Loss factor	0.38
Energy generation cost	0.067 $/KWh	Annual Load growth	1.2%
Load factor	0.57		

S/N	year	Capital cost [USD/km]	O&M cost [USD]	Loss cost [USD/km]	Total Cost [USD]	PV factor	PV Cost [USD]	NPV [USD]
1	2016	873,977.02	13,109.66	26,899.22	913,985.90	0.91	(830,896.27)	(830,896.27)
2	2017	812,798.63	13,655.89	47,851.32	874,305.84	0.83	722,566.81	(108,329.46)
3	2018	755,902.73	14,224.89	68,566.18	838,693.79	0.75	630,123.06	521,793.60
4	2019	702,989.54	14,817.59	87,397.87	805,204.99	0.68	549,965.85	1,071,759.45
5	2020	653,780.27	15,434.99	104,517.58	773,732.84	0.62	480,427.22	1,552,186.67
6	2021	608,015.65	16,078.11	120,080.96	744,174.73	0.56	420,067.23	1,972,253.90
7	2022	565,454.56	16,748.04	134,229.49	716,432.08	0.51	367,642.94	2,339,896.84
8	2023	525,872.74	17,445.87	147,091.78	690,410.39	0.47	322,081.54	2,661,978.38
9	2024	489,061.65	18,172.78	158,784.78	666,019.21	0.42	282,457.16	2,944,435.54
10	2025	454,827.33	18,929.98	169,414.78	643,172.09	0.39	247,970.68	3,192,406.22
11	2026	422,989.42	19,718.73	179,078.41	621,786.56	0.35	217,932.40	3,410,338.62
12	2027	393,380.16	20,540.34	187,863.53	601,784.04	0.32	191,746.94	3,602,085.56
13	2028	365,843.55	21,396.19	195,850.01	583,089.75	0.29	168,900.33	3,770,985.89
14	2029	340,234.50	22,287.70	203,110.44	565,632.64	0.26	148,948.75	3,919,934.64
15	2030	316,418.08	23,216.35	209,710.83	549,345.27	0.24	131,508.89	4,051,443.53
16	2031	294,268.82	24,183.70	215,711.19	534,163.71	0.22	116,249.59	4,167,693.11
17	2032	273,670.00	25,191.36	221,166.06	520,027.41	0.20	102,884.65	4,270,577.77
18	2033	254,513.10	26,241.00	226,125.03	506,879.13	0.18	91,166.67	4,361,744.43
19	2034	236,697.18	27,334.37	230,633.19	494,664.74	0.16	80,881.64	4,442,626.07
20	2035	220,128.38	28,473.30	234,731.51	483,333.19	0.15	71,844.40	4,514,470.47
21	2036	204,719.39	29,659.69	238,457.26	472,836.34	0.14	63,894.64	4,578,365.11
22	2037	190,389.04	30,895.51	241,844.30	463,128.85	0.12	56,893.51	4,635,258.63
23	2038	177,061.80	32,182.82	244,923.43	454,168.06	0.11	50,720.65	4,685,979.28
24	2039	164,667.48	33,523.77	247,722.65	445,913.90	0.10	45,271.68	4,731,250.96
25	2040	153,140.75	34,920.60	250,267.38	438,328.73	0.09	40,455.99	4,771,706.94
26	2041	142,420.90	36,375.62	252,580.78	431,377.30	0.08	36,194.91	4,807,901.85
27	2042	132,451.44	37,891.27	254,683.87	425,026.58	0.08	32,420.04	4,840,321.90
28	2043	123,179.84	39,470.08	256,595.77	419,245.68	0.07	29,071.90	4,869,393.79
29	2044	114,557.25	41,114.66	258,333.86	414,005.77	0.06	26,098.68	4,895,492.47
30	2045	106,538.24	42,827.78	259,913.94	409,279.95	0.06	23,455.24	4,918,947.72
31	2046	99,080.56	44,612.27	261,350.37	405,043.20	0.05	21,102.22	4,940,049.93
32	2047	92,144.93	46,471.11	262,656.23	401,272.26	0.05	19,005.23	4,959,055.17
33	2048	85,694.78	48,407.41	263,843.36	397,945.55	0.04	17,134.25	4,976,189.42
34	2049	79,696.15	50,424.38	264,922.58	395,043.11	0.04	15,462.98	4,991,652.40
35	2050	74,117.42	52,525.40	265,903.69	392,546.50	0.04	13,968.42	5,005,620.81

New HVAC 400KV line

Economic analysis

Interest rate	10%	IRR	24%
Energy cost [Sep 2015]	0.0291 $/KWh	Loss factor	0.38
Energy generation cost	0.067 $/KWh	Annual Load growth	1.2%
Load factor	0.57		

S/N	year	Capital cost [USD/km]	O&M cost [USD]	Loss cost [USD]	Total Cost [USD]	PV factor	PV Cost [USD]	NPV [USD]
1	2016	1,600,977.21	24,014.66	55,537.00	1,680,528.87	0.91	(1,527,753.52)	(1,527,753.52)
2	2017	1,488,908.81	25,015.27	98,796.19	1,612,720.27	0.83	(1,332,826.67)	(2,860,580.18)
3	2018	1,384,685.19	26,057.57	141,565.11	1,552,307.87	0.75	1,166,271.88	(1,694,308.31)
4	2019	1,287,757.23	27,143.30	180,445.94	1,495,346.47	0.68	1,021,341.76	(672,966.55)
5	2020	1,197,614.22	28,274.27	215,792.15	1,441,680.64	0.62	895,170.25	222,203.70
6	2021	1,113,781.22	29,452.37	247,925.07	1,391,158.66	0.56	785,272.80	1,007,476.50
7	2022	1,035,816.54	30,679.55	277,136.81	1,343,632.90	0.51	689,496.13	1,696,972.63
8	2023	963,309.38	31,957.87	303,692.94	1,298,960.19	0.47	605,974.51	2,302,947.15
9	2024	895,877.72	33,289.44	327,834.88	1,257,002.05	0.42	533,091.57	2,836,038.72
10	2025	833,166.28	34,676.50	349,782.09	1,217,624.88	0.39	469,447.10	3,305,485.82
11	2026	774,844.64	36,121.36	369,734.11	1,180,700.11	0.35	413,828.19	3,719,314.01
12	2027	720,605.52	37,626.42	387,872.30	1,146,104.24	0.32	365,184.13	4,084,498.14
13	2028	670,163.13	39,194.18	404,361.57	1,113,718.89	0.29	322,604.69	4,407,102.83
14	2029	623,251.71	40,827.27	419,351.81	1,083,430.80	0.26	285,301.19	4,692,404.02
15	2030	579,624.09	42,528.41	432,979.31	1,055,131.81	0.24	252,590.17	4,944,994.19
16	2031	539,050.41	44,300.43	445,367.94	1,028,718.77	0.22	223,879.18	5,168,873.36
17	2032	501,316.88	46,146.28	456,630.33	1,004,093.49	0.20	198,654.54	5,367,527.91
18	2033	466,224.70	48,069.04	466,868.87	981,162.61	0.18	176,470.72	5,543,998.63
19	2034	433,588.97	50,071.92	476,176.63	959,837.52	0.16	156,941.10	5,700,939.73
20	2035	403,237.74	52,158.25	484,638.23	940,034.22	0.15	139,730.10	5,840,669.83
21	2036	375,011.10	54,331.51	492,330.60	921,673.20	0.14	124,546.23	5,965,216.05
22	2037	348,760.32	56,595.32	499,323.66	904,679.30	0.12	111,136.21	6,076,352.26
23	2038	324,347.10	58,953.46	505,680.98	888,981.54	0.11	99,279.82	6,175,632.08
24	2039	301,642.80	61,409.85	511,460.37	874,513.03	0.10	88,785.46	6,264,417.54
25	2040	280,527.81	63,968.60	516,714.36	861,210.76	0.09	79,486.31	6,343,903.85
26	2041	260,890.86	66,633.95	521,490.71	849,015.53	0.08	71,237.03	6,415,140.88
27	2042	242,628.50	69,410.37	525,832.85	837,871.72	0.08	63,910.91	6,479,051.80
28	2043	225,644.50	72,302.47	529,780.25	827,727.23	0.07	57,397.38	6,536,449.17
29	2044	209,849.39	75,315.07	533,368.80	818,533.26	0.06	51,599.85	6,588,049.03
30	2045	195,159.93	78,453.20	536,631.11	810,244.24	0.06	46,433.93	6,634,482.95
31	2046	181,498.74	81,722.08	539,596.85	802,817.67	0.05	41,825.74	6,676,308.70
32	2047	168,793.83	85,127.17	542,292.98	796,213.97	0.05	37,710.64	6,714,019.33
33	2048	156,978.26	88,674.13	544,744.00	790,396.39	0.04	34,031.91	6,748,051.25
34	2049	145,989.78	92,368.89	546,972.21	785,330.88	0.04	30,739.82	6,778,791.07
35	2050	135,770.49	96,217.59	548,997.85	780,985.94	0.04	27,790.68	6,806,581.75

Appendix G : 400 kv HVAC single circuit investment cost

No	Description	Unit	Qty	Unit cost [USD]	Total cost [USD]
	Switch yard upgrade at Gibee III				
1	400 kV line bay, double bus	no	1	1,200,000.00	1,200,000.00
2	400 kV incoming line bay, double bus	no	1	1,200,000.00	1,200,000.00
3	400 kV outgoinging line bay, double bus	no	1	1,200,000.00	1,200,000.00
4	400 kV transformer bay, double bus	no	1	1,200,000.00	1,200,000.00
5	Transformer				-
	750 MVA, 400/132/33 KV auto transformer with complete terminal connector, all auxiliaries, and internal cabling and termination	no	1	18,000,000.00	18,000,000.00
	110 MVAR line shunt reactor, 3 phase , with complete	no	1	264,000.00	264,000.00
	terminal connector, all auxiliaries, and internal cabling and termination	no	1	15,000.00	15,000.00
6	Circuit breaker				-
	400 Kv SF6 spring operated circuit brakers with 3ph,2000A,40KA closing resistorsuuitable for single and three phase operation along with support structure	no	6	96,428.00	578,568.00
7	Current transformer				-
	400KV,2000A,40KA 6 core current transformer 1 phase complete with terminal connector	no	6	19,285.00	115,710.00
8	Capacitor voltage transformer				-
	400KV. 4440pF, CVT, 1 phase complement with line terminal connector	no	6	30,535.00	183,210.00
9	Isolator				-
	420KV ,2000 A , 3 phase Horizintal double break isolator (Eelectrically ganged motor) with two earth switch (manually operated) completer with 9 support insulators per e phase isolator and terminal connector	no	6	32,141.00	192,846.00
	420KV, 2000A line insulator	no	6	42,559.00	255,354.00
10	Wave trap				-
	420KV,200ma 0.5mH, I phase wave trap with 3 support insulator	no	1	26,786.00	26,786.00
11	Bus post insulator				-
	420KV post insulator for bus support with terminal connector	no	6	1,687.00	10,122.00
	BUS BAR MATERIALS	no	6	1,687.00	10,122.00
12	String Insulator and Hardware				-
	String insulator with double anchoring point (anchor spacing 450mm) string comprising 2x25Nos 120kn ant fog type disc with hardware accessories including tension clamp and turn buckle for double AAAC conductor spacing 400mm	no	12	24,900.00	298,800.00
13	Conductor				-
	AAAC Aster 851 condcutor for bus/jack bus connection, droppers equipment connection, bus bar jumpering along with spacers TEE connectors PG clamps	km	402	21,996.00	8,842,392.00
14	Site work including cabling, trench and earthing	set	1		-
15	Marshash kiosk and junction box, cable trenceh and other accessories	set	6	2,410.00	14,460.00
16	Earthing all 400 KV switch yard equipment	set			-
	65x8mm galvanised MS flat riser	km	3250	1,607.00	5,222,750.00
	50x6mm galvanised MS	km	2500	1,607.00	4,017,500.00
17	Substation auxilaries	set	1	128,500.00	128,500.00
					42,976,120.00

	Substation upgrade at Akaki II susbtation				
1	400 kV line bay, double bus	no	1	1,200,000.00	1,200,000.00
2	400 kV incoming line bay, double bus	no	1	1,200,000.00	1,200,000.00
3	400 kV outgoinging line bay, double bus	no	1	1,200,000.00	1,200,000.00
4	400 kV transformer bay, double bus	no	1	1,200,000.00	1,200,000.00
5	Transformer				-
	750 MVA, 400/132/33 KV auto transformer with complete terminal connector, all auxiliaries, and internal cabling and termination	no	1	18,000,000.00	18,000,000.00
	110 MVAR line shunt reactor, 3 phase , with complete	no	1	264,000.00	264,000.00
	terminal connector, all auxiliaries, and internal cabling and termination	no	1	15,000.00	28,000.00
6	Circuit breaker				-
	400 Kv SF6 spring operated circuit brakers with 3ph,2000A,40KA closing resistorsuuitable for single and three phase operation along with support structure	no	6	96,428.00	578,568.00
7	Current transformer				-
	400KV,2000A,40KA 6 core current transformer 1 phase complete with terminal connector	no	6	19,285.00	115,710.00
8	Capacitor voltage transformer				-
	400KV. 4440pF, CVT, 1 phase complement with line terminal connector	no	6	30,535.00	183,210.00
9	Isolator				-
	420KV ,2000 A , 3 phase Horizintal double break isolator (Eelectrically ganged motor) with two earth switch (manually operated) completer with 9 support insulators per e phase isolator and terminal connector	no	6	32,141.00	192,846.00
	420KV, 2000A line insulator	no	6	42,559.00	255,354.00
10	Wave trap				-
	420KV,200ma 0.5mH, I phase wave trap with 3 support insulator	no	1	26,786.00	26,786.00
11	Bus post insulator				-
	420KV post insulator for bus support with terminal connector	no	6	1,687.00	10,122.00
	BUS BAR MATERIALS	no	6	1,687.00	10,122.00
12	String Insulator and Hardware				-
	String insulator with double anchoring point (anchor spacing 450mm) string comprising 2x25Nos 120kn ant fog type disc with hardware accessories including tension clamp and turn buckle for double AAAC conductor spacing 400mm	no	12	24,900.00	298,800.00
13	Conductor				-
	AAAC Aster 851 condcutor for bus/jack bus connection, droppers equipment connection, bus bar jumpering along with spacers TEE connectors PG clamps	km	402	21,996.00	8,842,392.00
14	Marshash kiosk and junction box	set	6	2,410.00	14,460.00
15	Earthing material				
	Earthing all 400 KV switch yard equipment	set			
	65x8mm galvanised MS flat riser	km	1250	1,607.00	2,008,750.00
	50x6mm galvanised MS	km	1300	1,607.00	2,089,100.00
16	Substation auxilaries	set	1	98,500.00	98,500.00
	Total				37,816,720.00
1	Transmission tower				
	One single Ckt,Steel Tower with composite insulator for all three phase lines fromGibe III- wolyita	Km	58	1,400,000.00	81,200,000.00
	One single Ckt,Steel Tower with composite insulator for all three phase lines from wolyita - Gelan	Km	344	1,400,000.00	481,600,000.00
	Total				562,800,000.00
	Grand Total				**643,592,840.00**